Development of new methods to study DNA methyltransferase function and protein interactions in living cells

Kourosh Zolghadr

Dissertation
an der Fakultät für Biologie
der Ludwig-Maximilians-Universität
München

vorgelegt von
Kourosh Zolghadr
aus Teheran

München, den 18.12.2007

Erstgutachter: Prof. Dr. Heinrich Leonhardt
Zweitgutachter: Prof. Dr. Harry MacWilliams

Tag der mündlichen Prüfung: 19.03.2008

INDEX

SUMMARY 3

CHAPTER I. INTRODUCTION 5

I.1. How to detect protein interactions? 6
  I.1.1. Antibodies and derivates thereof to identify proteins 6
  I.1.2. Biochemical methods to study protein interactions 8
  I.1.3. Genetic yeast two-hybrid screens to detect protein-protein interactions 9
  I.1.4. Fluorescently labeled proteins and applications in living cells 10

I.2. DNA methylation in mammalian cells 16
  I.2.1. Function and localization of Dnmt1 18
  I.2.2. Molecular mechanism of DNA methylation 20

CHAPTER II. RESULTS 25

II.1. A fluorescent two-hybrid (F2H) assay for direct visualization of protein-protein interactions in living cells 25

II.2. Targeting and tracing antigens in live cells with fluorescent nanobodies 61

II.3. A versatile nanotrap for biochemical and functional studies with fluorescent fusion proteins 77

II.4. Trapped in action: direct visualization of DNA methyltransferase activity in living cells 97

II.5. Regulation of DNA methyltransferase 1 109

CHAPTER III. DISCUSSION 123

III.1. A new assay to visualize protein-protein interactions *in vivo* 123

III.2. A new antibody-format to follow endogenous antigens in living cells 125

III.3. A GFP-binding protein for biochemical and functional studies 127

III.4. Direct visualization of enzyme-activity in living cells 128

III.5. Combinatorial approaches and outlook 130

CHAPTER IV. ANNEX 135

IV.1. Abbreviations 135

IV.2. Contributions 137
  IV.2.1. Declarations of Contributions to II.1 137
  IV.2.2. Declarations of Contributions to II.2 137
  IV.2.3. Declarations of Contributions to II.3 137
  IV.2.4. Declarations of Contributions to II.4 138
  IV.2.5. Declarations of Contributions to II.5 138
  IV.2.6. Declaration according to the "Promotionsordnung der LMU München für die Fakultät Biologie" 138

IV.3. Acknowledgements 139

IV.4. References 140

CHAPTER V. CURRICULUM VITÆ 155

V.1. Publications 156

V.2. Awards and conference contributions 157

SUMMARY

Interactions between proteins are central to essentially all cellular processes. Many methods for the investigation of proteins have been developed in the last years, requiring either removal of the proteins from their normal cellular environment, perturbation of the cells or costly instrumentation and high technical expertise. Therefore we aimed at designing assays for *in vivo* studies of protein interaction, distribution, dynamics, characterization, manipulation and enzyme activity focusing on proteins essential for DNA methylation.

During this thesis we developed a novel fluorescent two-hybrid (F2H) assay for a direct analysis of protein-protein interactions in real-time in mammalian cells using a simple co-localization read-out of fluorescent bait and prey proteins at a stably integrated chromosomal *lac* operator array. The F2H assay can in principle be automated and therefore be used for high-throughput protein-protein interaction analysis in living cells.

To study localization and mobility of endogenous proteins inside cells we took advantage of antibodies derived from alpacas (*Lama pacos*). Alpacas and other *Camelidae* posses so-called heavy-chain antibodies that lack light chains. We isolated the heavy chain variable domain (V_HH) of these single chain antibodies, fused this antigen-binding fragment to a fluorescent protein and expressed the resulting chimeric protein (referred to as chromobody) in cells. Chromobodies allow for the first time targeting and tracing of endogenous antigens, i.e. proteins as well as non-protein components in living cells.

An additional, highly versatile application of V_HHs is to couple them on solid support for biochemical methods or to fuse them to a structural protein. We generated a V_HH against the green fluorescent protein GFP (referred to as GFP-binding protein; GBP) and tethered it to the nuclear lamina (referred to as GFP-nanotrap). With this intracellular GFP-nanotrap we could ectopically capture GFP-fusion proteins and their interacting endogenous factors. Such directed manipulation of cellular components opens up new possibilities to study protein dynamics, function and regulation including the role and organization of nuclear architecture.

To gain insight into the regulation and maintenance of cytosine-5 methylation by DNA methyltransferases (Dnmts), an epigenetic hallmark leading to transcriptional silencing, we developed an *in vivo* trapping assay that directly visualizes the activity and subnuclear targeting of Dnmts in the context of dynamic chromatin structures and simultaneously ongoing DNA replication. The trapping assay offers an approach to test new types of Dnmt inhibitors including small molecules.

In summary, we developed new, simple, versatile and efficient methods and tools to study the regulation and function of proteins involved in complex cellular processes such as DNA methylation in living cells in real-time.

CHAPTER I. INTRODUCTION

The understanding of cellular processes and regulatory networks requires quantitative data on all cellular components including their concentration, modifications, interactions, distributions, dynamics and activity in living cells. Biological processes such as DNA replication or DNA methylation are strictly coordinated and mostly take place in complex, dynamic networks and clusters where many proteins are involved. In the case of DNA replication, being an essential part of the cell cycle, this implies assembly of several thousand replication clusters throughout the cell which comprise specialized proteins to unwind the DNA, stabilize the single strand state and precisely duplicate each and every base pair of the genome exactly one time on the leading strand as well as on the lagging strand where in addition, maturation of Okazaki fragments is required (Sclafani and Holzen, 2007). At the same time countless processes occur within cells involving an only partly known number of cellular factors. To gain an insight into such cellular events it is necessary to identify the involved factors, their functions and their interactions.

Closely associated with the highly complex task of DNA replication is the maintenance of epigenetic information, i.e. DNA methylation and specific histone modifications during each cell cycle. Epigenetic information is defined as the information, which is inherited through mitosis or meiosis but is not contained within the basic sequence of DNA. So far, we owe part of our basic knowledge about DNA methylation, the most common epigenetic modification, to classical biochemical *in vitro* approaches, which cannot reproduce the complexity of living, mammalian cells. Therefore, the body of this thesis project aimed at developing new methods and tools to study proteins involved in DNA methylation, more precisely DNA methyltransferase 1 (Dnmt1) in their normal environment of living cells. First, we aimed at designing a new assay to directly visualize protein-protein interactions in living cells, including detection of interactions between Dnmt1 and proteins involved in DNA replication independently of cell cycle progression. The next objective was to generate a novel, versatile tool to recognize, trace and manipulate proteins *in vivo*. This tool should also be applicable to isolate proteins for biochemical and functional studies e.g. to determine enzymatic activity *in vitro* or chromatin immunoprecipitations (ChIPs). A further goal was to develop a method to directly visualize DNA methyltransferase activity in living cells, particularly to monitor kinetic properties of Dnmt1 in its native environment.

I.1. HOW TO DETECT PROTEIN INTERACTIONS?

I.1.1. ANTIBODIES AND DERIVATES THEREOF TO IDENTIFY PROTEINS

Many methods that are applied to detect and gain insight into biological functions depend on the recognition of an antigen by a specific antibody. Conventional antibodies are heteromeric molecules composed of light (L) and heavy (H) chains with constant and variable domains. The combination of variable domains of an H- and L-chain considerably diversifies the antigen-binding repertoire of conventional antibodies (Fig. 1a).

Antibodies are widely used as detection reagents in many biochemical, cellular and histological applications. However, despite being generally applied, conventional antibodies yield fundamental disadvantages. Antibodies are naturally designed to function in the extracellular milieu. Essential disulfide bonds are formed through a complex process of assembly. Therefore, antibodies expressed inside cells (within the reducing environment of the cytoplasm) are folded improperly and prone to aggregation. Additionally, batch-to-batch variations in monoclonal antibody quality and their limited amount of availability are common problems. To circumvent these limitations recombinant antibody formats such as antigen binding fragments (Fab fragments) or single chain variable fragments (scFvs) are being developed. Currently, widely used recombinant antibody-derivates are scFvs, a fusion of the variable heavy and light chains of immunoglobulins (Ig), linked together with a short, usually serine-glycine-linker (Fig. 1a). Nevertheless, scFvs and other formats do not solve all problems of conventional antibodies, as antigen recognition of scFvs in living cells also mostly is impaired by aggregation (Cardinale et al., 2004).

Interestingly, camelids (Bactrian camels, dromedaries and llamas) developed in addition to their conventional antibodies, so-called heavy-chain antibodies solely composed of truncated H-chains (Hamers-Casterman et al., 1993). Isolation of the variable domain of these single-chain antibodies yields the smallest intact antigen-binding fragment (15 kDa), the heavy chain variable (V_HH) domain (Fig. 1b) (Muyldermans et al., 1994; Muyldermans and Travers, 1994). Sequence analysis and elucidation of the crystal structure revealed that V_HHs contain four framework regions forming the core structure of the immunoglobulin domain and three complementarity-determining regions (CDRs) involved in antigen binding (Desmyter et al., 2001; Desmyter et al., 1996; Harmsen et al., 2000). It has been shown that V_HHs bind their antigen specifically with nanomolar affinity (Muyldermans and Lauwereys, 1999). Furthermore, V_HHs are highly soluble and stable because of unique hydrophilic residues in their structural region (Davies and Riechmann, 1995; Muyldermans, 2001; van der Linden et al., 1999; Vu et al., 1997).

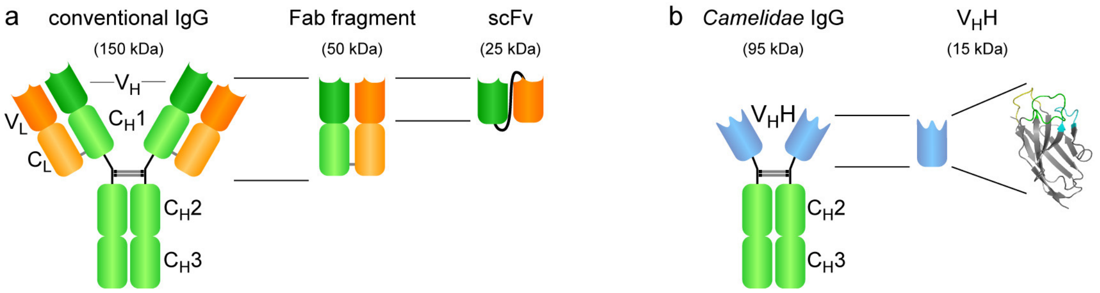
a
conventional IgG
(150 kDa)
Fab fragment
(50 kDa)
scFv
(25 kDa)
V_H
V_L
C_H1
C_L
C_H2
C_H3
b
Camelidae IgG
(95 kDa)
V_HH
(15 kDa)
V_HH
C_H2
C_H3

Fig. 1 | (a) Schematic outline of conventional antibodies composed of heavy (H) and light (L) chains with variable (v) and constant (c) domains. Recombinant derivates thereof are Fab fragments and single chain variable fragments (scFv). (b) In comparison, a *Camelidae*-derived heavy-chain antibody and the isolated heavy chain variable (V_HH) domain. Within the crystal structure of the V_HH, the three antigen binding loops (CDRs) are shown in yellow, cyan and green. Adapted from (Harmsen and De Haard, 2007)

In contrast to scFvs, V_HHs are encoded by only one gene, so they can easily be amplified by one RT-PCR reaction from total mRNA isolated from antibody producing cells (lymphocytes). For efficient selection of specific V_HHs, the V_HH repertoire of one animal is cloned in a phage display vector leading to a library. This library can then be screened for antigen-binding V_HHs using the phage display technology. Several rounds of affinity purification and amplification lead to the isolation of candidate-V_HHs, which then can be tested by e.g. enzyme-linked immunosorbent assay (ELISA) and further characterized through Biacore measurements (Fig. 2). Once, specific V_HHs are identified and selected they can easily be produced as recombinant proteins in bacteria in infinite amounts with constant quality (Muyldermans, 2001).

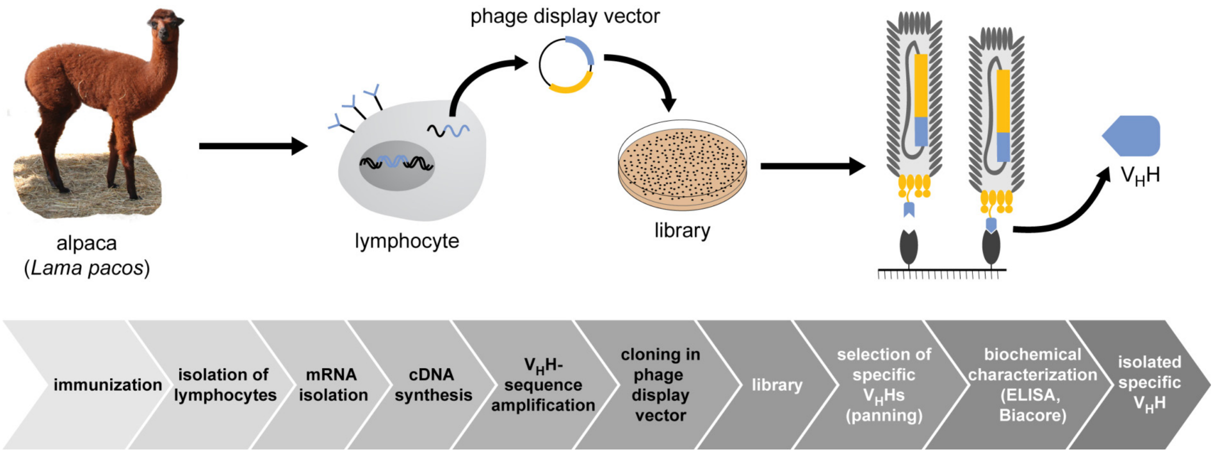
alpaca
(*Lama pacos*)
lymphocyte
phage display vector
library
V_HH
immunization
isolation of lymphocytes
mRNA isolation
cDNA synthesis
V_HH-sequence amplification
cloning in phage display vector
library
selection of specific V_HHs (panning)
biochemical characterization (ELISA, Biacore)
isolated specific V_HH

Fig. 2 | Workflow of the isolation of specific V_HHs from an immunized alpaca. Adapted from (Muyldermans, 2001)

We show in chapter II.2 that fluorescently labeled V_HHs (chromobodies) are capable to detect and visualize antigens in living cells. In chapter II.3 we demonstrate that immobilized V_HHs (nanotraps) can also be applied for biochemical and functional studies as well as a tool to manipulate cellular proteins.

I.1.2. BIOCHEMICAL METHODS TO STUDY PROTEIN INTERACTIONS

Widely used biochemical methods to analyze proteins and interacting factors are affinity purification, immunoprecipitation (IP), co-immunoprecipitation (Co-IP) or pull-down assays. These methods are all based on the binding of a specific antibody or a ligand to the protein of interest and require removal of the proteins from their native environment. The antibody/ligand is immobilized on a solid support and binds specifically the protein of interest from a complex protein mixture. After elution of the isolated protein (Fig. 3) it can be further analyzed by e.g. gel electrophoresis, western blotting or mass spectrometry. With these techniques the presence, molecular mass, quantity, enzymatic activity or post-translational modifications of the protein of interest but especially interactions with other proteins can be determined. Presumably the most significant method to identify a specifically precipitated protein and interacting components is western blotting. After protein-isolation, gel electrophoresis is uses to separate proteins according to their size. The proteins are then transferred to a membrane, where they are detected with specific antibodies. This reveals their presence, quantity, size and also provides information about potential interaction partners. A further method to identify proteins, particularly unknown proteins and interactors is mass spectrometry. The protein of interest is precipitated together with interacting proteins and separated by gel electrophoresis. Candidate bands are cut out and the masses of proteolytic peptides in that protein band determined. Subsequent *in silico* data analysis and comparison with protein databases provides the best match proteins.

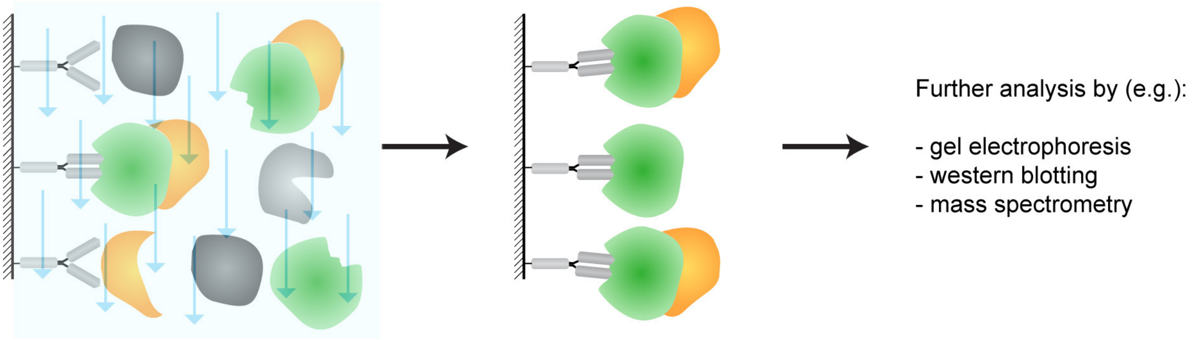

Fig. 3 | Schematic representation of precipitation of a particular protein (green) from a crude mixture of proteins by binding to a specific antibody (or ligand) immobilized on solid support. Interacting proteins (yellow) can be co-precipitated.

Dependant on the properties of the analyzed proteins detergent solubilization of cells during biochemical studies can promote artificial protein-aggregation leading to false positive results (Pfleger and Eidne, 2003). Artificial introduction of expression vectors into cells can induce overexpression of the corresponding protein of interest, which then may lead to protein-aggregation. Additionally, it is not possible to distinguish between direct and indirect interactions when the protein of interest is assembled in a large multi-component complex. The disassembly of complexes may then lead to disruption of the protein interactions to be assayed for, giving false negatives. Slight variation of protocols may therefore lead to contrary results. To some extend proteins can be embedded in complexes in such a way, so that the specific antibody has no access to and can therefore not detect its epitope. Furthermore, it is very demanding to detect weak respectively transient interactions between proteins or very low abundant proteins. Nevertheless biochemical approaches to detect protein interactions are mostly considered to be the "gold standard" among the diversity of present techniques (Cho et al., 2004).

I.1.3. GENETIC YEAST TWO-HYBRID SCREENS TO DETECT PROTEIN-PROTEIN INTERACTIONS

Another frequently used technique is the genetic identification of protein-protein interactions with yeast two-hybrid (Y2H) screens. The Y2H technique uses two protein domains of a transcriptional activator that have specific functions: a DNA-binding domain (DB), which recognizes and binds to a defined promoter sequence upstream of a reporter gene and an activation domain (AD) which interacts with the RNA polymerase II complex, thereby activating transcription.

For a Y2H screen, first, a cDNA encoding the protein of interest (X) is cloned into a bait vector, creating a fusion of the DB and X. Second, a cDNA encoding an interacting protein Y (or a library of cDNAs encoding an entire collection of different potential interactors) is cloned into a prey vector, creating a fusion of the AD and Y. Finally, bait and prey protein are expressed in yeast and if they interact, the AD is recruited to a reporter gene, creating a hybrid transcription factor. The downstream reporter gene, e.g. an auxotrophic marker such as *HIS3* or *ADE2* or a colony color marker like *lacZ*, is transcribed (Fig. 4). Yeast cells expressing HIS3 or ADE2 protein are able to grow on selective medium lacking the amino acid histidine or the metabolite adenine, respectively. Expression of β-galactosidase (LacZ) results in blue coloration of the yeast cells growing on medium containing X-gal (Durfee et al., 1993; Fields and Song, 1989; Vidal et al., 1996b; Vojtek et al., 1993). Thus, the interaction of two proteins is measured by the reconstitution of a transcription factor and the consequent activation of a set of specific reporter genes. (Vidal et al., 1996a).

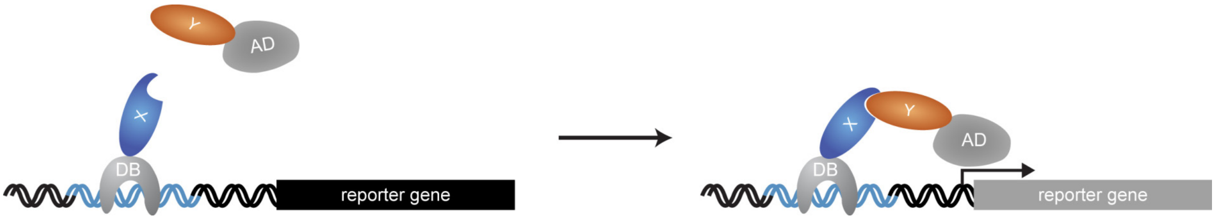

Fig. 4 | Schematic representation of the yeast two hybrid screen. The bait protein (X) is fused to the DNA-binding domain (DB) of a transcription factor. The prey protein (Y) is fused to the transcription activation domain (AD) of a transcription factor. Reporter gene expression can then efficiently be selected for in yeast. Modified from (Vidal and Legrain, 1999)

Although Y2H screens are very suitable to identify whole protein networks and to develop interactome maps in an efficient and inexpensive high-throughput manner (Vidal, 2005) they also have some disadvantages: (I) Y2H screens yield a high number (up to 50%) of false positive or false negative identifications (Deane et al., 2002); (II) mammalian proteins expressed in yeast can be misfolded and therefore dysfunctional; (III) lack of some post-translational modifications of mammalian proteins in yeast may prevent interactions; (IV) no spatial or dynamic resolution where and when the detected interactions normally occur in higher eukaryotic cells is obtained (Kim et al., 2007). Additionally, before performing Y2H screens self-activation of transcription by the bait proteins has to be tested for. Modification of the classical Y2H screen like forward or reverse 'n' -hybrid screens (reviewed in (Vidal and Legrain, 1999)) and combinations thereof have been made to further improve the reliability of the screens. However, a second line of evidence for confirmation of interactions by higher confidence assays such as Co-IPs remains necessary (Uetz et al., 2004).

An analogous system to the yeast two-hybrid screen is the bacterial two-hybrid (B2H) selection system, which facilitates the rapid interaction analysis of large libraries (more than 10^8 in size), due to the higher transformation efficiency and faster growth rate of *E.coli* (Hu et al., 2000; Joung et al., 2000).

I.1.4. FLUORESCENTLY LABELED PROTEINS AND APPLICATIONS IN LIVING CELLS

The combined use of genetic and biochemical approaches has led to the identification of thousands of potential protein interactions, but the cell specificity and the subcellular localization of these interactions often remain unknown. Therefore more and more cellular approaches are being developed and applied in order to investigate distribution and dynamics of fluorescently labeled proteins as well as interactions between proteins in their physiological environment with minimal perturbation. Kinetic data on protein localization and mobility acquired from live cell microscopic methods can be modeled to quantify biophysical properties of molecules and processes (Phair and Misteli, 2001). Generally, with fusion proteins it has to be taken into account that they are artificially introduced into cells. Controls, including antibody stainings against the endogenous protein are therefore crucial to assure that the fusion protein is distributed and regulated like its endogenous counterpart. Furthermore, potential influences on cellular properties and interference with cellular processes such as cell cycle have to be considered (Sporbert et al., 2005).

PHOTOMANIPULATION TO MEASURE PROTEIN DYNAMICS

The mobility of fluorescently labeled proteins can be measured with fluorescence recovery after photobleaching (FRAP) and fluorescence loss in photobleaching (FLIP). Both techniques involve deliberate photobleaching an area with a short intense laser beam that results in localized destruction of fluorophores. For FRAP evaluation the time it takes for fluorescence to recover in the bleached area is measured. In a FLIP experiment the selected area is repeatedly bleached and the time it takes for adjacent areas to loose fluorescence is measured (Fig. 5). The kinetics of the fluorescence recovery respectively loss provide a quantitative measure of the mobility of the labeled proteins.

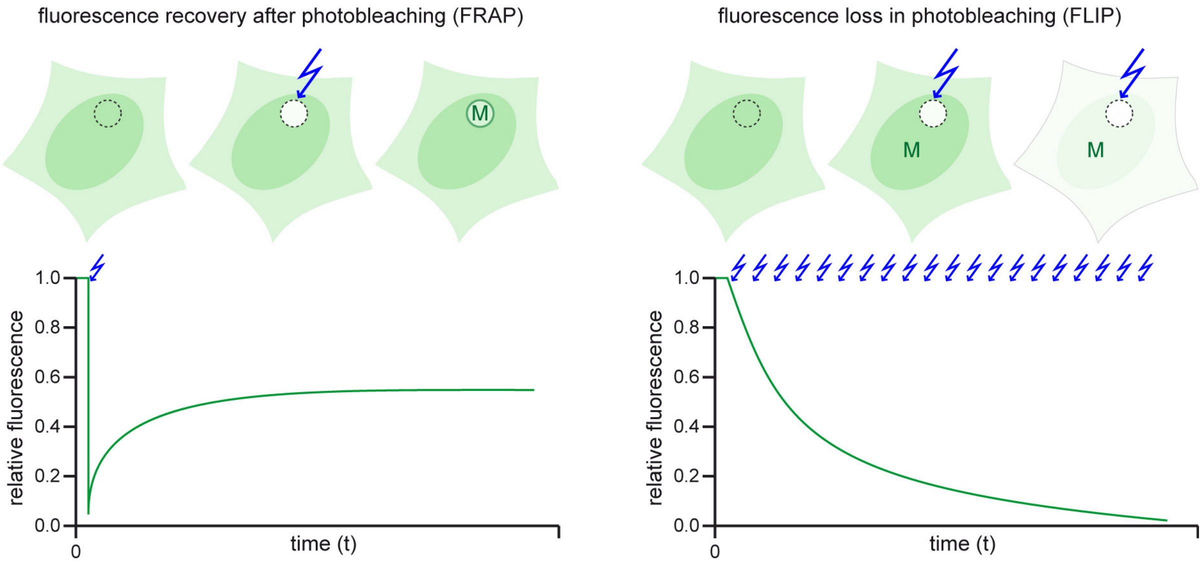

Fig. 5 | Graphical presentations of FRAP and FLIP experiments. The arrow indicates photobleaching with an intense laser beam (in the outlined area); M the region where fluorescence intensity is measured.

Photoactivatable (PA) fluorescent proteins generally display little or no initial fluorescence under excitation at the imaging wavelength. After activation by irradiation at a different (usually shorter) wavelength they dramatically increase their fluorescence intensity. Photoconvertible (PC) proteins, on the other hand, undergo a change in the fluorescence emission profile upon optically-induced changes (a strong laser pulse) to the chromophore. These effects result in a direct and controlled highlighting of distinct molecular pools within the cell and changes in fluorescent protein distribution can then be monitored and evaluated (Lippincott-Schwartz et al., 2003).

FRAP, FLIP, PA and PC are all based on conventional laser scanning microscopy. This enables the detection of localization of fluorescently labeled molecules within the optical spatial resolution defined by the diffraction limit (Abbe limit), at best 200 nanometers (Abbe, 1873). However, in order to understand the physical interactions between protein partners involved in a typical biomolecular process, the relative proximity of the molecules must be determined more precisely than diffraction-limited optical imaging methods permit. Techniques such as fluorescence resonance energy transfer (FRET), bimolecular fluorescence complementation (BiFC) or fluorescence correlation spectroscopy (FCS) permit determination of the vicinity between two molecules within several nanometers, a distance sufficiently close for molecular interactions to occur.

FLUORESCENCE ENERGY TRANSFER AS A MEASURE FOR PROTEIN INTERACTIONS

Förster radius energy transfer, mostly called fluorescence resonance energy transfer (FRET) is a non-destructive spectroscopic method that can monitor the proximity and relative angular orientation of fluorophores *in vivo* by the energy transfer between two fluorophores (Miyawaki et al., 1997). For monitoring the complex formation between two molecules in cells, one molecule is labeled with a donor-fluorophore and the other with an acceptor. The donor fluorescent dye has shorter excitation/emission wavelengths that allow excitation of the acceptor fluorescence dye. Typically two fluorophores with overlapping emission and excitation wavelengths are used, classically cyan fluorescent protein (CFP) and yellow fluorescent protein (YFP) (Mc Intyre et al., 2007) (Fig. 6a). An alternative technique to FRET is bioluminescence resonance energy transfer (BRET), a very similar technique, based on a bioluminescent donor and a fluorescent acceptor.

When the donor and acceptor are in close proximity (1-10 nm) on account of an interaction of the two analyzed molecules, the donor transfers the excitation energy directly to the second fluorochrome (the acceptor) without the emission of a photon. Therefore, if energy transfer occurs, the donor channel signal will be quenched and the acceptor channel signal will be increased (Periasamy, 2001) (Fig. 6a).

FRET quantification is most often based on measuring changes in fluorescence intensity or fluorescence lifetime upon changing the experimental conditions. The fluorescence lifetime refers to the average time the molecule stays in its excited state before emitting a photon. A common FRET microscopy and quantification technique is photo acceptor bleaching. To this end images of donor emission are taken with the acceptor being present. The acceptor is then bleached, such that it is incapable of accepting energy transfer. Further donor emission images are then acquired. A pixel-based quantification should then reveal a brighter fluorescence or a longer fluorescence lifetime of the donor in case of interaction (Sekar et al., 2003).

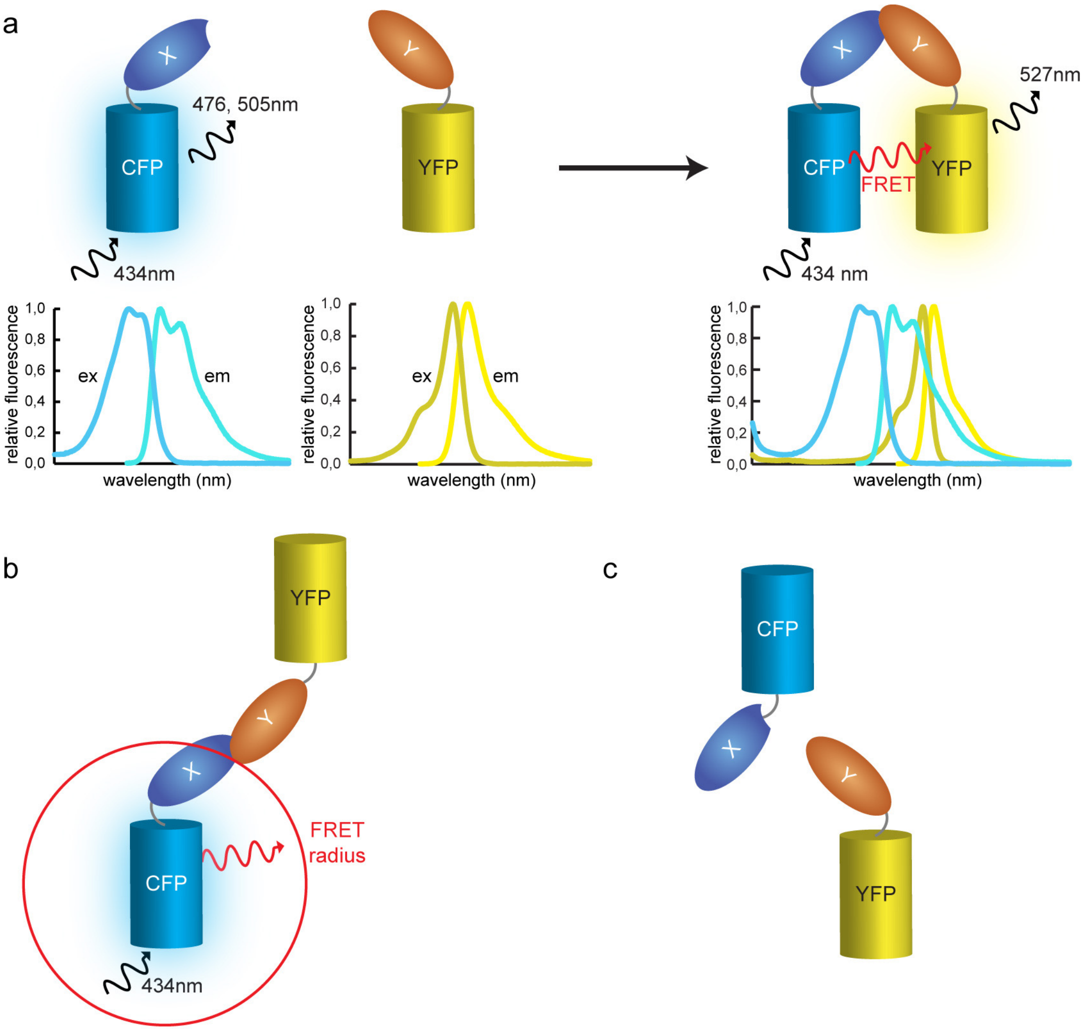

Fig. 6 | (a) Principle of fluorescence resonance energy transfer (FRET). Interaction between proteins X and Y fused to cyan fluorescent protein (CFP) and yellow fluorescent protein (YFP) respectively results in FRET between the donor and the acceptor fluorophore. Plot: excitation (ex) / emission (em) spectra with maxima at 434nm / 476, 505nm (CFP) and 514nm / 527nm (YFP) (b) Head- or tail-fusions of fluorescent proteins can result in a distance larger than the FRET radius. (c) The fusion to the fluorescent protein may mask the interaction site and thus prevent an interaction that occurs under normal conditions.

However, the quantitative or semi-quantitative determination of protein interactions with FRET is very complex and extensive positive as well negative controls are crucial (Miyawaki et al., 1997). Fluorescent proteins fusion to the studied proteins can be N- or C-terminal. Opposite orientations of the fusions can easily result in a distance between the two fluorophores too large for a detectable FRET effect (Fig. 6b). Depending on the geometry of interactions fluorophore fusions can inhibit interactions, which occur under normal conditions (Fig. 6c). Therefore many potential protein-protein interactions might not be detected. Recently, it has been confirmed that photobleaching of YFP induces photoconversion of the protein and generation of a fluorescent byproduct emitting CFP-like fluorescence (Kirber et al., 2007; Valentin et al., 2005). On account of these results, this mainly used FRET pair appears to be less suitable for interaction studies or at least careful controls need to be done.

FLUORESCENCE COMPLEMENTATION TO VISUALIZE PROTEIN INTERACTIONS

A more recent approach to determine protein-protein interactions in living cells is the bimolecular fluorescence complementation (BiFC) assay. This approach is based on the complementation between two non-fluorescent fragments of e.g. the yellow fluorescent protein (YFP). Reconstruction of the fluorescent protein due to interactions between the proteins fused to each of the fragments then recovers the fluorescence (Hu et al., 2002) (Fig. 7).

In the last years complementation assays based on fragments of different proteins including other GFP variants (Magliery et al., 2005), monomeric red fluorescent protein 1 (mRFP1) (Jach et al., 2006), firefly luciferase (Paulmurugan et al., 2002), Gaussia luciferase (Remy and Michnick, 2006) or TEV protease (Wehr et al., 2006) have been developed. These various complementary fragments differ in their functional characteristics and cover a wide range of possible applications. Therefore, interactions between peptides, nuclear proteins, membrane proteins or proteins involved in signaling cascades in mammalian cells, *E.coli* or several other organisms could be visualized (an extended list of described interaction is available at: http://sitemaker.umich.edu/kerppola.bifc). A further modification of the BiFC assay is the simultaneous monitoring of expression and interaction of proteins (Wolff et al., 2006).

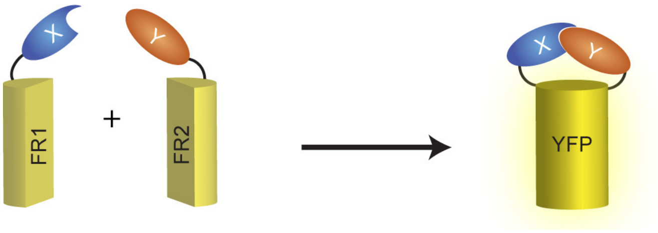

Fig. 7 | Principle of bimolecular fluorescence complementation (BiFC). Non-fluorescent fragments of YFP (FR1 and FR2) are fused to the proteins X and Y to be tested. Interaction of X and Y bring the two fragments together thereby reconstituting the yellow fluorescent protein YFP

The BiFC approach is capable to detect protein-protein interactions in living cells however, steric constraints can prevent the association of the fragment with the interactors. The present generation of fluorescence complementation assays has proven to be versatile, but they have some characteristics limiting their usage. One of these limitations is the irreversible association of the fluorescent protein fragments (Kerppola, 2006b). A second limitation is the intrinsic ability of fluorescent-protein fragments to associate with each other independently of an interaction between the proteins that are fused to the fragments. Finally, the chemical reactions required for fluorophore formation are very slow and temperature-sensitive making it so far impossible to directly visualize the protein-protein interactions in real-time (reviewed in (Kerppola, 2006a)).

ANALYSIS OF SINGLE FLUORESCENT MOLECULES IN LIVING CELLS

In fluorescence correlation spectroscopy (FCS) diffusion and interaction of fluorescent molecules are studied by analyzing fluorescence intensity fluctuations arising from single molecules diffusing in and out of the illuminated volume of a focused laser beam (Magde et al., 1974). An important extension of FCS is the simultaneous detection of two color channels, using two spectrally distinct dyes (Schwille et al., 1997). With two-color FCS, a cross-correlation (FCCS) analysis can be made, where the signals of the two channels are time-correlated with each other and the interaction between two molecules results in a positive cross-correlation amplitude. Single molecule tracing (SMT) allows the direct observation of movements in the nanometer-scale. This makes it possible to discriminate between specific classes of mobility, such as diffusion, binding, direct transport or motion confined to spatially restricted zones (Grunwald et al., 2006).

Measuring fluorescence of single molecules is a highly complex task demanding a very specialized microscopic instrumentation optimized for highest sensitivity and acquisition speed. Furthermore, in living cells the signal-to-noise ratio is largely influenced by auto-fluorescence and scattering. Additionally, the big complexity of the biological systems under investigation requires individual adaptation, optimization and extensive testing of each experimental setup (Haustein and Schwille, 2007). On account of the huge amounts of data generated during any of the methods and the lack of robust automated evaluation software additional expertise in data analysis and interpretation is required.

In summary, numerous cell biological methods based on microscopy of fluorescent proteins, biochemical or genetic approaches are available for addressing whether proteins interact or not. However many of these methods can be technically very demanding, can be limited by the strength of the interaction, or cannot resolve whether the interaction indeed occurs inside cells. To this end our goal was to develop new and simple assays that are adaptable to high-throughput formats primarily to study function, regulation and inhibition of DNA methylation as well as interactions between proteins involved in this process.

I.2. DNA METHYLATION IN MAMMALIAN CELLS

In mammalian organisms cells differ dramatically in their function, shape and organization despite of an identical genetic information. During development cellular differentiation is established by epigenetic modifications such as DNA methylation and histone tail modifications regulating the expression of cell-type specific sets of genes (Berger, 2007; Bird, 2002; Bird, 2007; Leonhardt and Cardoso, 2000; Reik, 2007; Robertson, 2002). DNA methylation pattern changes along with cellular differentiation and once established, it is stably inherited from one cell generation to the next.

Addition of methyl groups to the 5-position of cytosine residues in palindromic cytosine-guanine dinucleotides (CpGs) in the vertebrate genome (Gruenbaum et al., 1981) is a postreplicative modification catalyzed by DNA (cytosine-5-)-methyltransferases (Dnmts). CpG dinucleotides are not randomly distributed in the mammalian genome; instead, they are highly enriched at promoter regions while being greatly under-represented in the rest of the genome. About 70% of CpGs in mammalian genomes are methylated (Ehrlich et al., 1982), predominantly in repressive heterochromatic region and in repetitive sequences (Baylin and Bestor, 2002; Yoder et al., 1997). Cytosine methylation generally is associated with transcriptional inactivation (Bird and Wolffe, 1999; Kass et al., 1997) partly through inhibition of sequence-specific DNA binding factors (Tate and Bird, 1993). Additionally, the recruitment of methyl binding proteins, which interact with histone deacetylases to modify histones, creates a chromatin structure refractory to transcriptional initiation (Jones et al., 1998; Nan et al., 1998). In the promoters of about half of all human genes, clusters of CpG-rich regions termed CpG islands are present (Bird, 1986; Gardiner-Garden and Frommer, 1987). These CpG islands represent about 15% of all CpG sites and were found to be mostly unmethylated (Shen et al., 2007; Weber et al., 2007). Therefore, the role of CpG island methylation in normal development however remains poorly understood. It is now widely held that CpG islands associated with both housekeeping and tissue-specific genes are unmethylated at any developmental stage, except when associated with certain imprinted genes and genes subject to X inactivation (Saxonov et al., 2006).

Controversially discussed aspects of mammalian development are the molecular mechanisms underlying the two major waves of genome-wide demethylation and remethylation: one during germ-cell development and the other after fertilization (reviewed in (Reik et al., 2001)). The genome-wide demethylation could either occur passively through the lack of maintenance methylation following DNA replication and cell division (Howlett and Reik, 1991; Rougier et al., 1998) or could be due to an active process (Oswald et al., 2000). Recently, it has been shown that Gadd45a (growth arrest and DNA-damage-inducible protein 45 alpha), a nuclear protein involved in maintenance of genomic stability, DNA repair and suppression of cell growth, promotes active DNA demethylation by interaction with DNA repair endonuclease XPG (Barreto et al., 2007).

In contrast to developmental genes, which need to be epigenetically regulated with flexibility, imprinted genes need to be stably silenced. To imprint genes, DNA methylation is introduced during gametogenesis, by the *de novo* methyltransferases Dnmt3a (Chedin et al., 2002; Jia et al., 2007; Kaneda et al., 2004) and/or Dnmt3b and their cofactor Dnmt3L (for Dnmt3-*like*) (Hata et al., 2002; Margot et al., 2003; Suetake et al., 2004). Dnmt3L is closely related to Dnmt3 but appears to be inactive on its own (Bourc'his et al., 2001). After fertilization, the methylation is later on stably maintained by Dnmt1 (Goll and Bestor, 2005; Reik, 2007). The importance of maintaining DNA methylation patterns is underlined by the observation that homozygous null deletions of mouse *Dnmt1* result in an 80% reduction of global genomic methylation in embryonic stem cells and embryos and are lethal early in development (Lei et al., 1996; Li et al., 1992).

As mentioned, CpG islands in the promoter region of many genes on the inactive copy of the X chromosome are methylated (Panning and Jaenisch, 1996). However, it has been shown that on a chromosome-wide scale, the active copy is actually more highly methylated, mostly occurring within the bodies of genes (the transcribed regions), rather than in upstream promoters or intergenic areas (Hellman and Chess, 2007; Lock et al., 1986; Viegas-Pequignot et al., 1988; Weber et al., 2005b).

DNA methylation has also been postulated to play a role in cancer for many decades since methylation patterns are significantly altered in many tumor types. In cancer cells, the transcriptional silencing of tumor-suppressor genes by CpG island promoter hypermethylation correlates with tumor development (Hanahan and Weinberg, 2000; Jones and Baylin, 2002). Another effect of hypermethylation is a higher frequency of point mutations; CpGs are mutation hotspots. This results from increased deamination of 5-methylcytosine (5mC) to thymine, resulting in a C→T transition mutation, which is not recognized and repaired before the next round of DNA replication (Jones et al., 1992; Laird and Jaenisch, 1994). In contrast, spontaneous deamination of cytosine forms uracil, which is efficiently recognized and removed by DNA repair enzymes like uracil DNA glycosylases (Craig and Bickmore, 1994; Sved and Bird, 1990). Additionally, genome-wide hypomethylation in cancer cells induces chromosomal instability and promotes insertional mutagenesis by retroviral elements (such as IAPs) (Brown and Robertson, 2007; Eden et al., 2003; Gaudet et al., 2003; Gaudet et al., 2004; Howard et al., 2007; Walsh et al., 1998). In summary, DNA methylation and the maintenance of proper DNA methylation plays a central role in the epigenetic control of mammalian gene expression during development and is required for X inactivation (Beard et al., 1995), genomic imprinting

(Li et al., 1993) and silencing of retroviral elements (Jaenisch and Bird, 2003; Jones and Takai, 2001).

In mammals DNA methylation is catalyzed by a family of four active DNA methyltransferases: Dnmt1, Dnmt2, Dnmt3a and Dnmt3b where Dnmt2 mainly methylates aspartic acid transfer RNA (tRNA(Asp)) (Goll et al., 2006) but is not required for DNA methylation (Okano et al., 1998b). Dnmt3a and Dnmt3b are essential for the methylation of previously unmethylated DNA (*de novo* methylation) during development (Okano et al., 1999; Okano et al., 1998a). The most abundant DNA methyltransferase in mammals is Dnmt1 designated as the maintenance methyltransferase, ensuring the established methylation patterns are preserved over many cell divisions (Bestor, 2000; Li, 2002; Robertson and Wolffe, 2000).

I.2.1. FUNCTION AND LOCALIZATION OF DNMT1

DNA methylation occurs in the context of other epigenetic modifications and once established it needs to be maintained over many cell division cycles. This means that both, genetic and epigenetic information have to be faithfully duplicated, implying a tight coordination between the DNA replication machinery and epigenetic regulators. The first eukaryotic DNA methyltransferase to be identified and cloned was later named Dnmt1 (Bestor et al., 1988; Bestor, 1988; Bestor and Ingram, 1983; Bestor and Ingram, 1985). Dnmt1 is ubiquitously expressed in mammalian cells, and considered to be the key maintenance methyltransferase (reviewed in (Goll and Bestor, 2005)). It predominantly methylates hemimethylated CpG dinucleotides in the genome. *In vitro* assay show a 10- to 40-fold higher activity of Dnmt1 on hemimethylated DNA as compared with unmethylated substrates (Pradhan et al., 1999).

The enzyme comprises 1620 amino acids. The first ~1100 amino acids constitute the regulatory domain and the remaining residues form the catalytic domain containing the 10 conserved motifs (I-X). These motifs are characteristic for cytosine-5-methyltransferases including the invariant catalytic center (Pro-Cys-/PC-motif) in motif IV (Leonhardt and Bestor, 1993). The substitution of the PC dipeptide has been shown to result in a loss of enzymatic activity (Hsieh, 1999). The regulatory and catalytic domain are joined by seven Lys-Gly repeats (Fig. 8).

Mouse oocytes and preimplantation embryos express an oocyte-specific variant called Dnmt1o. At the mouse *Dnmt1* locus an oocyte-specific promoter initiates translation at the second, downstream ATG. This yields the shortened Dnmt1o, lacking 118 amino acids at the N-terminus (Carlson et al., 1992; Gaudet et al., 1998; Mertineit et al., 1998). The truncated Dnmt1o is retained in the cytoplasm of mouse oocytes and early embryos (Cardoso and Leonhardt, 1999; Doherty et al., 2002; Howell et al., 2001) with restricted mobility, while it has a higher mobility in the nucleus of preimplantation embryos (Grohmann et al., 2005). Apart from the development specific isoforms of Dnmt1 also proliferation dependent mRNA expression has been described (Robertson et al., 2000b).

The postreplicative maintenance of methylation patterns is mediated and secured by association of Dnmt1 with the replication machinery throughout S phase (Chuang et al., 1997; Leonhardt et al., 1992; Robertson et al., 1999). Replication-independent loading on (peri-)centromeric heterochromatin from mid-late S to G2 and M phase has also been described (Easwaran et al., 2004) (Fig. 8). During S phase Dnmt1 transiently interacts with the central loading platform PCNA at replication foci. This interaction was shown not to be essential for methylation activity but to increase the maintenance activity in a twofold manner (Schermelleh et al., 2007; Spada et al., 2007).

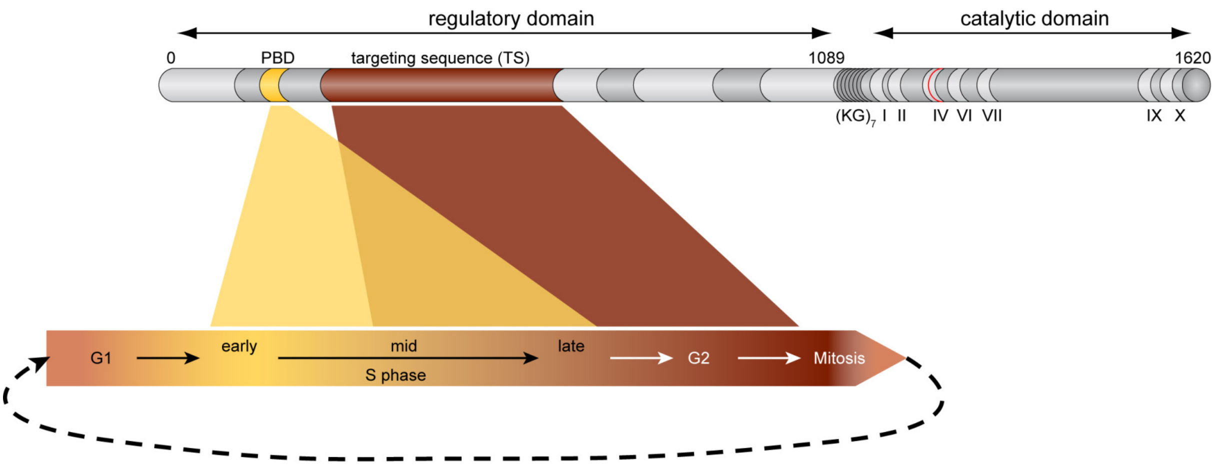

Fig. 8│Structure of DNA methyltransferase 1 (Dnmt1). In the regulatory domain the PCNA binding domain (PBD) and the targeting sequence (TS) mediate association of Dnmt1 with chromatin during the cell cycle. The catalytic domain contains 10 conserved motifs (I-X) characteristic for C5-methyltransferases and the catalytic center (red line in motif IV). Regulatory and catalytic domains are joined by seven Lys-Gly repeats $(KG)_7$.

Furthermore, it has been suggested that the recruitment of Dnmt1 to DNA damage sites (via the PCNA binding domain; PBD) is responsible for coupling DNA repair and subsequent restoration of DNA methylation patterns (Mortusewicz et al., 2005). Many additionally interactions of Dnmt1 with a range of nuclear proteins including UHRF1, G9a, pRb, DMAP1, E2F1, HDAC 1/2, MeCP2, p23, PARP-1, Annexin V, p53, SUV39H1 and HP1b and the nucleolar chromatin remodeling complex Tip5/Snf2h have also been described (Bostick et al., 2007; Esteve et al., 2006; Fuks et al., 2000; Fuks et al., 2003; Geiman et al., 2004a; Geiman et al., 2004b; Kimura and Shiota, 2003; Reale et al., 2005; Robertson et al., 2004; Robertson et al., 2000a; Robertson et al., 2000b; Santoro et al., 2002; Smallwood et al., 2007). The regulation of Dnmt1 during development and cell cycle as well as disease related defects are reviewed in more detail in chapter II.5.

In summary, Dnmt1 interacts with a large number of various proteins. These interactions involve different types of proteins ranging from transcription factors to histone methyltransferases. This places Dnmt1 at the center of a complex network connecting two epigenetic pathways - both resulting in the establishment and maintenance of transcriptionally inactive chromatin - DNA methylation and histone modification. All interactions occur in a highly dynamic fashion and are mainly cell cycle dependently regulated. Our aim was now to develop new *in vivo* assays and tools to analyze which of them occur where and when and what their functional consequences are.

I.2.2. MOLECULAR MECHANISM OF DNA METHYLATION

Having a closer look at DNA methylation being a postreplicative process reveals an interesting problem. DNA replication is highly processive taking about ~2 kbp/ min (Jackson and Pombo, 1998). A certain discrepancy emerges since *in vitro* steady-state kinetic analysis of purified recombinant Dnmt1 revealed a much lower turn-over rate of about 70–450 s per methyl group transfer (Bacolla et al., 1999; Pradhan et al., 1999). Assuming *in vivo* DNA methylation to be faster, it is still not likely to come close to the 30–40 times faster DNA replication, especially taking into account cytosine-methylation being a highly complex reaction (Fig. 9).

The methyl transfer reaction process is initiated with nonspecific binding of Dnmts to DNA, recognition of specific hemimethylated CpG sites and recruitment of the methyl group donor S-adenosyl methionine (SAM) to the active site of the enzyme (Chiang et al., 1996). Dnmts transfer a methyl group onto carbon 5 of cytosines through a covalent intermediate between the PC dipeptide in the active site and the carbon 6 of the target cytosine (Bestor and Verdine, 1994; Chen et al., 1991; Santi et al., 1983). During this covalent complex formation, the cytidine base is flipped out of the DNA doublehelix into an active site pocket of the enzyme (Horton et al., 2004; Klimasauskas et al., 1994). The base pairing hydrogen bonds are broken and the stacking interactions with the adjacent base pairs are lost (Cheng and Roberts, 2001; O'Gara et al., 1996). Through the methyl group transfer the cofactor SAM is transformed into the demethylated S-adenosyl homocysteine (SAH). Subsequently, an unidentified enzyme base or water molecule abstracts a proton from the cytosine-5 position, which allows release of free enzyme by β-elimination (Erlanson et al., 1993).

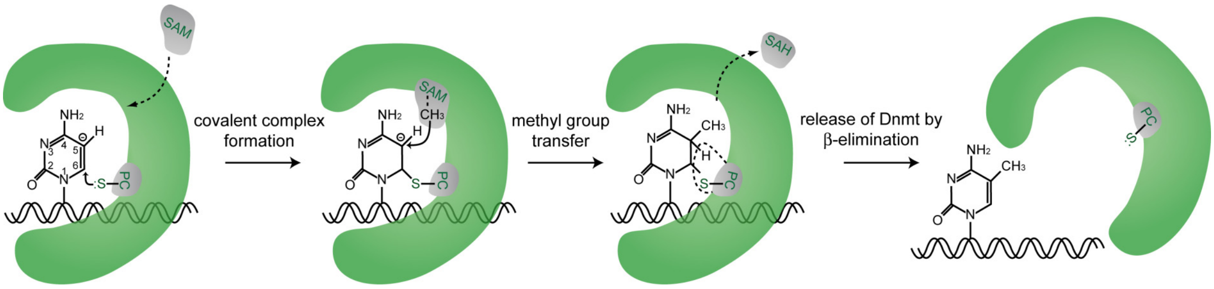

Fig. 9|Schematic representation of the methylation reaction catalyzed by Dnmts (green). A covalent complex is formed between the sulfhydryl group of cysteine in the PC dipeptide in the active site of Dnmts and the carbon 6 position of the cytosine base ring. Then a methyl group is transferred from S-adenosyl methionine (SAM) followed by the release of S-adenosyl homocysteine (SAH) and the enzyme. Adapted from (Goll and Bestor, 2005).

The enzymatic activity of Dnmts can be measured *in vitro*. For this, isolated protein is mixed with [^{3}H]-SAM and hemimethylated double stranded DNA. The methylation reaction catalyzed by Dnmt, transfers labeled methyl groups on the DNA template. The incorporation of ^{3}H into the DNA can then be measured by (liquid) scintillation counting. Various other methods are available to determine global methylation levels of genomic DNA or local levels at certain promoters.

A very common and efficient technique is the treatment of DNA with bisulfite (i.e. sodium bisulfite), which converts non-methylated cytosine residues in DNA to uracil, whereas 5-methylcytosine remains unaltered (Shapiro et al., 1973; Shapiro et al., 1974). In a PCR amplification of the region of interest the uracil is subsequently replaced by a thymine, which can be detected by DNA sequencing (bisulfite sequencing) (Frommer et al., 1992). The combined bisulfite restriction analysis (COBRA) is an alternative detection method to quantitatively determine methylation levels of CpG dinucleotides at specific gene loci (Xiong and Laird, 1997). Bisulfite treatment of DNA and PCR amplification introduces different restriction sites for specific enzymes in methylated DNA and unmethylated DNA, which then can be analyzed by restriction analysis.

A different approach to analyze CpG methylation is methylation sensitive restriction enzyme digestion of DNA with enzyme pairs like *Hpa*II and its methylation insensitive isoschizomer *Msp*I. Methylated and unmethylated DNA is digested and the resulting restriction fragments can be detected by southern blotting or PCR (Sadri and Hornsby, 1996). Immunostainings with specific 5mC-antibodies visualize the overall distribution of methylation pattern inside single cells. With the recently developed methyl-DIP technique methylated DNA is immunoprecipitated with 5mC-antibodies followed by hybridization to genomic microarrays, allowing the identification of methyl-CpG-rich sequences (Keshet et al., 2006; Weber et al., 2005a; Zhang et al., 2006). However, none of the methods listed is capable of visualizing the enzymatic activity or monitoring protein interactions in living cells.

During this work we developed new, versatile methods and tools for *in vivo* and *in vitro* approaches, which all can be applied to study DNA methylation in its natural environment. With our novel trapping assay we are able to study DNA methyltransferase activity in defined chromatin domains e.g. heterochromatin or euchromatin in living cells. Furthermore we designed a fluorescent two-hybrid assay, which enables us to easily analyze interactions of Dnmts, mutant Dnmts or isolated domains of Dnmts with other proteins in real-time *in vivo*. Additionally, we generated small antigen-binding proteins (V_HHs) and labeled them fluorescently (chromobodies) to trace protein in living cells. Furthermore, we immobilized V_HHs on a matrix (nanotrap) to precipitate proteins for biochemical studies respectively to alter their ectopic localization in cells. The applicability of these new methods is not restricted to research on DNA methylation but can generally be implemented to obtain data on proteins including their concentrations, modifications, interactions, distributions, dynamics and activity in living cells to help understanding cellular processes and regulatory networks.

CHAPTER II. RESULTS

II.1. A FLUORESCENT TWO-HYBRID (F2H) ASSAY FOR DIRECT VISUALIZATION OF PROTEIN-PROTEIN INTERACTIONS IN LIVING CELLS

A fluorescent two-hybrid (F2H) assay for direct visualization of protein interactions in living cells

Kourosh Zolghadr[1], Oliver Mortusewicz[1], Ulrich Rothbauer[1], Regina Kleinhans[1], Heike Goehler[2,3], Erich E. Wanker[2], M. Cristina Cardoso[2] and Heinrich Leonhardt[1]

[1]Munich Center for Integrated Protein Science (CiPS^M) and Department of Biology, Ludwig Maximilians University Munich, 82152 Planegg-Martinsried, Germany

[2]Max Delbrueck Center for Molecular Medicine, 13125 Berlin, Germany

[3]present address: Medizinisches Proteom Center, Ruhr University Bochum, Germany

Correspondence should be addressed to H.L. (E-mail: h.leonhardt@lmu.de)

Running Title: A fluorescent two-hybrid assay to study protein interactions

Abbreviations

aa: amino acid

BAH: bromo adjacent homology domain

BiFC: bimolecular fluorescence complementation

BHK: baby hamster kidney

CFP: enhanced cyan fluorescent protein

Co-IP: co-immunoprecipitation

DAPI: 4',6-diamidino-2-phenylindole

DDP1: deafness dystonia peptide 1

Dnmt1: DNA methyltransferase 1

DPSS: Diode-Pumped Solid-State

FP: fluorescent protein

FRET: fluorescence resonance energy transfer

GFP: enhanced green fluorescent protein

HEK: human embryonic kidney cell line

IMS: intermembrane space

NLS: nuclear localization signal

PARP: Poly (ADP-ribose) polymerase

PBD: PCNA binding domain

PBHD: polybromo homology domain

PCNA: proliferating cell nuclear antigen

RFP: monomeric red fluorescent protein

SUMO3: small ubiquitin-related modifier 3

TS: targeting sequence (of Dnmt1)

Vim: Vimentin

XRCC1: X-ray repair cross-complementing protein 1

Y2H: yeast two-hybrid

YFP: enhanced yellow fluorescent protein

ZnF: Zn^{2+}-binding region

Summary

Genetic high-throughput screens have yielded large sets of potential protein-protein interactions now to be verified and further investigated. Here we present a simple assay to directly visualize protein-protein interactions in single living cells. Using a modified lac repressor system, we tethered a fluorescent bait at a chromosomal *lac* operator array and assayed for co-localization of fluorescent prey fusion proteins. With this fluorescent two-hybrid (F2H) assay we successfully investigated the interaction of proteins from different subcellular compartments including nucleus, cytoplasm and mitochondria. In combination with an S phase marker we also studied the cell cycle dependence of protein-protein interactions. These results indicate that the F2H assay is a powerful tool to investigate protein-protein interactions within their cellular environment and to monitor the response to external stimuli in real-time.

Introduction

After sequencing the human genome the next challenge is now to analyze the complex protein-networks underlying cellular functions. In the last decade a wide variety of methods to study protein-protein interactions ranging from biochemical to genetic or cell-based approaches have been developed. Biochemical methods like affinity purification or co-immunoprecipitation (Co-IP) allow the detection of protein complexes *in vitro*. Genetic methods, such as the yeast two-hybrid (Y2H) system (1), enable efficient high-throughput screening of interactions within the cellular environment (2). The analysis of mammalian protein interactions in yeast may, however, suffer from the absence or insufficient conservation of cellular factors modulating protein-protein interactions, e.g. through posttranslational modifications (3).

In recent years new fluorescence-based methods for in-cell visualization of protein-protein interactions have been introduced. Two established techniques, fluorescence resonance energy transfer (FRET) (4, 5) and bimolecular fluorescence complementation (BiFC) (6), are based on the expression of fluorescently labeled proteins or fragments thereof. However, FRET requires costly instrumentation and advanced technical expertise, while BiFC is based on the irreversible complementation and slow maturation of fluorophores which does not allow real-time detection of protein-protein interactions (6).

All these methods have inherent shortcomings and are typically combined to obtain more reliable results. We have now developed a novel fluorescent two-hybrid (F2H) assay for the direct visualization of protein-protein interactions in living mammalian cells. The simple optical readout of this F2H assay allows observation of protein-protein interactions in real time and should also be suitable for high-throughput screens.

Experimental Procedures

Expression constructs

The LacI encoding sequence was PCR amplified from the p3'SS EGFP-LacI expression vector (7) using the following primers: forward primer 5'-TCT AGA *AAG CTT* TCC ATG GTG AAA CCA GTA-3' and reverse primer 5'-CCA TG*C CCG GG*A CAG GCT GCT TCG GGA AAC-3' (restriction sites in italic). This PCR fragment was digested with *Hind*III and *Xma*I and cloned into the same sites of two Dnmt1-YFP expression vectors (MTNY.2 and PBHD-YFP)(8) generating PBD-LacI-YFP and ΔPBD-LacI-YFP. The NLS-PCNA-LacI-RFP and XRCC1-LacI-RFP constructs were generated by PCR amplification of the PCNA and XRCC1 cDNA using the following primers (restriction sites in italic):

PCNA forward	5´- CCCC*CTCGAG*ATGTTCGAGGCGCGC -3´
PCNA reverse	5´- GGGG*AAGCTT*GGAGATCCTTCTTCATCCTC- 3`
XRCC1 forward	5´- CCCC*AGATCT*ATGCCGGAGATCCGC -3´
XRCC1 reverse	5´- GGGG*GAATTC*GGGGCTTGCGGCACCAC -3´

Subsequently the PCR fragments were cloned into a LacI-RFP expression vector using the *Xho*I/*Hind*III sites for the NLS-PCNA-LacI-RFP and the *Bgl*II/*EcoR*I sites for the XRCC1-LacI-RFP expression vector.

All other F2H constructs were generated by PCR amplification of coding cDNAs and subsequent ligation into the *AsiS*I and *Not*I sites of the bait and prey expression vectors described in **Fig. 1a**. The following primers were used with the restriction site indicated in italics:

DDP1 forward	5´-CCCC*GCGATCGC*GATTCCTCCTCCTCTTCCTC-3´
DDP1 reverse	5´-CCCC*GCGGCCGC*TCAGTCAGAAAGGCTTTCTG-3´
TIMM13 forward	5´-CCCC*GCGATCGC*CGAGGGCGGCTTCGGCTCC-3´
TIMM13 reverse	5´-CCCC*GCGATCGC*GAGGGCGGCTTCGGCTCC-3´
HZFH forward	5´-GGGG*GCGATCGC*CACGCCCGCTTCC-3´
HZFH reverse	5´-CCCC*GCGGCCGC*TTAGTCGTCTATACAGATCACCTCC-3´
SUMO3 forward	5´-CCCC*GCGATCGC*GCCGACGAAAAGCCCAAG-3´
SUMO3 reverse	5´-CCCC*GCGGCCGC*TCAGTAGACACCTCCCG-3´
Vim forward	5´-GGGGTGTACA*GCGATCGC*ATGTCGACCCACGCGT-3´
Vim reverse	5´-CCCCGAATTC*GCGGCCGC*TTATTCAAGGTCATCGTGATGCT-3´

Mammalian expression constructs encoding translational fusions of human DNMT1, DNA Ligase I, DNA Ligase III, p21, FEN I, Polymerase δ p66 subunit, PARP-1, PARP-2 and PCNA were previously described (9-14). Deletion constructs and isolated domains of DNA Ligase I and III were described in Mortusewicz et al (15). Immunoprecipitations were performed with a GFP-nanotrap (16) as described before (15). All fusions constructs were tested for correct expression and localization.

Cell culture and transfection

Transgenic BHK cells (clone #2) and U2OS cells (clone 2-6-3) containing *lac* operator repeats were cultured under selective conditions in DMEM supplemented with 10% fetal calf serum and 150 μg/ml hygromycin B (PAA Laboratories) as described (17, 18). For microscopy cells were grown to 50-70% confluence either on 18x18 glass coverslips or in µ-slides (ibidi, Munich, Germany) and then co-transfected with the indicated expression constructs using Polyplus transfection reagent jetPEI™ (BIOMOL GmbH, Hamburg, Germany) according to the manufacturer's instructions. After 6-10 hours the transfection medium was changed to fresh culture medium and cells were then incubated for another 12-24 hours before live cell microscopy or fixation with 3.7% formaldehyde in PBS for 10 min at room temperature. Fixed cells were permeabilized with 0.2% Triton X-100 in PBS for 3 min, counterstained with DAPI and mounted in Vectashield (Vector Laboratories, CA, USA).

Microscopy

Live or fixed cells expressing fluorescent proteins were analyzed using a Leica TCS SP2 AOBS or a Leica TCS SP5 confocal microscope equipped with a 63x/1.4 NA Plan-Apochromat oil immersion objective. Fluorophores were excited with a 405 nm Diode laser, a 488 nm and a 514 nm argon laser and a 561 nm Diode-Pumped Solid-State (DPSS) laser. Confocal image stacks of living or fixed cells were typically recorded with a frame size of 512x512 pixels, a pixel size of 50-100 nm, a z-step size of 250 nm and the pinhole opened to 1 Airy unit. A maximum intensity projection of several mid z-sections was generated with ImageJ (Version 1.38, http://rsb.info.nih.gov/ij/).

Results

To visualize protein-protein interactions in living cells in real time we developed a fluorescent two-hybrid (F2H) assay. The rationale for the F2H assay is based on the fact that proteins are freely roaming the cell unless interactions with other cellular components immobilize them at specific structures (19).

We used a previously described BHK and an U2OS cell line, which both harbor a stable integration of about 200-1000 copies of a plasmid carrying 256 copies of the *lac* operator sequence (17, 18). We generated an expression construct encoding a fluorescent bait protein consisting of a fluorescent protein (FP), the lac repressor (LacI) and the protein X to be tested for interactions (bait) resulting in the triple fusion protein *FP-LacI-X* (**Fig. 1a**) or *X-LacI-FP*. This fusion protein binds to the operator array, which then becomes visible due to the focal enrichment of the FP signal. A second, differently labeled fusion protein (FP-Y, prey) may either interact with the bait protein X leading to co-localization of the FP signals (**Fig. 1b**) or may not interact, resulting in a dispersed distribution of the prey fluorescence (**Fig. 1c**).

Visualization of interactions between DNA repair proteins

To test the F2H assay, the previously described interaction between the two DNA repair proteins DNA Ligase III and XRCC1 (20, 21) was analyzed and the results were compared with data obtained from pull down assays. We have previously shown that this interaction is mediated by the BRCT domain of DNA Ligase III which targets it to DNA repair sites (15). We generated a bait fusion protein consisting of XRCC1 followed by the LacI and the monomeric red fluorescent protein RFP (mRFP). As expected this fusion protein localized at the *lac* operator array in transiently transfected BHK cells (**Fig. 2a**). Both, the full length GFP-tagged DNA Ligase III as well as the isolated GFP-labeled BRCT domain co-localize with XRCC1 at the *lac* operator array, while a fusion protein missing the BRCT domain shows a dispersed distribution. Notably, the highly homologous DNA Ligase I, which catalyzes the same reaction as DNA Ligase III, does not bind to XRCC1 (**Fig. 2a** and **supplementary Fig. 1**). A direct comparison of the F2H data with data obtained from Co-IP experiments reveals that these two methods gave similar results (**Fig. 2b**). In addition, we could also observe the recently described interaction of XRCC1 with PCNA (22) and the two DNA-damage dependent PARPs, PARP-1 and PARP-2 (23, 24) (**supplementary Fig. 2**). These results demonstrate that the F2H assay is well suited to study protein-protein interactions in living cells.

Analysis of cell cycle dependence of protein-protein interactions

A challenge in the analysis of protein-protein interactions is to monitor transient changes caused by for example cell cycle progression or other external stimuli. We analyzed the previously described interaction between DNA methyltransferase 1 (Dnmt1) and PCNA which is mediated by the PCNA binding domain (PBD) and targets Dnmt1 to sites of DNA replication in S phase (8, 25). These findings raised the question whether this interaction occurs only in S phase at replication foci or throughout the cell cycle. We generated two bait-proteins comprising parts of Dnmt1 fused to the LacI and YFP. One bait (PBD-LacI-YFP) comprises aa 118-427 of Dnmt1 including the PBD, while the second bait (∆PBD-LacI-YFP) lacks the PBD and comprises aa 629-1089 of Dnmt1 (**Fig. 3a**). As a prey-protein we used RFP-PCNA, which in addition marks sites of DNA replication allowing the identification of cells in S phase (9, 26). The binding possibilities of these fusion proteins at the *lac* operator array and the replication fork are summarized in **Fig. 3b**.

In non S phase the LacI part of the bait proteins only binds to the chromosomally integrated *lac* operator array, which – dependent on the ploidy of the cell – becomes visible as one or two fluorescent spots in the nucleus. Interaction of RFP-PCNA with the PBD part of the bait protein results in co-localization of the fluorescent signals at the *lac* operator array (**Fig. 3c upper panel)**, while deletion of the PBD in the bait protein leads to a dispersed distribution of RFP-PCNA in non S phase cells (**Fig. 3d upper panel)**. This clearly illustrates that the PBD-dependent interaction of Dnmt1 with PCNA also occurs outside of S phase.

In S phase cells, RFP-PCNA localizes at sites of ongoing DNA replication and in addition is recruited to the *lac* operator array by the PBD-LacI-YFP bait protein (**Fig. 3c lower panel)**. In contrast, when RFP-PCNA is co-expressed together with a bait protein lacking a functional PBD (ΔPBD-LacI-YFP), RFP-PCNA is exclusively enriched at DNA replication sites and not at the *lac* operator array highlighted by ΔPBD-LacI-YFP (**Fig. 3d lower panel)**.

These results clearly show that the localization of RFP-PCNA (prey) at the *lac* operator array depends on the presence of the PBD in the bait construct and that this interaction is not restricted to S phase.

Next, we analyzed the interaction of other PBD-containing proteins with PCNA. We generated a bait fusion protein comprising PCNA fused to an additional NLS followed by LacI and RFP (NLS-PCNA-LacI-RFP). When co-expressed with GFP-Ligase I, both fusion proteins localized to the *lac* operator array indicating interaction between PCNA and DNA Ligase I. Deletion of the PBD lead to a dispersed distribution of DNA Ligase I, while the PBD of DNA Ligase I alone was sufficient for binding to PCNA at the *lac* operator array (**supplementary Fig. 3**). This is in agreement with previous studies showing that the PBD of DNA Ligase I is necessary and sufficient for its targeting to DNA replication and repair sites (15, 27, 28). Notably, using the F2H assay we could demonstrate that DNA Ligase I, as well as the isolated PBD are capable of binding to PCNA also outside of S phase. Likewise we could show binding of various additional replication and repair proteins like FEN1, p21 and the Polymerase δ subunit p66 to PCNA in non S phase cells (**supplementary Fig. 4**). Taken together we could show that the interaction between replication proteins and PCNA is not limited to S phase but also occurs in non S phase cells and outside the replication machinery. This illustrates that the F2H assay offers the unique potential to analyze cell cycle specific changes in protein-protein interactions in living cells.

Detection of interactions between proteins related to Huntington´s disease

To investigate whether the F2H assay can also detect protein-protein interactions taking place in other cellular compartments, we tested the F2H assay with protein interactions identified in the context of Huntington´s disease by yeast two-hybrid (Y2H) assays (29). We analyzed the interaction of one cytoplasmatic (Vimentin) and two nuclear (HZFH and SUMO3) proteins. Vimentin has been described to be a cytoskeleton component and participates in transport processes, whereas HZFH and SUMO3 are involved in transcriptional regulation and DNA maintenance (29). These proteins were either fused with a red fluorescent mCherry-LacI-NLS or with NLS-GFP to generate sets of bait and prey proteins. BHK cells carrying a *lac* operator array were transfected with all possible combinations of expression constructs and subjected to microscopic analysis. We could detect an interaction between Vimentin and HZFH independent of whether these two proteins were used as bait or prey (**Fig.4** and data not shown). We could also detect the reported interaction between SUMO3 and HZFH while Vimentin and SUMO3 did not interact, as previously described (**Fig. 4**) (29). These results show that interactions of nuclear and cytoplasmic proteins can be studied with the F2H assay.

Detection of interactions between mitochondrial proteins

Next, we investigated whether the F2H assay is also suitable to detect protein-protein interactions occurring in other cellular organelles. To this end, we analyzed the interaction between two mitochondrial proteins, DDP1 (deafness dystonia peptide 1) and TIMM13. Both proteins are nuclear encoded and imported into the mitochondrial intermembrane space (IMS) forming a hexameric complex (**Fig. 5a**). Within the IMS the DDP1-TIMM13 complex facilitates the import of hydrophobic proteins of the mitochondrial import machinery into the mitochondrial innermembrane (30). A mutation of the *DDP1* gene was associated with the Mohr-Tranebjaerg-Syndrome, which is a progressive, neurodegenerative disorder (31). This C66W missense mutation is known to cause a full blown phenotype and affects the highly conserved Cys(4) motif of DDP1. Previous studies have shown, that this amino acid exchange abolishes the interaction between DDP1 and TIMM13 in the IMS (32).

Using a red fluorescent bait fusion protein comprising LacI-NLS-TIMM13 and GFP-tagged wildtype (GFP-DDP1) or mutant DDP1 (GFP-DDP1^{C66W}) prey proteins we analyzed this specific mitochondrial protein interaction with the F2H assay. We found that GFP-DDP1 co-localizes with TIMM13 at the *lac* operator array (**Fig. 5b**), while GFP-DDP1^{C66W} was evenly distributed (**Fig. 5c**). These results demonstrate that the F2H assay is also suitable for the analysis of protein-protein interactions occurring outside the nucleus and the characterization of disease related point mutations disrupting these interactions.

Discussion

Here we describe a new method to detect and visualize protein-protein interactions in living cells, which we termed fluorescent two-hybrid assay (F2H). This method is based on the immobilization of a fluorescently labeled bait protein at a distinct subcellular structure enabling the detection of protein-protein interactions as co-localization of a differently labeled prey protein at this defined structure. The F2H assay described takes advantage of cell lines with a stable integration of a *lac* operator array to immobilize a lac repressor fused to fluorescently labeled proteins of interest (bait). Readily usable cell lines have already been described for human, mouse, hamster and *Drosophila* (7, 17, 18, 33-35). To be independent of specific transgenic cell lines this assay could be modified by using various cellular structures like the lamina, the cytoskeleton or centrosomes as anchoring structures to locally immobilize bait proteins.

Like other genetic two-hybrid methods also the F2H assay may yield false positive or false negative results, which need to be controlled for. Prey proteins that bind to the *lac* operator array in the absence of a bait protein can be identified by an initial screen and then be only used as baits. We analyzed more than 20 protein-protein interactions from different subcellular compartments with the F2H assay and obtained identical results as previously described with other genetic or biochemical methods. Only one protein (SUMO3) was found to bind by itself to the *lac* operator array and could therefore only be used as a bait protein. These results show that the F2H assay is a reliable and broadly applicable method to study protein-protein interactions.

In some cases, proteins may accumulate at subnuclear foci and thus complicate the F2H analysis. To bypass this problem, the *lac* operator array could be visualized and identified with a third fluorescent fusion protein like CFP-LacI.

In summary, this new F2H assay allows the direct visualization of protein-protein interactions and should be ideally suited to investigate cell cycle or differentiation dependent changes in real-time in living cells. A significant advantage of the F2H assay over other cell-based techniques is its simplicity that does neither require costly instrumentation nor advanced technical expertise. The simple optical read-out of the F2H assay additionally offers the possibility to use this assay in automated high-throughput screens to systematically analyze the protein interactome in living cells.

Acknowledgements

We thank D.L. Spector for providing BHK clone#2 and U2OS.2-6-3 cells containing a *lac* operator array, V. Schreiber for GFP-tagged PARP-1 and PARP-2 constructs and R.Y. Tsien for mRFP1 and mCherry cDNA. We thank L. Schermelleh and F. Spada for helpful comments and suggestions. We are grateful to G. Li for help in plasmid construction. This work was supported by the Center for NanoScience (CeNS), by the Nanosystems Initiative Munich (NIM) and by grants from the Deutsche Forschungsgemeinschaft (DFG) to M.C.C and H.L.

References

1. Fields, S., and Song, O. (1989) A novel genetic system to detect protein-protein interactions. *Nature* 340, 245-246.

2. Rual, J. F., Venkatesan, K., Hao, T., Hirozane-Kishikawa, T., Dricot, A., Li, N., Berriz, G. F., Gibbons, F. D., Dreze, M., Ayivi-Guedehoussou, N., Klitgord, N., Simon, C., Boxem, M., Milstein, S., Rosenberg, J., Goldberg, D. S., Zhang, L. V., Wong, S. L., Franklin, G., Li, S., Albala, J. S., Lim, J., Fraughton, C., Llamosas, E., Cevik, S., Bex, C., Lamesch, P., Sikorski, R. S., Vandenhaute, J., Zoghbi, H. Y., Smolyar, A., Bosak, S., Sequerra, R., Doucette-Stamm, L., Cusick, M. E., Hill, D. E., Roth, F. P., and Vidal, M. (2005) Towards a proteome-scale map of the human protein-protein interaction network. *Nature* 437, 1173-1178.

3. Parrish, J. R., Gulyas, K. D., and Finley, R. L., Jr. (2006) Yeast two-hybrid contributions to interactome mapping. *Curr Opin Biotechnol* 17, 387-393.

4. Sekar, R. B., and Periasamy, A. (2003) Fluorescence resonance energy transfer (FRET) microscopy imaging of live cell protein localizations. *J Cell Biol* 160, 629-633.

5. Miyawaki, A. (2003) Visualization of the spatial and temporal dynamics of intracellular signaling. *Dev Cell* 4, 295-305.

6. Kerppola, T. K. (2006) Visualization of molecular interactions by fluorescence complementation. *Nat Rev Mol Cell Biol* 7, 449-456.

7. Robinett, C. C., Straight, A., Li, G., Willhelm, C., Sudlow, G., Murray, A., and Belmont, A. S. (1996) In vivo localization of DNA sequences and visualization of large-scale chromatin organization using lac operator/repressor recognition. *J Cell Biol* 135, 1685-1700.

8. Easwaran, H. P., Schermelleh, L., Leonhardt, H., and Cardoso, M. C. (2004) Replication-independent chromatin loading of Dnmt1 during G2 and M phases. *EMBO Rep* 5, 1181-1186.

9. Sporbert, A., Domaing, P., Leonhardt, H., and Cardoso, M. C. (2005) PCNA acts as a stationary loading platform for transiently interacting Okazaki fragment maturation proteins. *Nucleic Acids Res* 33, 3521-3528.

10. Mortusewicz, O., Schermelleh, L., Walter, J., Cardoso, M. C., and Leonhardt, H. (2005) Recruitment of DNA methyltransferase I to DNA repair sites. *Proc Natl Acad Sci U S A*.

11. Schermelleh, L., Spada, F., Easwaran, H. P., Zolghadr, K., Margot, J. B., Cardoso, M. C., and Leonhardt, H. (2005) Trapped in action: direct visualization of DNA methyltransferase activity in living cells. *Nat Methods* 2, 751-756.

12. Cazzalini, O., Perucca, P., Riva, F., Stivala, L. A., Bianchi, L., Vannini, V., Ducommun, B., and Prosperi, E. (2003) p21CDKN1A does not interfere with loading of PCNA at DNA replication sites, but inhibits subsequent binding of DNA polymerase delta at the G1/S phase transition. *Cell Cycle* 2, 596-603.

13. Maeda, Y., Hunter, T. C., Loudy, D. E., Dave, V., Schreiber, V., and Whitsett, J. A. (2006) PARP-2 interacts with TTF-1 and regulates expression of surfactant protein-B. *J Biol Chem* 281, 9600-9606.

14. Meder, V. S., Boeglin, M., de Murcia, G., and Schreiber, V. (2005) PARP-1 and PARP-2 interact with nucleophosmin/B23 and accumulate in transcriptionally active nucleoli. *J Cell Sci* 118, 211-222.

15. Mortusewicz, O., Rothbauer, U., Cardoso, M. C., and Leonhardt, H. (2006) Differential recruitment of DNA Ligase I and III to DNA repair sites. *Nucleic Acids Res* 34, 3523-3532.

16. Rothbauer, U., Zolghadr, K., Muyldermans, S., Schepers, A., Cardoso, M. C., and Leonhardt, H. (2007) A versatile nanotrap for biochemical and functional studies with fluorescent fusion proteins. *Mol Cell Proteomics*.

17. Tsukamoto, T., Hashiguchi, N., Janicki, S. M., Tumbar, T., Belmont, A. S., and Spector, D. L. (2000) Visualization of gene activity in living cells. *Nat Cell Biol* 2, 871-878.

18. Janicki, S. M., Tsukamoto, T., Salghetti, S. E., Tansey, W. P., Sachidanandam, R., Prasanth, K. V., Ried, T., Shav-Tal, Y., Bertrand, E., Singer, R. H., and Spector, D. L. (2004) From silencing to gene expression: real-time analysis in single cells. *Cell* 116, 683-698.

19. Phair, R. D., and Misteli, T. (2000) High mobility of proteins in the mammalian cell nucleus. *Nature* 404, 604-609.

20. Caldecott, K. W., McKeown, C. K., Tucker, J. D., Ljungquist, S., and Thompson, L. H. (1994) An interaction between the mammalian DNA repair protein XRCC1 and DNA ligase III. *Mol Cell Biol* 14, 68-76.

21. Wei, Y. F., Robins, P., Carter, K., Caldecott, K., Pappin, D. J., Yu, G. L., Wang, R. P., Shell, B. K., Nash, R. A., Schar, P., and et al. (1995) Molecular cloning and expression of human cDNAs encoding a novel DNA ligase IV and DNA ligase III, an enzyme active in DNA repair and recombination. *Mol Cell Biol* 15, 3206-3216.

22. Fan, J., Otterlei, M., Wong, H. K., Tomkinson, A. E., and Wilson, D. M., 3rd (2004) XRCC1 co-localizes and physically interacts with PCNA. *Nucleic Acids Res* 32, 2193-2201.

23. Schreiber, V., Ame, J. C., Dolle, P., Schultz, I., Rinaldi, B., Fraulob, V., Menissier-de Murcia, J., and de Murcia, G. (2002) Poly(ADP-ribose) polymerase-2 (PARP-2) is required for efficient base excision DNA repair in association with PARP-1 and XRCC1. *J Biol Chem* 277, 23028-23036.

24. Masson, M., Niedergang, C., Schreiber, V., Muller, S., Menissier-de Murcia, J., and de Murcia, G. (1998) XRCC1 is specifically associated with poly(ADP-ribose) polymerase and negatively regulates its activity following DNA damage. *Mol Cell Biol* 18, 3563-3571.

25. Chuang, L. S., Ian, H. I., Koh, T. W., Ng, H. H., Xu, G., and Li, B. F. (1997) Human DNA-(cytosine-5) methyltransferase-PCNA complex as a target for p21WAF1. *Science* 277, 1996-2000.

26. Easwaran, H. P., Leonhardt, H., and Cardoso, M. C. (2005) Cell Cycle Markers for Live Cell Analyses. *Cell Cycle* 4.

27. Cardoso, M. C., Joseph, C., Rahn, H. P., Reusch, R., Nadal-Ginard, B., and Leonhardt, H. (1997) Mapping and use of a sequence that targets DNA ligase I to sites of DNA replication in vivo. *J Cell Biol* 139, 579-587.

28. Montecucco, A., Savini, E., Weighardt, F., Rossi, R., Ciarrocchi, G., Villa, A., and Biamonti, G. (1995) The N-terminal domain of human DNA ligase I contains the nuclear localization signal and directs the enzyme to sites of DNA replication. *Embo J* 14, 5379-5386.

29. Goehler, H., Lalowski, M., Stelzl, U., Waelter, S., Stroedicke, M., Worm, U., Droege, A., Lindenberg, K. S., Knoblich, M., Haenig, C., Herbst, M., Suopanki, J., Scherzinger, E., Abraham, C., Bauer, B., Hasenbank, R., Fritzsche, A., Ludewig, A. H., Bussow, K., Coleman, S. H., Gutekunst, C. A., Landwehrmeyer, B. G., Lehrach, H., and Wanker, E. E. (2004) A protein interaction network links GIT1, an enhancer of huntingtin aggregation, to Huntington's disease. *Mol Cell* 15, 853-865.

30. Rothbauer, U., Hofmann, S., Muhlenbein, N., Paschen, S. A., Gerbitz, K. D., Neupert, W., Brunner, M., and Bauer, M. F. (2001) Role of the deafness dystonia peptide 1 (DDP1) in import of human Tim23 into the inner membrane of mitochondria. *J Biol Chem* 276, 37327-37334.

31. Tranebjaerg, L., Schwartz, C., Eriksen, H., Andreasson, S., Ponjavic, V., Dahl, A., Stevenson, R. E., May, M., Arena, F., Barker, D., and et al. (1995) A new X linked recessive deafness syndrome with blindness, dystonia, fractures, and mental deficiency is linked to Xq22. *J Med Genet* 32, 257-263.

32. Hofmann, S., Rothbauer, U., Muhlenbein, N., Neupert, W., Gerbitz, K. D., Brunner, M., and Bauer, M. F. (2002) The C66W mutation in the deafness dystonia peptide 1 (DDP1) affects the formation of functional DDP1.TIM13 complexes in the mitochondrial intermembrane space. *J Biol Chem* 277, 23287-23293.

33. Tumbar, T., Sudlow, G., and Belmont, A. S. (1999) Large-scale chromatin unfolding and remodeling induced by VP16 acidic activation domain. *J Cell Biol* 145, 1341-1354.

34. Dietzel, S., Zolghadr, K., Hepperger, C., and Belmont, A. S. (2004) Differential large-scale chromatin compaction and intranuclear positioning of transcribed versus non-transcribed transgene arrays containing {beta}-globin regulatory sequences. *J Cell Sci* 117, 4603-4614.

35. Vazquez, J., Belmont, A. S., and Sedat, J. W. (2001) Multiple regimes of constrained chromosome motion are regulated in the interphase Drosophila nucleus. *Curr Biol* 11, 1227-1239.

Figure Legends

Figure 1

Schematic outline of the fluorescent two-hybrid (F2H) assay. (a) Outline of pF2H-prey and pF2H-bait expression vectors coding for fluorescently labeled prey- and bait- proteins used for the F2H assay (b) The LacI domain of the bait-protein mediates binding to the chromosomally integrated *lac* operator array, which is visible as a fluorescent spot in nuclei of transfected cells. If the differentially labeled prey interacts with the bait it becomes enriched at the same spot resulting in co-localization of fluorescent signals at the *lac* operator (visible as yellow spot in the overlay image). (c) If the prey does not interact with the bait protein it remains dispersed in the nucleus and the *lac* operator array is only visualized by the bait protein (red spot). FP1 and FP2 refer to two distinguishable fluorescent proteins, e.g. GFP or YFP and mCherry or mRFP.

Figure 2

Specific interaction of DNA Ligase III with XRCC1 revealed by the F2H assay. (a) Transgenic BHK cells containing a chromosomal *lac* operator array were co-transfected with XRCC1-LacI-RFP and GFP-tagged DNA Ligase III or DNA Ligase I constructs. The lac repressor part of the XRCC1-LacI-RFP fusion protein mediates binding to the *lac* operator array (visible by fluorescence microscopy as red spot). DNA Ligase III is recruited to the *lac* operator array through interaction with XRCC1. Note that the highly homologous DNA Ligase I does not accumulate at the *lac* operator array indicating that it does not interact with XRCC1. Scale bars 5 µm. (b) Comparison of F2H results and co-immunoprecipitation (Co-IP) experiments. Co-IPs were performed with HEK 293T cells co-expressing RFP-XRCC1 and GFP-Ligase III or GFP-Ligase I, respectively. For interaction mapping the GFP-tagged BRCT domain of DNA Ligase III and a deletion construct lacking the BRCT domain were used. Immunoprecipitations were performed with a GFP-nanotrap (16) (as shown before (15)). Precipitated fusion proteins were then detected with specific antibodies against RFP and GFP on western blots. RFP-XRCC1 was co-precipitated with GFP-Ligase III but not with GFP-Ligase I. RFP-XRCC1 was also co-precipitated with GFP-Ligase III BRCT but not with GFP-N-Ligase III ΔBRCT. For comparison of F2H results the input (left) and bound (right) bands from Co-IPs were aligned with corresponding signals from the F2H assay. The LacI spot of the XRCC1-LacI-RFP bait construct shown in red and the bound fraction was aligned with the respective signal of the GFP-tagged prey constructs. Whole cell images of the respective F2H experiments are shown in (a) and **supplementary Fig. 1**.

Figure 3

F2H analysis of cell cycle independent interaction of Dnmt1 with PCNA. (a) Schematic outline of full-length mouse Dnmt1 and fusion proteins. PBD, PCNA binding domain; NLS, nuclear localization signal; TS, targeting sequence; ZnF, Zn^{2+}-binding region; BAH 1 and 2, two Bromo Adjacent Homology domains. (b) Outline of binding possibilities of fusion proteins at the *lac* operator (*lac* op) array and at the replication fork. (c) Transgenic BHK cells containing a chromosomal *lac* operator array were co-transfected with PBD-LacI-YFP and RFP-PCNA constructs. RFP-PCNA shows the characteristic cell cycle dependent distribution (dispersed in non S phase cells (top row) and focal patterns in S phase (bottom row)). The lac repressor part of the PBD-LacI-YFP fusion protein mediates binding to the *lac* operator array (visible as green spot and highlighted by arrowheads) and the PBD mediates binding to PCNA at replication sites (focal pattern in S phase). Notice, RFP-PCNA is localized at the *lac* operator array in S and non S phase cells indicating an interaction of the PBD of Dnmt1 with PCNA throughout the cell cycle and independent of the replication machinery. (d) BHK cells were transfected with expression vectors for ΔPBD-LacI-YFP and RFP-PCNA. As above, RFP-PCNA shows a dispersed distribution in non S phase (top row) and redistributes to replication sites in S phase (bottom row). The ΔPBD-LacI-YFP fusion protein binds to the *lac* operator array (green spot marked by arrowhead) but does not bind to replication sites in S phase since it lacks the PBD. Importantly, in these cells RFP-PCNA (prey) is not localized at the *lac* operator array (marked by arrowheads) indicating that binding depends on the presence of the PBD, which is absent in ΔPBD-LacI-YFP (bait). Scale bars 5 µm

Figure 4

Analysis of Huntington´s disease related interactions by F2H. Reported interactions between (a) SUMO3 and HZFH and (b) HZFH and Vimentin revealed by the F2H assay. (c) F2H analysis shows no interaction between SUMO3 and Vimentin as previously described (29). In (b) the nucleus is outlined by a dashed line and in (c) the *lac* operator array is indicated (arrowheads). Scale bars 5 µm.

Figure 5

Analysis of mitochondrial protein-protein interactions and the effect of a mutation associated with the Mohr-Tranebjaerg Syndrome. (a) Schematic overview of the hexameric DDP1-TIMM13 complex in the intermembrane space (IMS) of mitochondria. (b + c) BHK cells expressing the bait-protein mCherry-LacI-TIMM13 together either with GFP-DDP1 (b) or the loss-of-function mutant GFP-DDP1^{C66W} (c). While the functional wt fusion GFP-DDP1 shows interaction with TIMM13 revealed by co-localization of fluorescent signals at the *lac* operator array (b), the GFP-DDP1^{C66W} mutant is dispersedly distributed throughout the nucleus indicating no interaction (c). Scale bars 5 µm.

Figures

Figure 1

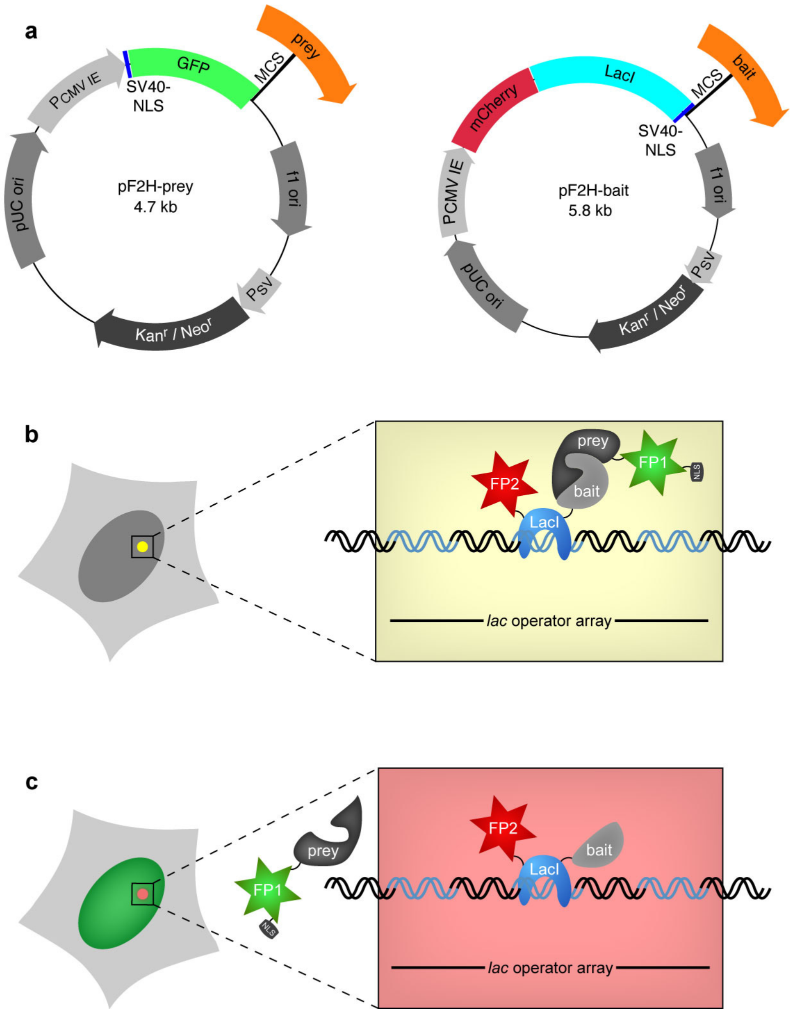
a
PCMV IE
SV40-NLS
GFP
MCS
prey
pF2H-prey
4.7 kb
f1 ori
PSV
Kanr / Neor
pUC ori
mCherry
LacI
MCS
bait
SV40-NLS
pF2H-bait
5.8 kb
PCMV IE
f1 ori
PSV
Kanr / Neor
pUC ori
b
prey
FP1
NLS
FP2
bait
LacI
lac operator array
c
FP2
bait
LacI
prey
FP1
NLS
lac operator array

Figure 2

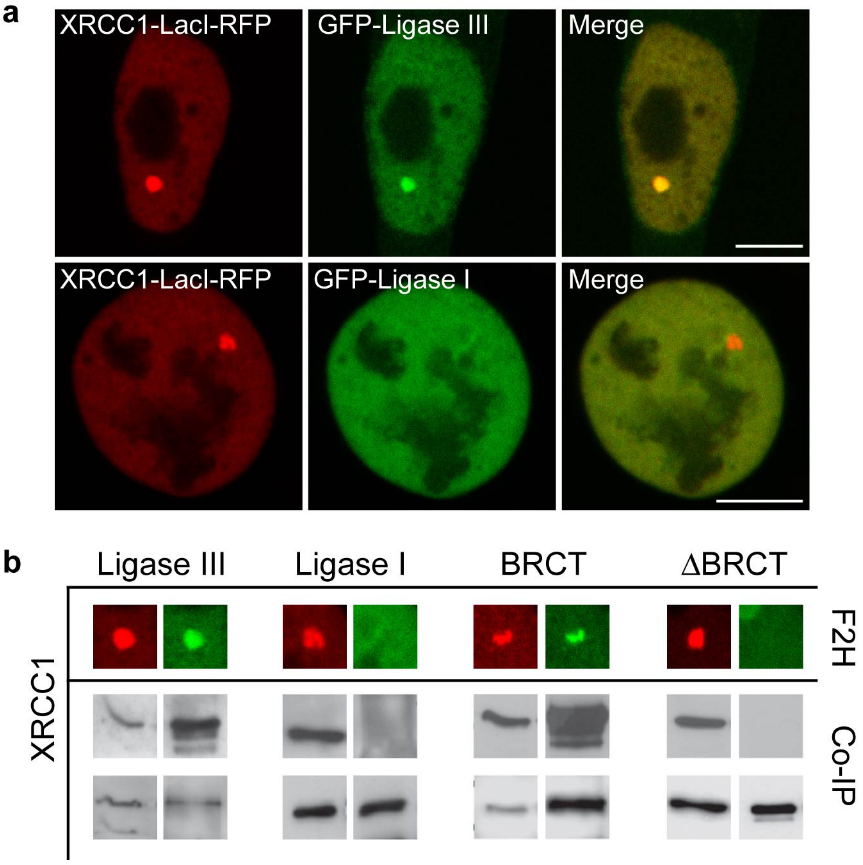
a
XRCC1-LacI-RFP
GFP-Ligase III
Merge
XRCC1-LacI-RFP
GFP-Ligase I
Merge
b
Ligase III
Ligase I
BRCT
ΔBRCT
XRCC1
F2H
Co-IP

Figure 3

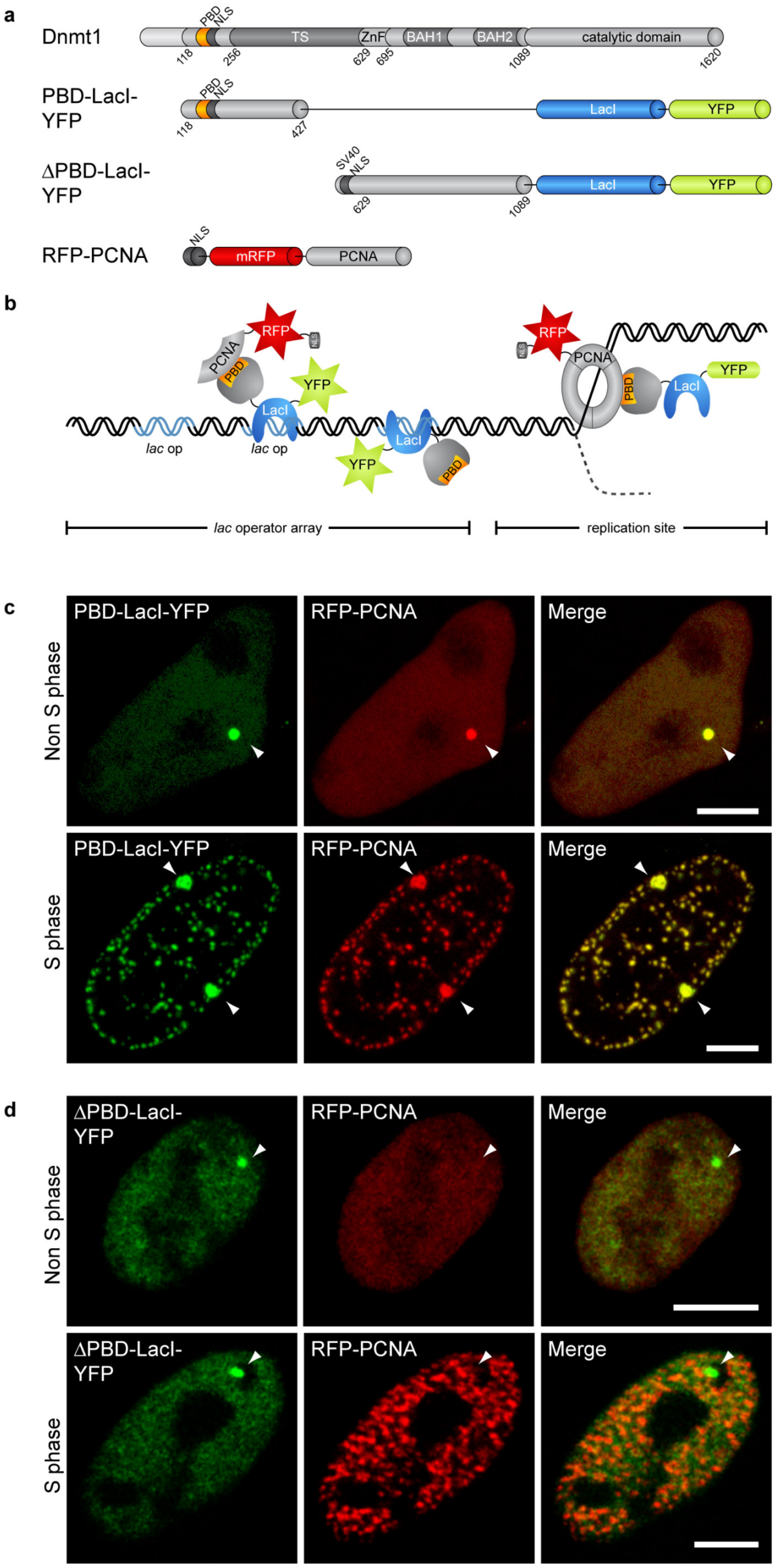
a
Dnmt1
PBD
NLS
TS
ZnF
BAH1
BAH2
catalytic domain
118
256
629
695
1089
1620
PBD-LacI-YFP
427
LacI
YFP
ΔPBD-LacI-YFP
SV40 NLS
RFP-PCNA
mRFP
PCNA
b
RFP
PCNA
PBD
YFP
LacI
lac op
lac op
lac operator array
replication site
c
Non S phase
S phase
PBD-LacI-YFP
RFP-PCNA
Merge
d
ΔPBD-LacI-YFP
RFP-PCNA
Merge

Figure 4

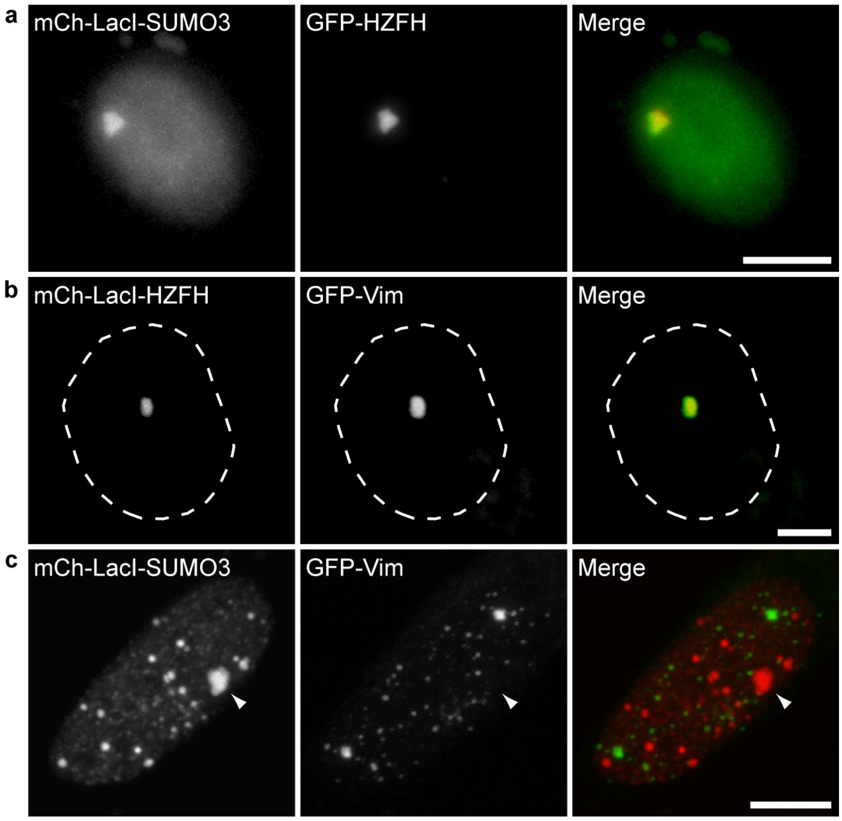
a
mCh-LacI-SUMO3
GFP-HZFH
Merge
b
mCh-LacI-HZFH
GFP-Vim
Merge
c
mCh-LacI-SUMO3
GFP-Vim
Merge

Figure 5

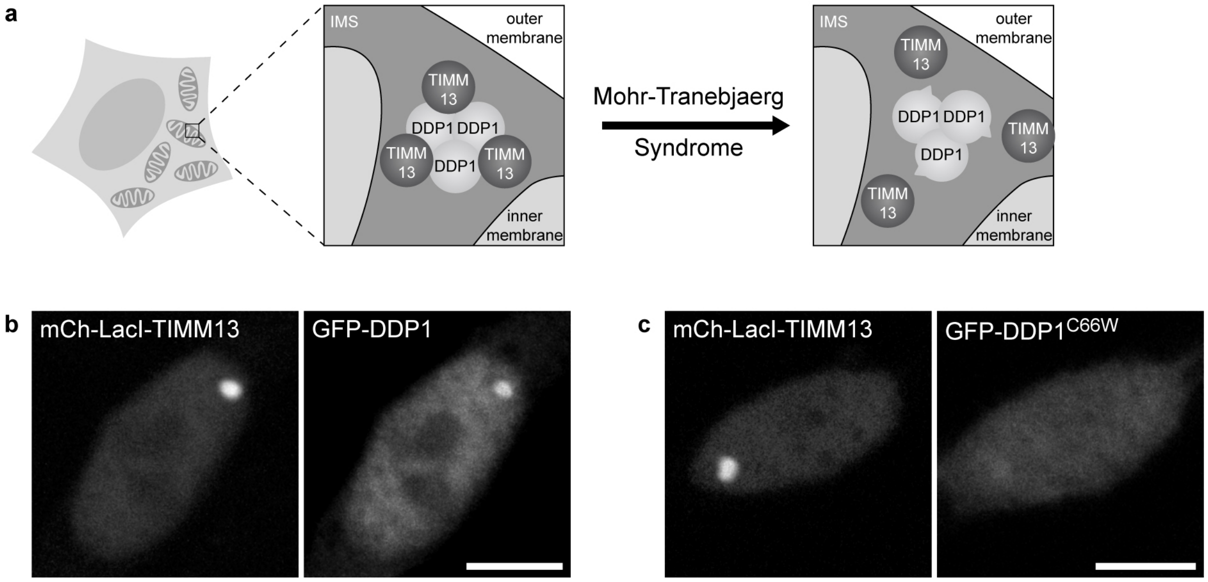
a
IMS
outer membrane
TIMM 13
DDP1 DDP1
TIMM 13
DDP1
TIMM 13
inner membrane
Mohr-Tranebjaerg
Syndrome
IMS
outer membrane
TIMM 13
DDP1 DDP1
TIMM 13
DDP1
TIMM 13
inner membrane
b
mCh-LacI-TIMM13
GFP-DDP1
c
mCh-LacI-TIMM13
GFP-DDP1^{C66W}

Supplementary Information

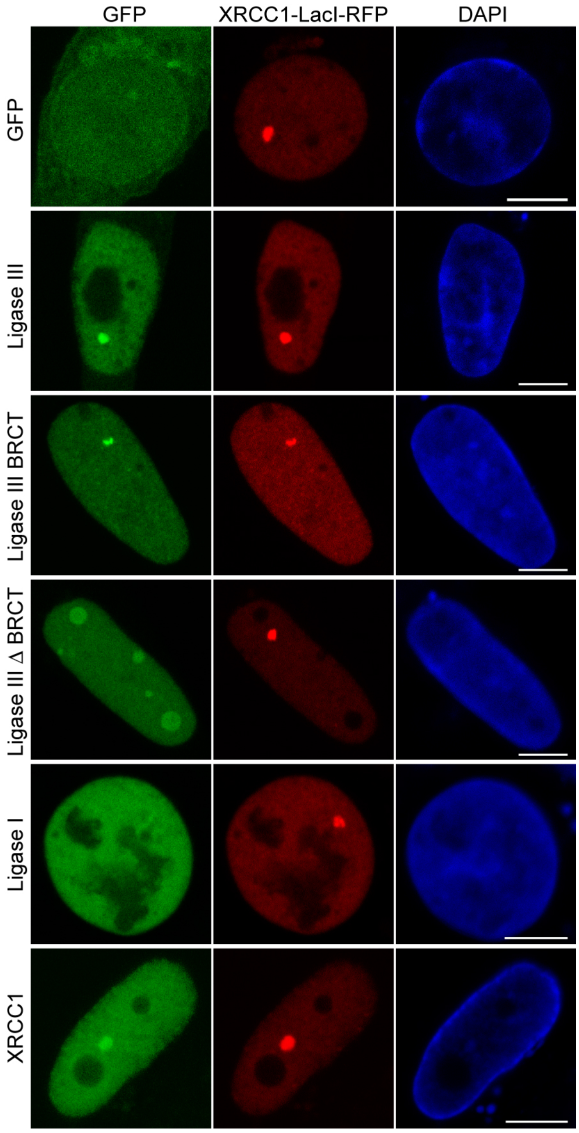
GFP
XRCC1-LacI-RFP
DAPI
GFP
Ligase III
Ligase III BRCT
Ligase III Δ BRCT
Ligase I
XRCC1

Supplementary Figure 1

BRCT mediated interaction of DNA Ligase III with XRCC1 revealed by the F2H assay. Transgenic BHK cells containing a *lac* operator array were co-transfected with XRCC1-LacI-RFP and various GFP-tagged DNA Ligase III constructs. The lac repressor part of the XRCC1-LacI-RFP fusion protein mediates binding to the *lac* operator array (visible as red spot). The BRCT domain is necessary and sufficient for targeting of DNA Ligase III to the *lac* operator array through interaction with XRCC1. Note that the highly homologous DNA Ligase I does not accumulate at the *lac* operator array indicating that it does not interact with XRCC1. Scale bars 5 µm.

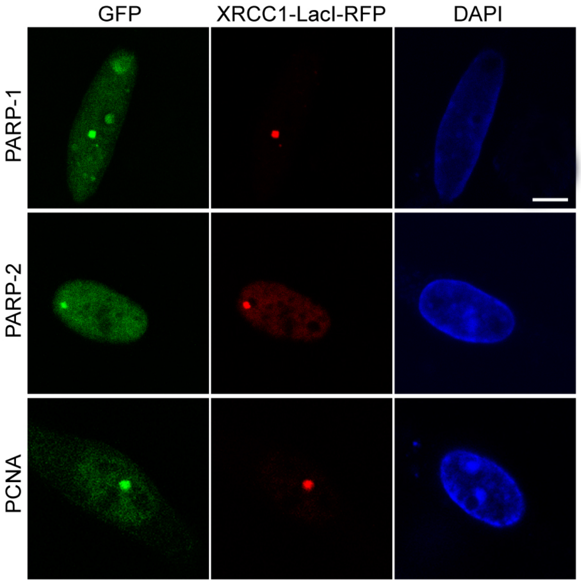

Supplementary Figure 2

The F2H assay reveals the interaction of XRCC1 with PCNA, PARP-1 and PARP-2. BHK cells containing a *lac* operator array were transfected with expression vectors for XRCC1-LacI-RFP and either GFP-PARP-1, GFP-PARP-2 or GFP-PCNA. The lac repressor part of the XRCC1-LacI-RFP fusion protein mediates binding to the *lac* operator array (visible as red spot). GFP-PARP-1, GFP-PARP-2 and GFP-PCNA are targeted to the *lac* operator array indicating an interaction with XRCC1. Scale bar 5 µm.

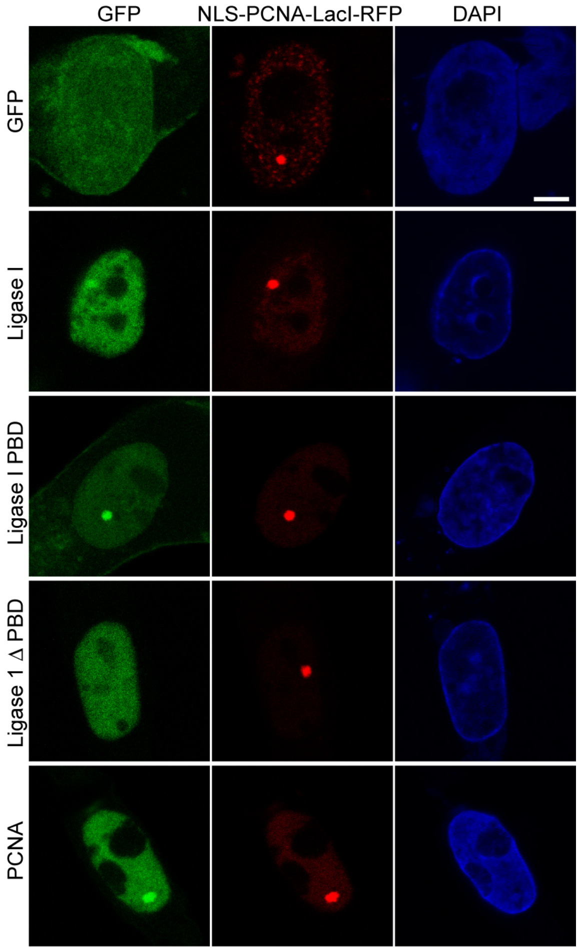
GFP
NLS-PCNA-LacI-RFP
DAPI
GFP
Ligase I
Ligase I PBD
Ligase 1 △ PBD
PCNA

Supplementary Figure 3

The F2H assay reveals the PBD-mediated interaction of DNA Ligase I with PCNA. Transgenic U2OS cells containing a *lac* operator array were co-transfected with NLS-PCNA-LacI-RFP and various GFP-tagged DNA Ligase I constructs. The lac repressor part of the NLS-PCNA-LacI-RFP fusion protein mediates binding to the *lac* operator array (visible as red spot). The PBD is necessary and sufficient for targeting of DNA Ligase I to the *lac* operator array through interaction with PCNA.

Scale bar 5 µm.

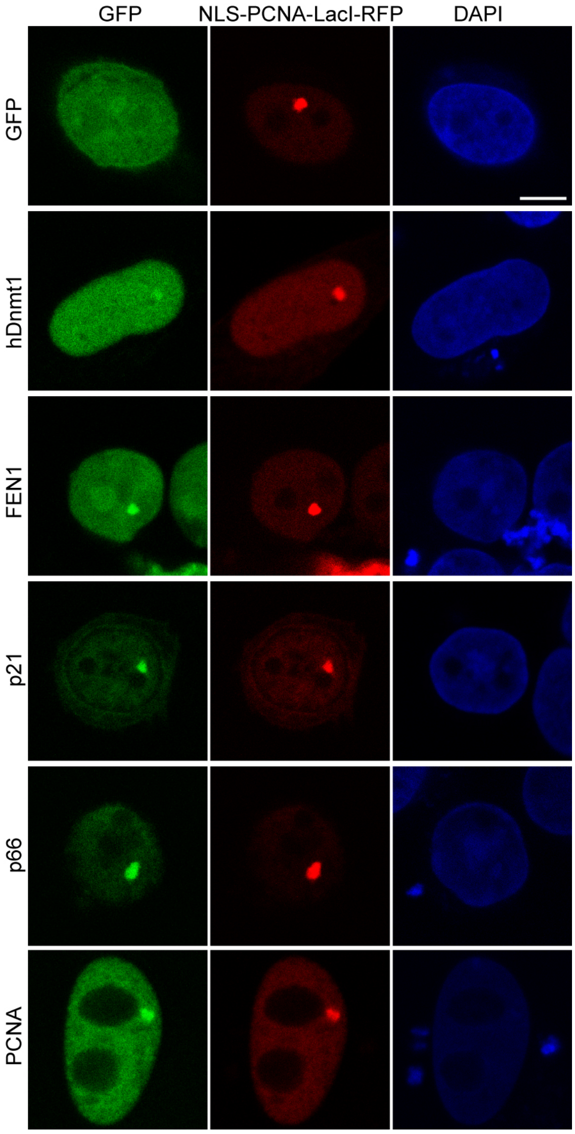
GFP
NLS-PCNA-LacI-RFP
DAPI
GFP
hDnmt1
FEN1
p21
p66
PCNA

Supplementary Figure 4

Interaction of various replication and repair proteins with PCNA revealed by the F2H assay. Transgenic BHK cells containing a *lac* operator array expressing NLS-PCNA-LacI-RFP and various GFP-tagged replication and repair proteins. All proteins tested interact with PCNA. Scale bar 5 µm.

II.2. TARGETING AND TRACING ANTIGENS IN LIVE CELLS WITH FLUORESCENT NANOBODIES

© 2006 Nature Publishing Group http://www.nature.com/naturemethods

Targeting and tracing antigens in live cells with fluorescent nanobodies

Ulrich Rothbauer[1,5], Kourosh Zolghadr[1,5], Sergei Tillib[2], Danny Nowak[3], Lothar Schermelleh[1], Anja Gahl[3], Natalija Backmann[4], Katja Conrath[4], Serge Muyldermans[4], M Cristina Cardoso[3] & Heinrich Leonhardt[1]

We fused the epitope-recognizing fragment of heavy-chain antibodies from *Camelidae* sp. with fluorescent proteins to generate fluorescent, antigen-binding nanobodies (chromobodies) that can be expressed in living cells. We demonstrate that chromobodies can recognize and trace antigens in different subcellular compartments throughout S phase and mitosis. Chromobodies should enable new functional studies, as potentially any antigenic structure can be targeted and traced in living cells in this fashion.

Antibodies are valuable tools for visualizing cellular components in fixed cells, but their use in living cells is limited owing to the inefficient folding and assembly of their variable heavy and light chains. So far, intracellular applications have mostly relied on direct microinjection of antibodies, which is technically demanding and stressful for cells. Fluorescent fusion proteins can easily be expressed in cells and whole organisms and provide information on protein localization and dynamics in living cells[1,2], but endogenous proteins, their post-translational modifications and nonprotein cell components remain invisible and cannot be studied. To overcome these limitations, we fused the antigen-binding fragment of a heavy-chain antibody with fluorescent proteins. Heavy-chain antibodies[3] from *Camelidae* sp. are devoid of light chains and recognize antigens via their variable domain (referred to as V_HH or nanobody; **Fig. 1a** and **Supplementary Fig. 1** online), which represents the smallest intact antigen-binding fragment[4]. On the basis of their chimeric nature, we termed these fluorescent antigen-binding nanobody fusions 'chromobodies'.

We chose green fluorescent protein (GFP) as a first target molecule to test the feasibility of this approach. GFP has previously been fused to a variety of proteins with well-characterized subcellular localization, providing 'visible' antigens to directly test chromobodies in different subcellular compartments. We isolated lymphocytes from an alpaca (*Lama pacos*) immunized with purified GFP. We amplified the coding sequence of the V_HH by PCR, cloned it into a phage display vector and identified a highly specific GFP-binding antibody fragment, α-GFP V_HH, after panning (**Supplementary Methods** online). Surface plasmon resonance measurements indicated a fast kinetic association rate of $7.68 \times 10^5\ M^{-1}s^{-1}$ and a slow dissociation rate of $1.74 \times 10^{-4}\ s^{-1}$ for the interaction of α-GFP V_HH with the GFP antigen. The low dissociation constant ($K_d = 0.23$ nM) calculated from these values was consistent with the interaction of an affinity-matured antibody recognizing its cognate antigen.

To test the distribution of α-GFP V_HH in living cells, we fused it to the monomeric red fluorescent protein (mRFP) to generate a 'visible' GFP-binding antibody termed the 'GFP-chromobody' (**Fig. 1a**). Gel filtration, immunoblotting and confocal microscopy showed that the GFP-chromobody was stable and dispersely distributed in mammalian cells and that there were no detectable signs of protein degradation (**Supplementary Fig. 2** online). We did not detect any aggregates such as have been described for intrabodies like scFvs[5].

We then investigated the ability of the GFP-chromobody to access and bind its epitope in different subcellular compartments and structures in living cells. As a typical epitope in the cytoplasm, we used GFP–β-actin (**Supplementary Fig. 3** online), which is incorporated into growing actin filaments and allows direct visualization of actin-containing structures[6]. We cotransfected HeLa cells with GFP–β-actin and GFP-chromobody expression vectors and analyzed them by live cell microscopy (**Supplementary Methods**). A representative confocal image of a double-transfected cell showed green and red fluorescence at the cytoskeleton (**Fig. 1b**), indicative of correct incorporation of GFP–β-actin into the actin filaments and efficient recognition by the GFP-chromobody. The efficient epitope binding of the α-GFP V_HH domain of the chromobody indicated that its intrinsic stability (ΔG = 30 kJ/mol)[7] was sufficient for proper folding and intracellular function.

We next chose three well-characterized GFP fusions to test antigen binding in different nuclear structures, by cotransfecting HeLa cells with GFP fusion proteins and the GFP-chromobody. We used a GFP–lamin B1 fusion that assembles into nuclear lamina of mammalian cells[8] (data not shown), a GFP fusion of proliferating cell nuclear antigen (PCNA) as an example of a nucleoplasmic epitope[9] (**Fig. 1c**), and an epitope embedded in chromatin using a HeLa cell line stably expressing a histone H2B-GFP fusion that assembles into nucleosomes[10] (**Fig. 1d**). In all experiments, the GFP-chromobody colocalized with the GFP fusion proteins. Moreover, the images of the untransfected cells clearly showed that no

---

[1]Ludwig Maximilians University Munich, Department of Biology II, Grosshaderner Str. 2, 82152 Planegg-Martinsried, Germany. [2]Institute of Gene Biology of the Russian Academy of Sciences, Vavilov Str. 34/5, 119334 Moscow, Russia. [3]Max Delbrueck Center for Molecular Medicine, Robert-Roessle Str. 10, 13125 Berlin, Germany. [4]Vrije Universiteit Brussel, Laboratory of Cellular and Molecular Immunology, Pleinlaan 2, 1050 Brussels, Belgium. [5]These authors contributed equally to this work. Correspondence should be addressed to H.L. (h.leonhardt@lmu.de).

RECEIVED 12 JUNE; ACCEPTED 6 SEPTEMBER; PUBLISHED ONLINE 23 OCTOBER 2006; DOI:10.1038/NMETH953

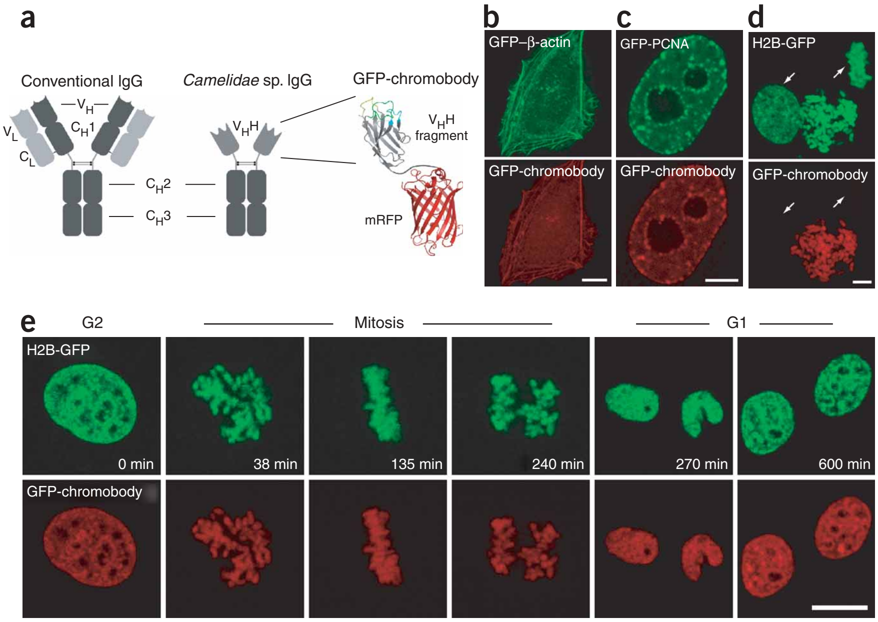

Figure 1 | Generation and characterization of a GFP-binding chromobody. (**a**) Schematic outline of a conventional IgG antibody in comparison with a *Camelidae*-derived heavy-chain IgG antibody and a generic chromobody. The putative structure of the chromobody, based on the known crystal structures of a V_HH and mRFP, is shown at right, with the three antigen-binding loops in yellow, cyan and green. (**b**–**d**) Targeting of the GFP-chromobody to GFP fusion proteins localizing in different cellular compartments and structures in HeLa cells. (**b**) GFP-chromobodies colocalize with GFP–β-actin on cytoskeletal actin filaments. (**c**) GFP-chromobodies bind to GFP-PCNA at replication foci; a cell in mid S phase is shown. (**d**) GFP-chromobodies bind to the histone H2B-GFP incorporated into chromatin. The cell transfected with the GFP-chromobody was in prometaphase and condensed chromosomes are visible. Untransfected cells in metaphase and interphase (marked by arrows) that did not express the chromobody indicate that no unspecific bleed-through of green fluorescence occured under these experimental conditions. Confocal mid-sections (**b**–**c**) and *z*-projection (**d**) of living cells are shown. Scale bars, 5 μm. (**e**) Tracing of a chromatin protein throughout mitosis. Time-lapse imaging of a HeLa cell stably expressing histone H2B-GFP transfected with GFP-chromobody. Selected frames from this time series are shown. At the time imaging was started (0 h), this cell was in late G2 phase. Scale bars, 10 μm. (See also **Supplementary Video 1**.)

fluorescence bleed-through occured under these experimental conditions (**Fig. 1d**; see arrows). These results demonstrated that the GFP-chromobody efficiently recognizes and binds its epitope in different structures and subcellular compartments.

We then tested the ability of the GFP-chromobody to trace its antigen throughout the cell cycle, again using H2B-GFP and GFP-PCNA. Time-lapse microscopy of transfected HeLa cells showed that colocalization of the GFP-chromobody with H2B-GFP persisted through various chromatin condensation states during mitosis (**Fig. 1e** and **Supplementary Video 1** online). GFP-PCNA constitutes a special challenge to live cell microscopy because it is an essential component of the replication machinery that concentrates at replication foci in S phase and shows a diffuse pattern in G1 and G2 (ref. 9). We followed the subcellular distribution of GFP-PCNA and GFP-chromobody from early S until G2 phase by taking confocal three-dimensional image stacks every 20 min (**Supplementary Fig. 4** and **Supplementary Video 2** online). Both GFP-PCNA and the chromobody showed typical punctate patterns followed by a disperse distribution, indicating progression through S phase and transition to G2 phase. These time-lapse analyses show that chromobodies can trace integral chromatin components such as H2B as well as essential components of the replication machinery without major impact on cell cycle progression and viability.

To test whether chromobodies can also recognize and trace endogenous epitopes, we generated chromobodies against cytoplasmic and nuclear antigens. We selected V_HHs that specifically bind to cytokeratin-8 and lamin Dm0, fused them to mRFP and tested the subcellular distribution of the resulting chromobodies in a variety of higher eukaryotic cells. The cytokeratin-8-chromobody highlighted cytoplasmic filaments, indicative of binding to the endogenous cytokeratin structures (**Fig. 2a**). In contrast, the lamin-chromobody was localized at the nuclear rim in *Drosophila melanogaster* S2 and HeLa cells (**Fig. 2b**), indicating efficient recognition of endogenous lamina lining the nucleus in cells derived from two organisms as different as insect and humans.

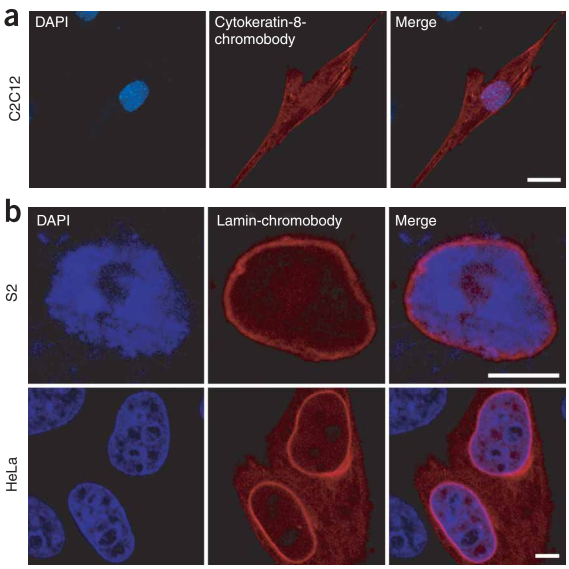

Figure 2 | Recognition of subcellular structures by chromobodies raised against endogenous epitopes. (**a**) Confocal microscopy images of mouse myoblast cells (C2C12) fixed and stained with 4′,6-diamino-2-phenylindole dihydrochloride (DAPI) 24 h after transfection with the cytokeratin-8-chromobody. The red fluorescence on cytoplasmic filaments indicates the recognition of cytokeratin fibers. Scale bar, 20 μm. (**b**) Confocal microscopy images of *D. melanogaster* S2 cells and human HeLa cells fixed and stained with DAPI 24 h and 48 h after transfection with the lamin-chromobody expression plasmid. The red fluorescence of the chromobody highlights a nuclear rim structure that is characteristic of the nuclear lamina. Scale bars, 5 μm.

© 2006 Nature Publishing Group http://www.nature.com/naturemethods

© 2006 Nature Publishing Group http://www.nature.com/naturemethods

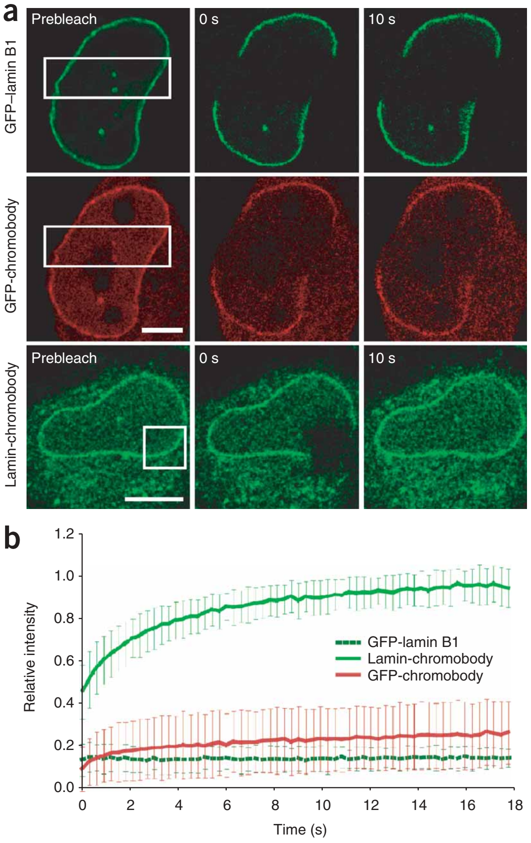

Figure 3 | *In vivo* binding properties of various chromobodies analyzed by FRAP. (**a**) FRAP of GFP–lamin B1 (top; green) and GFP-chromobody (middle; red) coexpressed in a HeLa cell. Photobleaching of a small region (box) resulted in no recovery of GFP–lamin B1 and only slow recovery of GFP-chromobody during the observation period. FRAP of lamin-chromobody (bottom; green) expressed in a different HeLa cell revealed a quick recovery of lamin chromobody within less than 20 s. Scale bars, 5 μm. (**b**) Quantitative evaluation of FRAP data showing mean curves, $n = 10$. Error bars, s.d.

Finally, we investigated the antigen-binding dynamics of chromobodies by measuring the fluorescence recovery after photobleaching (FRAP). We compared the binding of the lamin-chromobody and the GFP-chromobody with the recovery rate of the GFP–lamin B1 fusion, which is a stable component of the nuclear lamina with practically no turnover[11]. As expected, GFP–lamin B1 showed no detectable recovery after photobleaching and the GFP-chromobody showed very little recovery of fluorescence at the nuclear lamina, indicating high-affinity binding of its epitope (**Fig. 3a,b**). In contrast, the lamin-chromobody showed a quick recovery of fluorescence, with a halftime ($t_{1/2}$) of ∼1.9 s, indicating transient lamin binding with rapid turnover (**Fig. 3a,b**). These results demonstrate that chromobodies can be raised with different binding affinities and that even transient binding can be sufficient for visualization of cellular structures. Transient binding of chromobodies is likely to be less harmful to cells than permanent fusion with a fluorescent protein.

Chromobodies combine the wide target range of antibodies with the live cell capabilities of fluorescent protein fusions and thus potentially allow tracing of any cellular epitope, including endogenous proteins, their post-translational modifications and various conformational states as well as non-protein components in living cells. Recent work describing the detection of a specific protein conformation with scFvs[12] exemplifies new applications made possible with recombinant antibody technologies. As chromobodies can be selected against the entire antigen surface and their affinities adjusted by mutagenesis, it should be possible either to minimize functional interference for antigen tracing or to deliberately target catalytic or regulatory sites for functional studies. The small size and compact structure of the antigen-binding domain of the chromobodies supports their intracellular stability and should allow access to epitopes that are not reached by larger, conventional antibodies (**Supplementary Fig. 1**). This smaller size could, however, limit the maximally possible binding interface and strength of chromobodies.

The single V_HH domain required for chromobodies can be amplified in one step from bulk lymphocyte mRNA to generate libraries from naive or immunized animals for rapid selection of specific binders[13,14]. Thus in generating chromobodies one can take advantage of the affinity maturation occurring during the immunization process, which involves somatic mutations and *in vivo* selection of high-affinity binders. By comparison, Fab and scFv molecules require two matching fragments from heavy and light chains (**Supplementary Fig. 1**), which are usually obtained from monoclonal cell lines. The alpacas used in this study are the least demanding of all *Camelidae* and alpaca immunization is readily available in most countries. The availability of V_HH libraries, combined with continually improving maturation and selection techniques, will further facilitate the generation of new chromobodies. We anticipate that chromobodies and related tools will expand the possibilities of live cell microscopy and make entirely new functional studies possible, as potentially any antigenic cellular structure can be targeted and traced in living cells.

Note: Supplementary information is available on the Nature Methods website.

ACKNOWLEDGMENTS
We thank R.Y. Tsien, J. Ellenberg and K.F. Sullivan for providing expression vectors and cell lines, and J. Füner for the alpaca immunization. This work was supported by grants from the Deutsche Forschungsgemeinschaft to M.C.C. and H.L.

COMPETING INTERESTS STATEMENT
The authors declare that they have no competing financial interests.

Published online at http://www.nature.com/naturemethods/
Reprints and permissions information is available online at http://npg.nature.com/reprintsandpermissions/

1. Chalfie, M. *et al. Science* **263**, 802–805 (1994).
2. Tsien, R.Y. *Annu. Rev. Biochem.* **67**, 509–544 (1998).
3. Hamers-Casterman, C. *et al. Nature* **363**, 446–448 (1993).
4. Muyldermans, S. *J. Biotechnol.* **74**, 277–302 (2001).
5. Cardinale, A., Filesi, I., Mattei, S. & Biocca, S. *Methods* **34**, 171–178 (2004).
6. Westphal, M. *et al. Curr. Biol.* **7**, 176–183 (1997).
7. Saerens, D. *et al. J. Mol. Biol.* **352**, 597–607 (2005).
8. Daigle, N. *et al. J. Cell Biol.* **154**, 71–84 (2001).
9. Leonhardt, H. *et al. J. Cell Biol.* **149**, 271–280 (2000).
10. Kanda, T., Sullivan, K.F. & Wahl, G.M. *Curr. Biol.* **8**, 377–385 (1998).
11. Moir, R.D., Yoon, M., Khuon, S. & Goldman, R.D. *J. Cell Biol.* **151**, 1155–1168 (2000).
12. Nizak, C. *et al. Science* **300**, 984–987 (2003).
13. Jobling, S.A. *et al. Nat. Biotechnol.* **21**, 77–80 (2003).
14. Arbabi Ghahroudi, M. *et al. FEBS Lett.* **414**, 521–526 (1997).

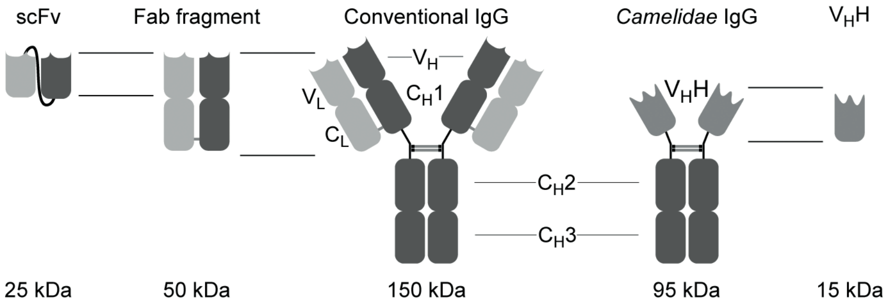

Supplementary Figure 1. Schematic comparison of a conventional IgG and a Heavy-chain IgG from *Camelidae* and various antigen-binding fragments derived thereof. The antigen binding domains of a conventional antibody are Fabs (fragment antigen binding) and Fv fragments. The Fab fragments are the antigen binding domains of an antibody molecule, containing V_H + C_H1 and C_L + V_L. The C_L and C_H1 are connected through an intrachain disulfide bond. The molecular weight of the heterodimer is around 50 kDa. Fab fragments can be prepared by papain digestions of whole antibodies. Normally, recombinant Fv fragments composed of both the variable heavy chain (V_H) and the variable light chain ($V_{L)}$ are unstable since the non-covalently associated domains tend to dissociate. To remediate this unstable behavior, the V_H and V_L domains are tethered by hydrophilic and flexible peptide linker $(Gly_4Ser)_3$. Such scFv (single chain Fv fragments) are the minimal fragments that still contain the whole antigen-binding site of an IgG antibody. Heavy-chain IgGs from *Camelidae* are only composed of the heavy chains and lack the light chain completely. Also the first constant region (C_H1) is missing in these Heavy-chain antibodies (spliced out during mRNA processing due to loss of a splice consensus signal). The antigen-binding domain, referred to as V_HH (15 kDa) to distinguish it from a V_H of the conventional IgG, contains some key mutations that prevent all pairing to possible V_L domains. The isolated V_HHs are the smallest available intact antigen-binding fragment that can be cloned after PCR amplification of one single exon, whereas a scFv requires separate V_H and V_L amplification and subsequent joining. The affinities of V_HHs to their cognate antigen are in the nanomolar range and comparable with those of Fab and scFv fragments. In contrast to other fragments, V_HHs are highly soluble and stable under challenging conditions as high salts, detergents or at elevated temperatures.

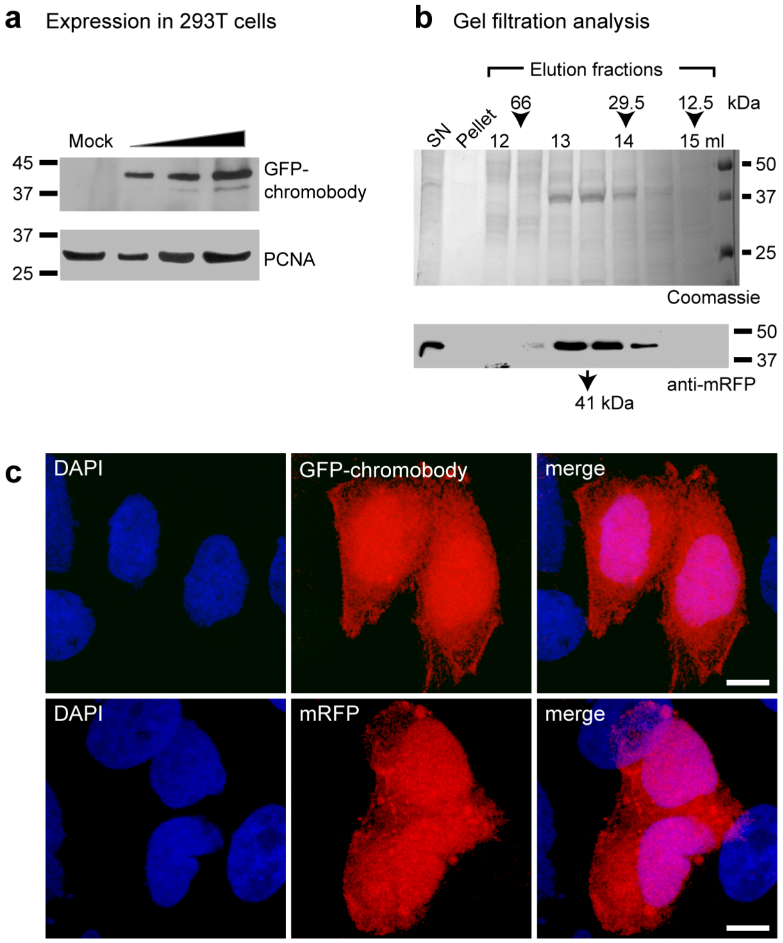
a
Expression in 293T cells
Mock
45
37
GFP-chromobody
37
25
PCNA
b
Gel filtration analysis
Elution fractions
66
29.5
12.5
kDa
SN
Pellet
12
13
14
15 ml
50
37
25
Coomassie
50
37
41 kDa
anti-mRFP
c
DAPI
GFP-chromobody
merge
DAPI
mRFP
merge

Supplementary Figure 2. The GFP-chromobody is present as a stable monomeric protein in mammalian cells. (**a**) Total cell extracts of GFP-chromobody expressing 293T cells or mock treated cells were prepared 72 h after transfection and were analyzed by SDS-PAGE and immunostaining. Lane 1: 30 µg of protein extract of mock transfected cells; lane 2-4: 10, 20 and 30 µg of protein extract of GFP-chromobody expressing cells. The predicted size of the chimeric protein is 41 kDa (upper panel). As a loading control, the blot was reincubated with an antibody against PCNA (lower panel). (**b**) Gel filtration analysis of extracts of mammalian cells expressing the chromobody. The GFP-chromobody elutes from the column in peak fractions corresponding to an apparent molecular mass of ~40 kDa. Arrowheads indicate the elution of calibration standards. (**c**) Expression of the GFP-chromobody in HeLa cells in the absence of any antigen shows a dispersed distribution of the protein throughout the cytoplasm and the nucleus (upper panel), which is comparable to the distribution of non-fused mRFP in the same cell type (lower panel).

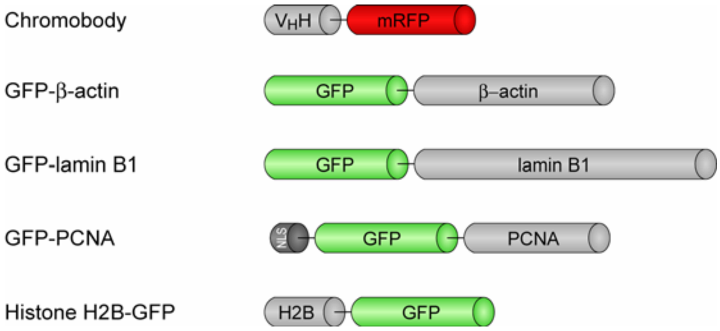
Chromobody
VHH
mRFP
GFP-β-actin
GFP
β–actin
GFP-lamin B1
GFP
lamin B1
GFP-PCNA
NLS
GFP
PCNA
Histone H2B-GFP
H2B
GFP

Supplementary Figure 3. Schematic representation of the fusion proteins used in this study.

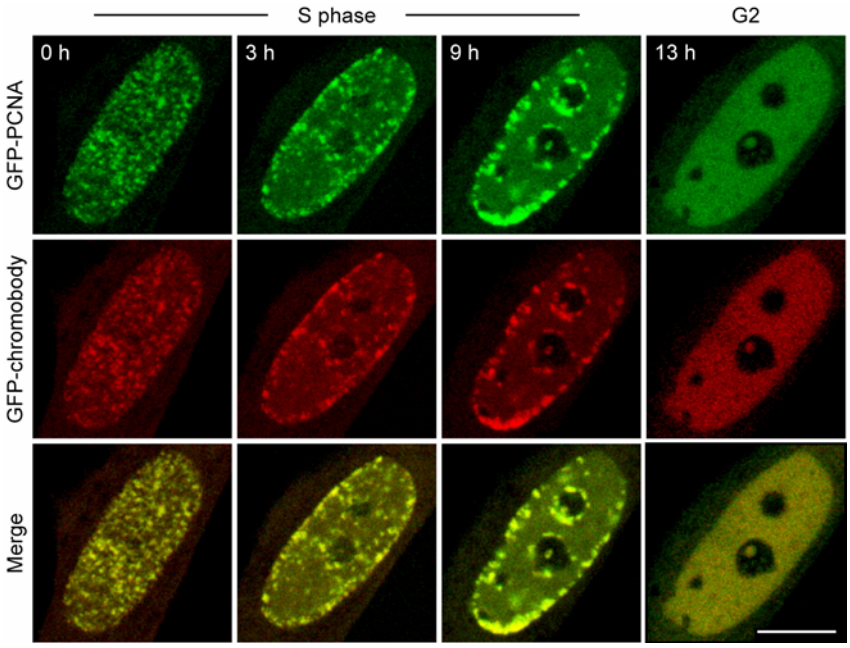
S phase
G2
0 h
3 h
9 h
13 h
GFP-PCNA
GFP-chromobody
Merge

Supplementary Figure 4. Antigen tracing with chromobodies. Tracing of a component of the replication machinery throughout S phase until G2. Time lapse imaging of cotransfected HeLa cell expressing GFP-PCNA and GFP-chromobody. Selected frames from this series are shown. At the start of imaging (0 h) the cell was in early to mid S phase. Scale bar, 10 µm. (See also **Supplementary Video 2**.)

Supplementary Methods

GFP expression, purification and llama immunization. *Escherichia coli* BL21DE3 cells were transformed with pRSETB-GFPS65T[1] (kindly provided by Roger Y. Tsien, UCSD) and overexpressed (His_6)-tagged GFPS65T was purified using ion-metal affinity chromatography according to the manufacturer's instructions (Talon, Clontech, CA, USA). One llama alpaca (*Lama pacos*) was immunized with recombinant purified GFP in Gerbu adjuvant according to the following scheme: day 0, 250 µg GFP; days 7, 14, 21, 28 and 35, 100 µg GFP; day 42, a bleed of 150 ml was collected.

V_HH library construction and selection of the antigen specific V_HH. Heparinized blood (36 ml) was diluted with prewarmed RPMI and layered on Lymphoprep™ (AXIS-Shield, Oslo, Norway) to purify the PBL cells according to the manufacturer's instructions. A total of 2×10^7 PBL cells were isolated and stored at -80°C in aliquots of 6×10^6 cells. The mRNA was extracted from 6×10^6 lymphocytes and cDNA was synthesized with SuperscriptII RNaseH$^-$ reverse transcriptase (Invitrogen, CA, USA) using an oligo-dT primer. The first PCR on the cDNA template was performed using CALL001 (5′-GTC CTG GCT GCT CTT CTA CA AGG-3′) and CALL002 (5′-GGT ACG TGC TGT TGA ACT GTT CC-3′) primers annealing at the leader sequence and at the CH2 exon of the heavy chains of all llama IgGs, respectively. The PCR products lacking the CH1 sequences (i.e. fragments with sizes between 650 -750 bp) were purified from an agarose gel using QIAquick PCR gel extraction kit (Qiagen-GmbH, Hilden, Germany). A nested PCR was done with an equimolar mixture of primers SM017 and SM018 (5′-CCA GCC GGC CAT GGC TCA GGT GCA GCT GGT GGA GTC TGG-3′and 5′-CCA GCC GGC CAT GGC TGA TGT GCA GCT GGT GGA GTC TGG-3′, respectively) and CALL002 primer, and the PCR product repurified from agarose gel as described before. The V_HH genes were finally re-amplified with primers A4short (5′-CAT GCC ATG ACT CGC GGC CAC GCC GGC CAT GGC-3′) and 38 (5′-

GGA CTA GTG CGG CCG CTG GAG ACG GTG ACC TGG GT-3′) and digested with restriction enzymes NcoI and NotI to obtain sticky DNA ends. The fragment was purified with QIAquick, ligated into pHEN4 vector [2] cut with the same enzymes and the ligation mixture used to transform *Escherichia coli* TG1 cells. After overnight growth on LB/ampicillin plates, the bacterial colonies were scraped from the plates in LB, washed in the same medium and stored in LB/15% glycerol at -80°C until further use. A V_HH library of 10^6 individual clones was obtained in *Escherichia coli* TG1 cells. A representative aliquot of this library was used to inoculate LB/ampicillin until cells reached the exponential growth phase before infection with M13K07 helper phages to display the cloned V_HH at the tip of the virions. The phage displayed V_HH library was panned for the presence of α-GFP V_HH on solid phase coated GFP (0.1 µg GFP / 100 µl per well) for three consecutive rounds. After the third round of selection, individual colonies were picked and expression of their soluble periplasmic protein was induced with 1 mM IPTG. The recombinant V_HH extracted from the periplasm was tested for antigen recognition in an ELISA. For further investigation of the binding specificity of the α-GFP V_HH, a C-terminal histidine (His_6)-tagged bacterial expression plasmid was constructed and the soluble recombinant antibody fragment was purified from *Escherichia coli* WK6 cells. The α-GFP V_HH was highly expressed and yielded 0.7 - 1 mg of soluble V_HH per 200 ml of IPTG-induced bacterial culture. The cytokeratin-8 and *Drosophila* lamin Dm0 specific V_HH's were obtained from an immunized camel using a similar protocol as for retrieving the α-GFP V_HH.

Expression and purification of the single-domain antibody fragment. The V_HH gene of the clone that scored positive in ELISA (α-GFP V_HH) was recloned into the pHEN6 expression vector and used to transform *Escherichia coli* WK6 cells. Large scale production and purification followed the protocol described by Saerens et al.[3]

Generation of chromobodies. The plasmid construct encoding a translational fusion of α-GFP V_HH and mRFP was derived by PCR amplification of the α-GFP V_HH coding region with primers gfp4#F (5´-GGG GGC TCG AGC CGG CCA TGG CCG ATG TGC AG-3´) and gfp4#RC (5´-GGG GGA ATT CCT TGA GGA GAC GGT GAC-3´). In the case of the α-lamin-V_HH and the α-cytokeratin V_HH the corresponding cDNA, was amplified by PCR with primers V_HH (BglII)#F (5´-GGG GAG ATC TCC GGC CAT GGC TCA GGT GCA G-3´) and gfp4#RC (5´-GGG GGA ATT CCT TGA GGA GAC GGT GAC-3´). The PCR product was purified as described and digested with restriction enzymes XhoI and EcoRI or BglII and EcoRI and ligated into a modified pEYFP-N1 vector (Clontech, CA, USA) where the YFP sequence had been replaced by the mRFP1 coding region [4].

Affinity measurements. Affinity measurements were done by addition of different concentrations of GFP, ranging from 500 nM to 7.5 nM, to purified his-tailed α-GFP V_HH attached on a nickel-nitrilo triacetic acid biochip (Biacore International AB, Uppsala, Sweden) according to the manufacturer's description. The kinetic binding parameters k_{on}, k_{off} and K_d were determined with the BIAevaluation software (version 3.0).

Mammalian expression constructs. The plasmid constructs encoding translational fusions of GFP were as follows: GFP-ß-actin (Clontech, CA, USA), GFP-lamin B1 [5], GFP-PCNA [6].

Mammalian cell culture and transfection. 293T cells, HeLa cells, HeLa cells stably expressing H2B-GFP [7] and C2C12 mouse myoblasts, were cultured in DMEM supplemented with 10% FCS and 20% FCS for C2C12. 293T cells were transfected with plasmid DNA using TransFectin™ reagent (Bio-Rad Laboratories, Hercules, CA, USA) according to the manufacturer's guidelines and incubated overnight, 48 h or 72 h respectively before performing the immunoblots. For microscopy HeLa cells were grown to 50-70 % confluence either on 18×18 mm glass coverslips, 40 mm round glass coverslips, in µ-Slides (ibidi®, Munich, Germany) or on Lab-Tek™ Chambered Coverglass (Nunc-GmbH, Wiesbaden, Germany) and were transfected with the indicated expression constructs using Polyplus transfection reagent jetPEI™ (BIOMOL GmbH, Hamburg, Germany) according to the manufacturer's instructions. After 4-6 hours the transfection medium was changed to fresh culture medium and cells were then incubated for another 24 hours before performing live cell microscopy or fixation with 3.7 % formaldehyde in PBS for 10 min at room temperature. Fixed cells were permeabilized with 0.2 % Triton X-100 in PBS for 3 min, counterstained with DAPI and mounted in Vectashield (Vector Laboratories, CA, USA).

Drosophila cell culture and transfection. Schneider S2 cells were cultured in Schneider´s Drosophila Medium containing 10% heat inactivated FBS at 26°C. Cells were transfected using Effectene™ reagent (QIAGEN Inc, Valenica, CA, USA) according to the manufacturer's guidelines and incubated for 48 hours at 26°C. After resuspension S2 cells were seeded on 18×18 mm glass coverslips. After 2 hours cells were fixed with 2.5% formaldehyde in PBS for 7 min on ice. Fixed cells were permeabilized with 0.2 % Triton X-100 in PBS for 3 min, counterstained with DAPI and mounted in Vectashield (Vector Laboratories, CA, USA).

Western blot analysis. Increasing protein amounts of total cell extracts of 293T cells either mock transfected or expressing the GFP-chromobody were separated on a 12% SDS–PAGE and then electrophoretically transferred to nitrocellulose membrane (Bio-Rad Laboratories, CA, USA). The membrane was blocked with 3% milk in PBS and incubated overnight at 4°C with an mRFP rabbit polyclonal antibody. After washing with PBS containing 0.1% Tween-20, the blots were incubated with rabbit IgG antibody conjugated with horseradish peroxidase. Immunoreactive bands were visualized with ECL plus Western Blot Detection Kit

(Amersham Biosciences, NJ, USA). As a loading control, membranes were reprobed with PCNA antibody.

Gel filtration. Extracts from 293T cells expressing the GFP-chromobody were subjected to gel filtration analysis. Briefly, 1×10^7 cells were homogenized in 500µl lysis buffer (20 mM Tris/HCl pH 7.5, 150 mM NaCl, 0.5 mM EDTA, 2 mM PMSF, 0.5% NP40). After a centrifugation step (10 min, 20,000×g, 4°C) the clear supernatant was loaded on a Superose-12 column (Amersham Pharmacia Biotech, NJ, USA) and chromatographed at a flowrate of 0.4 ml/min in column buffer (20 mM Tris/HCl pH 7.5, 150 mM NaCl, 0.5 mM EDTA). Fractions (500µl each) were analyzed by SDS-PAGE and proteins were either stained with Coomassie Brilliant Blue R-250 or probed further by western blotting followed by incubation with an antibody against mRFP as described above. As calibration standards bovine serum albumin (66 kDa), carbonic anhydrase (29.5 kDa) and cytochrome c (12.5 kDa) were used.

Microscopy. Live or fixed cells expressing fluorescent proteins were analyzed using a Leica TCS SP2 AOBS confocal microscope equipped with a 63×/1.4 NA Plan-Apochromat oil immersion objective. Fluorophores were excited with a 405 nm Diode laser, a 488 nm Ar laser, a 561 nm Diode-Pumped Solid-State (DPSS) laser. Confocal image stacks of living or fixed cells were typically recorded with a frame size of 512×512 pixels, a pixel size of 70-160 nm, a z step size of 280 nm and the pinhole opened to 1 Airy unit. A maximum intensity projection of several mid z-sections was then performed using ImageJ (Version 1.34, http://rsb.info.nih.gov/ij/). For long term live cell observation 40 mm diameter glass coverslips were mounted in a FCS2 live-cell chamber (Bioptechs, Butler, PA, USA) and maintained at 37°C. Light optical sections were acquired with a Zeiss LSM410 confocal laser scanning microscope using the 488 nm Ar laser line and the 543 nm HeNe laser line. Three mid z-sections at 1 µm intervals and the pinhole opened to 2 Airy Units were taken at indicated time intervals. Cells were followed up to 12 hours. Focus drift over time was compensated with a macro, which uses the reflection at the coverslip to medium interface as reference. After image acquisition, a projection of the three z-sections was performed from each time point. For colocalization analysis the "colocalization-finder" plug-in (Version 1.1) for ImageJ written by C. Laummonerie was used. For FRAP analysis, a region of interest was selected and photobleached by an intense laser beam (laser lines 458 nm, 476 nm, 488 nm, 496 nm, 514 nm and 561 nm set to maximum power at 100% transmission) for 300 ms. Before and after bleaching, confocal image series were recorded at 300 ms time intervals (typically 5 prebleach and 60 postbleach frames) with the pinhole opened to 1.5 Airy units. Mean fluorescence intensities of the bleached region were corrected for background and for total nuclear loss of fluorescence over the time course and normalized to the mean of the last 4 prebleach values. For the quantitative evaluation of FRAP experiments, data of 10 nuclei were averaged and the mean curve as well as the standard deviation was calculated.

References

1. Heim, R., Cubitt, A.B. & Tsien, R.Y. Improved green fluorescence. *Nature* **373**, 663-664 (1995).
2. Arbabi Ghahroudi, M., Desmyter, A., Wyns, L., Hamers, R. & Muyldermans, S. Selection and identification of single domain antibody fragments from camel heavy-chain antibodies. *FEBS Lett.* **414**, 521-526 (1997).
3. Saerens, D. *et al.* Identification of a universal VHH framework to graft non-canonical antigen-binding loops of camel single-domain antibodies. *J Mol Biol* **352**, 597-607 (2005).
4. Campbell, R.E. *et al.* A monomeric red fluorescent protein. *Proc. Natl Acad. Sci. U S A* **99**, 7877-7882 (2002).
5. Daigle, N. *et al.* Nuclear pore complexes form immobile networks and have a very low turnover in live mammalian cells. *J. Cell. Biol.* **154**, 71-84 (2001).
6. Leonhardt, H. *et al.* Dynamics of DNA replication factories in living cells. *J. Cell. Biol.* **149**, 271-280 (2000).
7. Kanda, T., Sullivan, K.F. & Wahl, G.M. Histone-GFP fusion protein enables sensitive analysis of chromosome dynamics in living mammalian cells. *Curr. Biol.* **8**, 377-385 (1998).

II.3. A VERSATILE NANOTRAP FOR BIOCHEMICAL AND FUNCTIONAL STUDIES WITH FLUORESCENT FUSION PROTEINS

A Versatile Nanotrap for Biochemical and Functional Studies with Fluorescent Fusion Proteins*ⓢ

Ulrich Rothbauer‡, Kourosh Zolghadr‡, Serge Muyldermans§, Aloys Schepers¶, M. Cristina Cardoso‖, and Heinrich Leonhardt‡**

AQ: A **Green fluorescent proteins (GFPs) and variants thereof are widely used to study protein localization and dynamics. We engineered a specific binder for fluorescent proteins based on a 13-kDa GFP binding fragment derived from a llama single chain antibody. This GFP-binding protein (GBP) can easily be produced in bacteria and coupled to a monovalent matrix. The GBP allows a fast and efficient (one-step) isolation of GFP fusion proteins and their interacting factors for biochemical analyses including mass spectroscopy and enzyme activity measurements. Moreover GBP is also suitable for chromatin immunoprecipitations** AQ: B **from cells expressing fluorescent DNA-binding proteins. Most importantly, GBP can be fused with cellular proteins to ectopically recruit GFP fusion proteins allowing targeted manipulation of cellular structures and processes** AQ: C **in living cells. Because of the high affinity capture of GFP fusion proteins *in vitro* and *in vivo* and a size in the lower nanometer range we refer to the immobilized GFP-binding protein as GFP-nanotrap. This versatile GFP-nanotrap enables a unique combination of microscopic, biochemical, and functional analyses with one and the same protein.** ***Molecular & Cellular Proteomics 7:xxx–xxx, 2008.***

After the identification of most components of the cell, further insights into their regulation and function require information on their abundance, localization, and dynamic interactions. Fn1 Green fluorescent proteins (GFPs)[1] and spectral variants thereof became popular tools to determine protein localization and, in combination with fluorescence photobleaching techniques, provided unique information on protein dynamics in living cells (1–4). Necessary additional information on DNA binding, enzymatic activity, and complex formation can be obtained with various methods including chromatin immunoprecipitation (ChIP) and affinity purification (5, 6). These methods, however, are hampered by the limited availability of specific antibodies. Those limitations are often bypassed by fusing the protein of interest to specific epitope or protein tags including hemagglutinin, c-Myc, FLAG, or GST (7, AQ: D 8). Curiously GFP, the most widely used labeling tag in cell biology, is rarely used for biochemical analyses, although various mono- and polyclonal antibodies have been described (9, 10). This may be due in part to limited availability and specificity as well as co-eluted heavy and light antibody chains that interfere with subsequent analyses. An alternative to conventional antibodies are variable single domain antibody fragments, also referred to as V_HH, derived from heavy AQ: E chain antibodies of Camelidae (11). These V_HH fragments, AQ: F which present the smallest intact antigen-binding units with a molecular mass of about ~15 kDa are highly soluble and AQ: G stable and can be efficiently produced in heterologous systems (12, 13). V_HH fragments have been used like conventional antibodies for various immunological applications (14–16).

Here we describe a novel application of a 13-kDa GFP binding fragment derived from a llama single chain antibody (17). This GFP-binding protein (GBP) has a small (2.5 × 4.5-nm) barrel-shaped structure and can easily be produced in bacteria. We immobilized the GBP to generate a GFP-nanotrap, which enables a fast and efficient isolation of GFP fusion proteins and their interacting factors for biochemical and ChIP analyses. Moreover we demonstrated that the GFP-binding AQ: H protein can be fused with structural proteins to ectopically recruit GFP fusion proteins and interacting factors at defined regions in living cells.

From the ‡Munich Center for Integrated Protein Science, $CiPS^M$ and Department of Biology, Ludwig Maximilians University Munich, 82152 Planegg-Martinsried, Germany, §Department of Molecular and Cellular Interactions, VIB and Laboratory of Cellular and Molecular Immunology, Vrije Universiteit Brussel, 1050 Brussels, Belgium, ¶Departments of Gene Vectors, GSF-National Research Center for Environment and Health, 81377 Munich, Germany, and ‖Max Delbrueck AQ: U Center for Molecular Medicine, 13125 Berlin, Germany

Received, July 26, 2007, and in revised form, October 15, 2007

Published, MCP Papers in Press, October 21, 2007, DOI 10.1074/mcp.M700342-MCP200

AQ: V [1] The abbreviations used are: GFP, green fluorescent protein; GBP, GFP-binding protein; ChIP, chromatin immunoprecipitation; V_HH, variable domain of heavy chain antibody; HEK, human embryonic kidney; IgG, immunoglobulin G; YFP, enhanced yellow fluorescent protein; CFP, enhanced cyan fluorescent protein; DsRed, *Discosoma* genus red fluorescent protein; mRFP, monomeric red fluorescent protein; PCNA, proliferating cell nuclear antigen; H2B, histone H2B; Dnmt1, DNA methyltransferase I; PBD, PCNA binding domain; HMGA1a, high mobility group protein A1a; Igf, insulin-like growth factor; PML, promyelocytic leukemia protein. AQ: W

© 2008 by The American Society for Biochemistry and Molecular Biology, Inc.

This paper is available on line at http://www.mcponline.org

EXPERIMENTAL PROCEDURES

Expression and Purification of the GBP—Llama immunization, V_HH library construction, and selection of the GBP were described previously (17). The coding sequence of the GFP-binding V_HH domain was cloned into the pHEN6 (18) vector using the NcoI and NotI restriction sites adding a C-terminal histidine (His_6) tag, and chemically competent *Escherichia coli* BL21 cells were transformed. For expression and purification a 500-ml *E. coli* culture was induced with 1 mM isopropyl AQ: I β-D-1-thiogalactopyranoside for 20 h at room temperature. Bacterial cells were harvested by centrifugation (10 min at 5000 × *g*), and the pellet was resuspended in 10 ml of binding buffer (1× PBS, pH 8.0, 0.5 M NaCl, 20 mM imidazole, 1 mM PMSF, 10 μg/μl lysozyme). The cell suspension was incubated for 1 h at 4 °C in a rotary shaker and then sonified (6 × 10-s pulse) on ice. After centrifugation (20 min at 20,000 × *g*) soluble proteins were loaded on a preequilibrated 1-ml HiTrap column (GE Healthcare) and purified. The His-tagged GBP was eluted by a linear gradient ranging from 20 to 500 mM imidazole. Elution fractions containing the GBP were pooled and dialyzed into PBS. Protein concentration was adjusted to 1 μg/μl. The yield of purified GBP/liter of bacterial culture was in the range of 10–15 mg.

Expression Plasmids—For bacterial expression and purification of GFP we used the bacterial expression plasmid pRSet5D containing the GFP coding sequence with a C-terminal His_6 tag kindly provided by B. Steipe. For mammalian cells we used the following expression AQ: J vectors encoding different fluorescent fusion proteins: pEGFP-C1, AQ: K pEYFP-C1, pECFP-C1, GFP-β-actin (all from Clontech), GFP-Lamin B1 (19), GFP-PCNA (20), mRFP-PCNA, GFP-Dnmt1, and GFP-Dnmt1(P1229W) (21). We also used mammalian expression vectors containing cDNAs coding for mRFP1 (22), mCherry, or mOrange (23) kindly provided by R. Tsien. Overlap extension PCR was performed to construct the CFP I147N and the CFP T154M using mutagenic primers CFP-I147N-FW (5′-GAGTACAACTACAACAGCCACAACGTCTATA-3′) in combination with CFP-I147N-Rev (5′-AACGTCTATATCATGGCCGACAAGCAG-3′) and CFP-T154M-FW (5′-AACGTCTATATCATGGCCGACAAGCAG-3′) in combination with CFP-T154M-Rev (5′-CTGCTTGTCGGCCATGATATAGACGTT-3′), respectively, and the flanking primer CFP FW (5′-GATCCGCTAGCGCTACCGGTCGCCACCATG-3′) and CFP-Rev (5′-AACGTCTATATCATGGCCGACAAGCAG-3′). The PCR fragment was cloned into the NheI/BsrGI site of the pECFP-C1 vector. For GBP-Lamin B1, the Lamin B1 was amplified from GFP-Lamin B1 by PCR with primers LaminB1EcoRV#F (5′-CCCCGATATCGGCGACTGCGACCCCC-3′) and LaminB1HisNotI#R (5′-GGGGGCGGCCGCCTAGTGATGGTGATGGTGGTGTTACATAATTGCACAGCTTC-3′). The PCR product was purified, digested with EcoRV and NotI, and ligated into the EcoRV/NotI sites of the GFP chromobody vector. All resulting constructs were sequenced and tested for expression in HEK 293T cells followed by Western blot analysis.

Antibodies—For immunoprecipitation and immunoblotting a mixture of two anti-GFP monoclonal antibodies (clones 7.1 and 13.1) from Roche Diagnostics and an affinity-purified polyclonal anti-GFP antibody raised in rabbit (a kind gift from D. Nowak, Berlin, Germany) were used. Precipitated proteins were detected with antibodies against GFP, mRFP, Lamin B (H-90, Santa Cruz Biotechnologies), β-actin (monoclonal anti-β-actin, Sigma), and PCNA (monoclonal anti-PCNA, clone 16D10). Promyelocytic leukemia protein (PML) bodies were detected with a monoclonal anti-PML antibody (5E10).

Immunoprecipitation—1×10^6–1×10^7 HeLa, HeLa H2B-GFP, or HEK 293T cells either mock-treated or transiently transfected with expression vectors coding for GFP, YFP, CFP, mRFP, mCherry, mOrange, GFP-β-actin, GFP-Lamin B1, GFP-PCNA, or GFP-Dnmt1 were homogenized in 200 μl of lysis buffer (20 mM Tris/HCl, pH 7.5, 150 mM NaCl, 0.5 mM EDTA, 2 mM PMSF, 0.5% Nonidet P-40). For extraction of GFP-Lamin B1 or H2B-GFP the lysis buffer was modified by adding 0.5 M NaCl, 1 μg of DNase I, 5 mM $MgCl_2$, and 0.1% SDS. After a centrifugation step (10 min at 20,000 × *g* at 4 °C) the supernatant was adjusted with dilution buffer (20 mM Tris/HCl, pH 7.5, 150 mM NaCl, 0.5 mM EDTA, 2 mM PMSF) to 1 ml. 20 μl (2%) were added to SDS-containing sample buffer (referred to as input). 1 μg of purified GBP or 2 μg of anti-GFP antibodies were added and incubated for 5–60 min on an end-over-end rotor at 4 °C. For pulldown of immunocomplexes 25 μl of an equilibrated mixture of protein A/G-Sepharose (Amersham Biosciences) were added, and incubation continued for 60 min. After a centrifugation step (2 min at 5000 × *g* at 4 °C) supernatant was removed, and 2% was used for SDS-PAGE (referred to as flow-through). The bead pellet was washed two times in 1 ml of dilution buffer containing 300 mM NaCl. After the last washing step the beads were resuspended in 2× SDS-containing sample buffer and boiled for 10 min at 95 °C.

Column-based GFP Purification—1 mg of purified GBP was covalently coupled to 1 ml of *N*-hydroxysuccinimide-Sepharose (GE Healthcare), according to the manufacturer's instructions, generating the GFP-nanotrap. Subsequently 50 μl of the GFP-nanotrap was transferred to a 1-ml column (MoBiTec) and preequilibrated with 5 ml of dilution buffer. Protein extracts of GFP-producing cells were prepared as described above, AQ: L and the soluble protein fraction was loaded onto the column. The protein solution (1 ml) passed through the column at 100–200 μl/min flow rate. Subsequently the column material was washed (two times) with 1 ml of dilution buffer containing 300 mM NaCl, and bound proteins were eluted with 100 μl 0.1 M glycine, pH 3.2. 2% of the input and flow-through and 10% of bound material were resuspended in 2× SDS-containing sample buffer and analyzed by SDS-PAGE and Coomassie Blue and by immunostaining.

Enzymatic Activity Test—Soluble protein extracts of HEK 293T cells producing GFP-Dnmt1 or GFP-Dnmt1(P1229W) were prepared, and immunoprecipitation was performed as described above. AQ: M Beads containing the GBP-GFP-Dnmt1 complexes were washed extensively in dilution buffer containing 300 mM NaCl, and after centrifugation the beads were resuspended in 500 μl of assay buffer (100 mM KCl, 10 mM Tris, pH 7.6, 1 mM EDTA, 1 mM DTT). Beads were washed (two times) in assay buffer, and after centrifugation (1000 × *g* for 1 min) 30 μl of methylation mixture (0.1 μCi of *S*-[^{3}H]adenosylmethionine (Am- AQ: N ersham Biosciences), 1.67 pmol/μl hemimethylated double-stranded 35-bp DNA (50 pmol/μl), 160 ng/μl BSA) were added. As a positive AQ: O control 2 μg of recombinant purified DNA methyltransferase I (DNMT1) was used. Incubation was carried out for 2.5 h at 37 °C, and the reactions were spotted onto DE81 cellulose filters. Subsequently filters were washed (three times) with 0.2 M $(NH_4)HCO_3$, once with H_2O, and once with 100% EtOH. After drying at 80 °C the filter was transferred into a Mini-Poly-Q vial with 5 ml of Ultima Gold LSC Mixture (PerkinElmer Life Sciences), and each sample was measured for 1 min in a scintillation counter (Beckman LS1801). A sample without enzyme addition was used as negative control.

Chromatin Immunoprecipitation Assay and Real Time PCR Analysis—For chromatin immunoprecipitation experiments, formaldehyde was diluted to 1% in serum-free medium, and 15 ml were added to monolayers of C2C12 and C2C12/HMGA1a-GFP cells for 10 min at AQ: P room temperature. The cross-link was stopped by adding 1.5 ml of 1.25 M glycine. After removal of the medium, cells were washed (two times) on plates with cold 1× PBS, scraped off, and washed again in cold 1× PBS and once with hypotonic LSB buffer (10 mM Hepes, pH 7.9, 10 mM KCl, 1.5 mM $MgCl_2$). Cells were resuspended in 2.7 ml of AQ: Q LSB buffer and lysed by adding 300 μl of 20% Sarkosyl. The chromatin was carefully layered onto a 40-ml sucrose cushion (LSB buffer plus 100 mM sucrose) and centrifuged (10 min at 4 °C at 4000 × *g*). Supernatant was removed, and the chromatin was resuspended in 2 ml of TE (10 mM Tris, 0.5 mM EDTA, pH 8.0) and sonicated (Branson sonifier 250-D, 35% amplitude, 2 min in 1-s intervals). For each

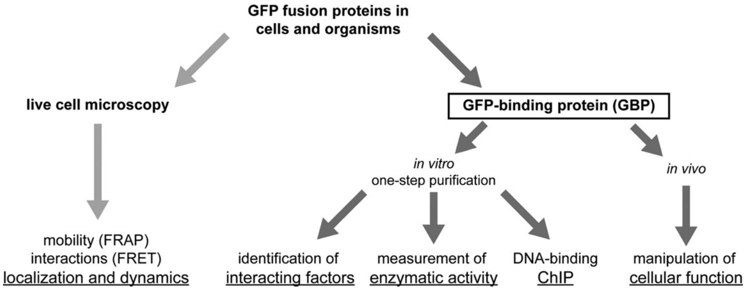
GFP fusion proteins in cells and organisms
live cell microscopy
GFP-binding protein (GBP)
in vitro one-step purification
in vivo
mobility (FRAP)
interactions (FRET)
localization and dynamics
identification of interacting factors
measurement of enzymatic activity
DNA-binding ChIP
manipulation of cellular function

AQ: Y FIG. 1. **Outline of possible GFP fusion protein applications with the GFP-nanotrap.** *FRAP*, fluorescence recovery after photobleaching; *FRET*, fluorescence resonance energy transfer.

AQ: R immunoprecipitation, 500 μg of the nucleoprotein were adjusted with 1/10 volume of 1× NET (50 mM Tris, 150 mM NaCl, 0.5 M EDTA, 0.5% Nonidet P-40). 10 μg of two anti-GFP monoclonal antibodies (clones 7.1 and 13.1; Roche Diagnostics), a mouse IgG1 isotype control, and 5 μg of GFP-nanotrap were incubated overnight at 4 °C. The purification of co-precipitated DNA was performed as described above. Real time PCR was performed with the Light Cycler instrument (Roche Diagnostics) using a ready-to-use "hot start" reaction mixture (FastStart DNA Master SYBR Green I; Roche Diagnostics). Real time PCR analysis was performed according to the manufacturer's instructions using the same parameters as described previously (24). The list of primer pairs is given in Supplemental Table 1.

RESULTS

F1 Ideally the subcellular localization and binding dynamics of fluorescent fusion proteins should be complemented with biochemical data on interacting factors, enzymatic activity, and DNA binding properties (Fig. 1). To generate a nanotrap for fast and efficient purification of GFP fusion proteins we used a small recombinant 13-kDa GBP comprising the epitope recognition domain of a heavy chain antibody raised in an alpaca (*Lama pacos*) against GFP (17). The GBP was fused with a C-terminal histidine (His$_6$) tag, produced in *E. coli*, and purified by IMAC (Supplemental Fig. S1A). Subsequent gel filtration analysis showed a single elution peak at about 13 kDa indicating that the GBP can easily be produced and purified as a stable monomer (Supplemental Fig. S1B). For a first functional analysis we tested the binding capacity of the GBP to purified GFP. Equimolar amounts of both proteins were mixed and incubated for about 20 min. Subsequent gel filtration analysis showed that the GBP and its antigen rapidly assemble into a stable, stoichiometric complex with a corresponding native molecular mass of 41 kDa (Supplemental Fig. S2). We then tested the ability of GBP to precipitate its antigen from cell extracts and directly compared its performance with mono- and polyclonal anti-GFP antibodies. GBP and anti-GFP antibodies were added to protein extracts of HEK 293T cells expressing GFP. Precipitated proteins were separated by SDS-PAGE and visualized by Coomassie Blue or immunoblot analysis (Fig. 2*A*). F2 After precipitation with GBP only two protein bands (GFP at ~28 kDa and the GBP itself at ~13 kDa) were detectable, whereas additional bands corresponding to the light and heavy chains of the denatured IgGs as well as unspecifically precipitated proteins could be observed in immunoprecipitations with the mono- and polyclonal anti-GFP antibodies. The quantitative comparison of precipitated GFP in relation to antibody input showed that the GBP is clearly more efficient than established mono- and polyclonal antibodies (Fig. 2*A* and Supplemental Fig. S3).

Conveniently GBP complexes can be immobilized and precipitated with protein A-agarose just like conventional antibodies (Fig. 2*A*, *left panel*). However, to prevent elution of the GBP itself and to avoid any interference with subsequent analyses we covalently coupled GBP to *N*-hydroxysuccinimide-Sepharose beads generating a stable GFP-binding matrix (GFP-nanotrap). This GFP-nanotrap allowed a very fast (5-min) column-based purification of GFP from total cell extracts yielding a single protein band without any visible unspecific protein contamination (Fig. 2*B*, *right panel*). Moreover the immunoblotting analysis revealed a quantitative precipitation of the antigen visible as depletion of GFP from the flow-through fraction.

To analyze the specificity of GBP we performed immunoprecipitation with a set of different fluorescent proteins. Besides GFP itself, GBP recognizes the yellow variant YFP but not CFP or any derivatives of DsRed like mRFP, mCherry, or mOrange (Supplemental Fig. S4). To further characterize the binding properties of GBP we tested different salt, temperature, and pH conditions. First, we increased the NaCl molarity of the binding buffer from 0.15 to 2 M and found that GBP precipitates its antigen even under high salt conditions (Supplemental Fig. S5A). Second, we tested different incubation temperatures and observed quantitative precipitation of GFP even at 65 °C (Supplemental Fig. S5B) demonstrating the temperature-stable folding and binding of GBP. Third, we tested the elution of bound epitope at different pH conditions. GFP was stably bound in the range from pH 4 up to pH 11. Lowering the pH to 3.2 caused quantitative release of GFP providing a fast and efficient method to elute bound antigen complexes from the GFP-nanotrap (Supplemental Fig. S5C).

To investigate whether GBP also precipitates GFP fusion proteins we chose four well characterized constructs from different subcellular compartments: GFP-β-actin (25), GFP-Lamin B1 (26), GFP-PCNA (20), and H2B-GFP (27). Cells transiently or stably expressing the fusion proteins were analyzed by confocal microscopy to determine the subcellular localization of the GFP fusion protein (Fig. 2*B*, *upper panel*). Subsequently cells were harvested, and GFP fusion proteins were precipitated with the GFP-nanotrap followed by Coomassie staining and Western blot analysis (Fig. 2*B*, *lower panel*). The results show that GBP efficiently precipitated N- or C-terminal GFP fusion proteins from different subcellular compartments and structures.

One of the most interesting applications of the GBP is the possibility to correlate subcellular localization, dynamics, and complex formation of specific proteins and mutants thereof. We had previously identified a deletion mutant of Dnmt1 lacking the PCNA interaction domain (Dnmt1Δ-PBD) (28). In comparison with wild-type Dnmt1 (GFP-Dnmt1) the fluorescent labeled mutant (GFP-Dnmt1Δ-PBD) showed no colocalization with the red fluorescent PCNA (mRFP-PCNA) during S phase (Fig. 2*C*, *upper panel*). We then compared this observation from living cells with biochemical data. Cells were lysed immediately after microscopic analysis and subjected to immunoprecipitation with the GFP-nanotrap. Immunoblot analysis showed that mRFP-PCNA co-precipitates with GFP-Dnmt1 but not with GFP-Dnmt1Δ-PBD (Fig. 2*C*, *lower panel*). The unbound mRFP-PCNA fraction reflects the transient nature of the Dnmt1-PCNA interaction during S phase (21). In addition, we also detected endogenous PCNA co-precipitating with GFP-Dnmt1 but not with GFP-Dnmt1Δ-PBD, demonstrating that GBP can also pick up interacting endogenous proteins. These results show that the GFP-nanotrap is suitable to identify (even) transiently interacting factors and cell cycle-dependent complexes. Taking advantage of its avid and specific binding we now routinely use the GFP-nanotrap to identify interacting factors by MALDI mass spectrometry.

F3

A critical question in live cell studies is whether the fluorescent fusion proteins are enzymatically active and have biochemical properties similar to their endogenous counterparts. For fast determination of enzymatic activity we chose fluorescent fusion constructs of the murine Dnmt1, which are actively investigated in our laboratory. With live cell microscopy we could not distinguish the active GFP-Dnmt1 (wild type) and an enzymatically inactive version, GFP-Dnmt1(P1229W) (Fig. 3, *upper panel*). After visualization of the fluorescent Dnmt1 constructs in nuclei of mammalian cells both proteins were one step-purified from cell extracts with the GFP-nanotrap (Fig. 3, *middle panel*) and directly assayed for enzymatic

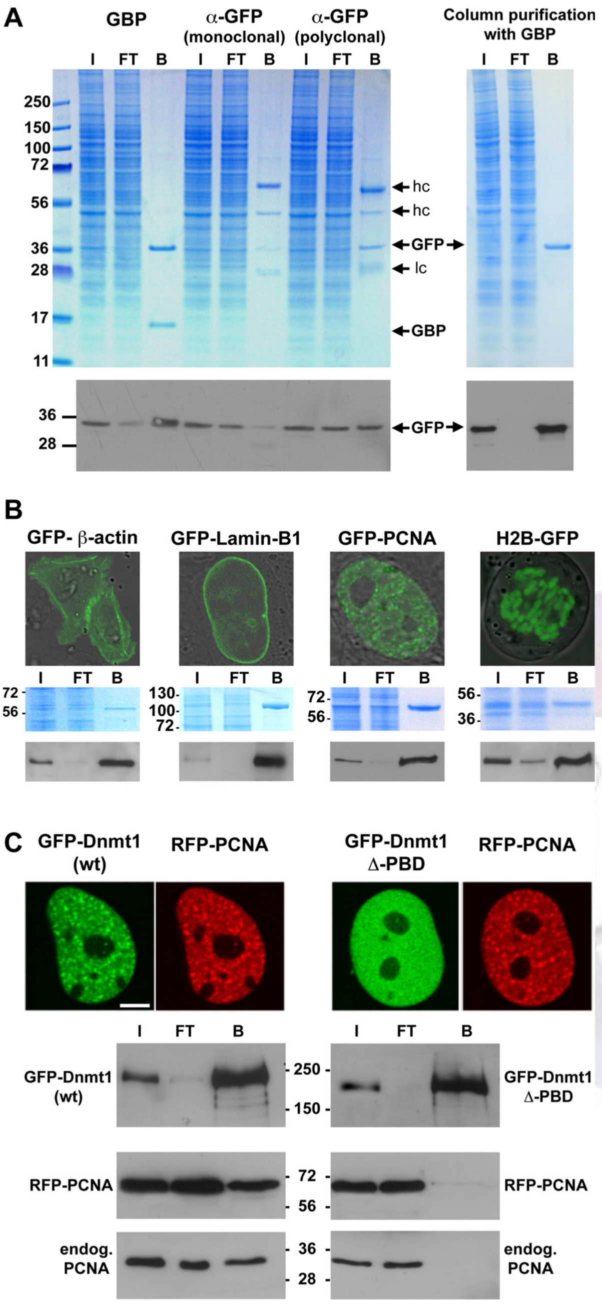

AQ: Z

FIG. 2. **One-step purification of fluorescent proteins.** *A*, immunoprecipitation of GFP. *Left panel*, comparison of GBP with mono- and polyclonal anti-GFP antibodies. Protein extracts of GFP-producing HEK 293T cells were subjected to immunoprecipitation with GBP, mono-, or polyclonal anti-GFP antibodies. Throughout (*A*–*C*) aliquots of input (*I*), flow-through (*FT*), and bound fraction (*B*) were separated by SDS-PAGE and visualized either by Coomassie Blue (*top*) or by immunoblot analysis (*bottom*). Precipitated GFP, denatured heavy (*hc*) and light chains (*lc*) of the IgGs, and the GBP are marked by *arrows*. *Right panel*, column-based purification with the GFP-nanotrap. GFP-containing protein extracts were loaded on a column containing GBP directly coupled to Sepharose (GFP-nanotrap), and bound proteins were eluted. *B*, one-step purification of GFP fusion proteins with the GFP-nanotrap. Representative images of HeLa cells producing GFP-β-actin, GFP-Lamin B1, GFP-PCNA, or H2B-GFP are shown (*upper panel*). Cells were lysed, and GFP fusion proteins were one step-purified with the GFP-nanotrap. *C*, co-precipitation of GFP fusion proteins and interacting factors. HeLa cells coexpressing either GFP-Dnmt1 or a deletion mutant of Dnmt1 (GFP-Dnmt1Δ-PBD) together with the red fluorescent version of PCNA (mRFP-PCNA) were analyzed by live cell microscopy. Representative confocal images of two cells in early-to-mid S phase are shown (*scale bar*, 5 μm). Subsequently cells were lysed and subjected to immunoprecipitation with the GFP-nanotrap. *wt*, wild type.

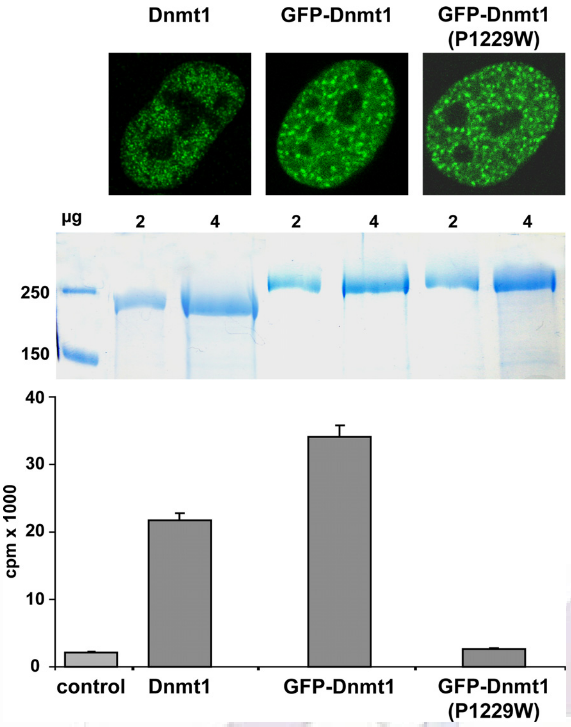

FIG. 3. **GFP fusion proteins retain their enzymatic activity after purification with the GFP-nanotrap.** Representative images of nuclei from HeLa cells show the endogenous Dnmt1, GFP-Dnmt1, or catalytically inactive mutant GFP-Dnmt1(P1229W) (*top*). Soluble protein extracts containing GFP-Dnmt1 or GFP-Dnmt1(P1229W) were one step-purified with the GFP-nanotrap and analyzed by SDS-PAGE followed by Coomassie Blue staining (*middle*). DNA methyltransferase activity of purified GFP fusion proteins (~4 µg each) and recombinant DNMT1 (~2 µg) were determined (*bottom*). $n = 4$; *error bars* show standard deviation. AQ: AA

AQ: S measurements. GFP-Dnmt1 showed a specific DNA methyltransferase activity similar to that of purified recombinant DNMT1 (Fig. 3, *lower panel*). The comparison with the catalytically inactive GFP-Dnmt1(P1229W) revealed that the endogenous DNA methyltransferase activities of mammalian cells were efficiently removed by this quick one-step purification. These results demonstrate that the GFP-nanotrap is a highly efficient tool for quick and reliable biochemical characterization of fluorescent fusion proteins.

To investigate whether the GFP-nanotrap has the required specificity to function in chromatin immunoprecipitations we performed ChIP experiments using a mouse myoblast cell line stably expressing a GFP fusion of the high mobility group Fn2 protein A1a (HMGA1a-GFP).[2] We analyzed the promoter regions of the Interleukin 6 and Igf-binding protein 1 genes that are known to preferentially bind HMGA1a (29–32). 500 µg of formaldehyde-cross-linked nucleoprotein were subjected to immunoprecipitation with the GFP-nanotrap and comparison with commercially available GFP-specific antibodies. Only the GFP-nanotrap showed a reproducible 3-fold enrichment of promoter fragments over distal sites. This preferential binding of HMGA1a-GFP at the specific promoter sites was not detectable with conventional GFP-specific antibodies (Fig. 4). F4 The parental C2C12 cells not expressing HMGA1a-GFP showed no specific enrichment of any sequences in comparison with the isotype control (data not shown). These data confirm the high specificity and sensitivity of the GFP-nanotrap.

These experiments show *in vitro* applications of the GFP-binding protein. In a second step we explored potential *in vivo* applications and placed the coding region of the GFP-binding protein at a defined position within the cell by fusing it to a structural component of the nuclear envelope. We fused the GBP with Lamin B1 (GBP-Lamin B1) to generate a cellular nanotrap at the nuclear lamina. As described above, GBP efficiently recognized and bound YFP but not the blue variant CFP *in vitro* (Supplemental Fig. S10). To compare these biochemical data with binding specificity in living cells we transfected HeLa cells with GBP-Lamin B1, GFP, and CFP and determined the distribution of GFP and CFP with respect to the GFP-nanotrap positioned at the nuclear lamina. Confocal microscopy showed that only GFP was exclusively localized at the nuclear lamina, whereas CFP showed a strikingly different, disperse distribution throughout the cell (Fig. 5*A*). F5 Sequence alignment of GFP, YFP, and CFP showed that CFP differs from the two other fluorescent proteins at two relevant amino acid positions (Fig. 5*B*). To define the epitope recognized by GBP we introduced single mutations reverting stepwise CFP to GFP. We found that the exchange of isoleucine at position 147 to asparagine (I147N) restored binding to the GFP-nanotrap, whereas mutating methionine at position 154 to a tryptophan (T154M) did not restore any detectable binding (Fig. 5*C*). This demonstrates the high selectivity and specificity of the GBP *in vitro* and *in vivo* even allowing detection of single amino acid substitutions. Finally we analyzed whether the GFP-nanotrap can be used to manipulate endogenous factors and cellular structures. As a target we chose the endogenous PML. AQ: T The PML is organized in nuclear PML bodies, which play a role in regulation of gene expression, apoptosis, DNA repair, and proteolysis (33, 34). We could detect 10–30 PML bodies by immunofluorescence staining of PML in HeLa cells where PML bodies are evenly distributed throughout the nucleus (data not shown). In transiently transfected cells PML bodies are highlighted by the green fluorescence of the GFP-PML (35) fusion protein and immunostaining with a specific antibody against PML (Fig. 6*A*). F6 Upon expression of GBP-Lamin B1 green fluorescent labeled PML bodies were exclusively found at the nuclear rim, and subsequent antibody staining confirmed the depletion of endogenous PML from the nuclear interior (Fig. 6*C*). These results demonstrate the potential of the GFP-nanotrap not only to recruit GFP fusion proteins but also interacting endogenous factors.

AQ: X [2] ■. Brocher and ■. Hock, manuscript submitted

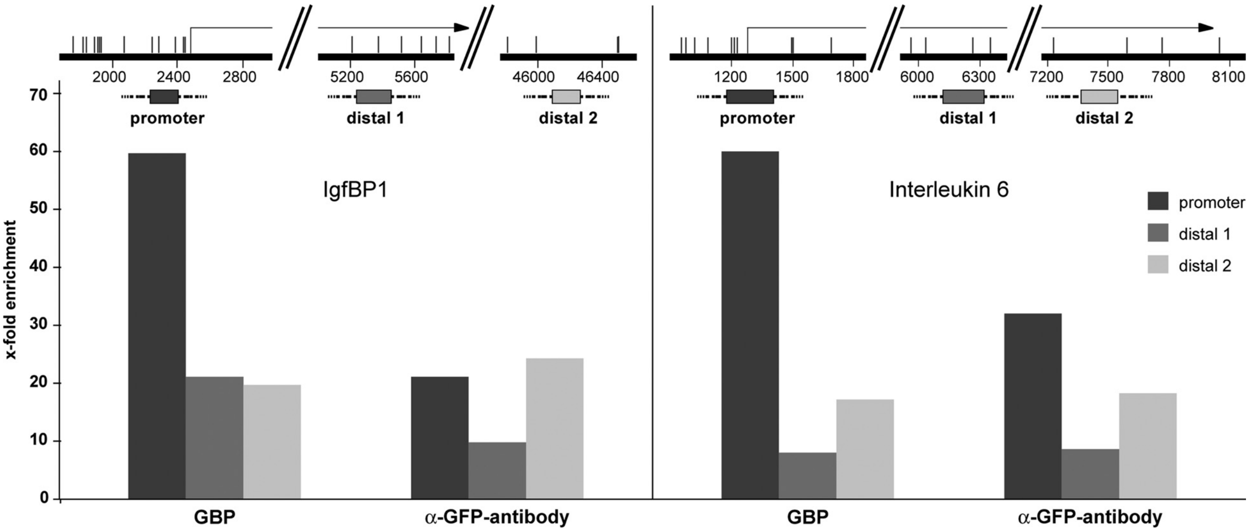

FIG. 4. **ChIP analysis with the GFP-nanotrap.** For ChIP experiments, 500 μg of C2C12/HMGA1a-GFP cells were subjected to immunoprecipitation using 5 μg of GFP-nanotrap, 10 μg of anti-GFP antibody (monoclonal), and 10 μg of mouse IgG1 isotype control, respectively. Co-precipitated DNA was quantified by real time PCR analysis using primer pairs of the IgfBP1 and Il6 promoter regions and indicated downstream regions (distal region 1/2). Results obtained for the Interleukin 6 and IgfBP1 promotor are shown in *dark gray*. *Column heights* indicate the relative enrichment obtained in two independent experiments as the difference between PCR values obtained with the GFP-nanotrap and anti-GFP antibodies over mouse IgG1 isotype control antibodies.

AQ: BB

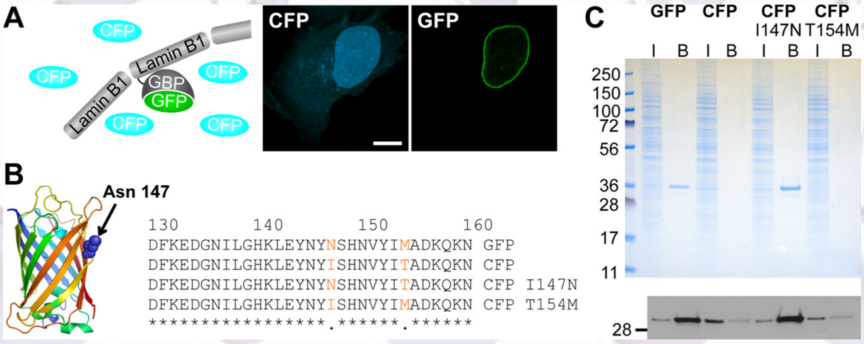

FIG. 5. **Specificity of the GFP-nanotrap.** *A*, in HeLa cells expressing GFP, CFP, and GBP-Lamin B1 GFP is exclusively localized at the nuclear lamina, whereas CFP is dispersedly distributed. *B*, amino acid sequence alignment of GFP, CFP, CFP I147N, and CFP T154M. Non-conserved residues are marked in *red*. The crystal structure of GFP (36) is shown, and the asparagine at position 147 is displayed as a *blue sphere* using PyMOL Version 0.99 (DeLano Scientific LLC). *C*, soluble protein extracts of HEK 293T cells expressing GFP, CFP, CFP I147N, and CFP T154M were subjected to one-step purification with the GFP-nanotrap. Input (*I*) and bound fractions (*B*) were separated by SDS-PAGE and analyzed by Coomassie Blue staining and by immunoblotting with anti-GFP antibody.

AQ: CC

AQ: DD

DISCUSSION

One challenge of the postgenomics era is the effective integration of genetic, biochemical, and cell biological data. This integration has in part been impeded by the simple fact that different protein tags are used for different applications. Here we present a GBP as a simple, robust, and versatile tool for biochemical analyses of GFP fusion proteins and even functional studies *in vivo*. The small and stable GBP has several decisive advantages over the conventional, 10 times larger, mono- and polyclonal antibodies. First, the GBP can be produced in bacteria in unlimited quantities and with reproducible quality and can easily be coupled to beads or matrices. Second, the high affinity of single chain GBP allows short (5–30-min) incubations to isolate fluorescent fusion proteins and even transiently bound factors from different cellular compartments. Third, its small size of about 13 kDa minimizes unspecific binding and entirely avoids contamination by heavy and light chains of conventional antibodies (50 and 25 kDa) that normally interfere with subsequent analyses.

The specificity of the GFP-nanotrap was further underlined by ChIP experiments with stable cells expressing a HMGA1a-GFP fusion. Analyzing DNA binding at two gene loci with the

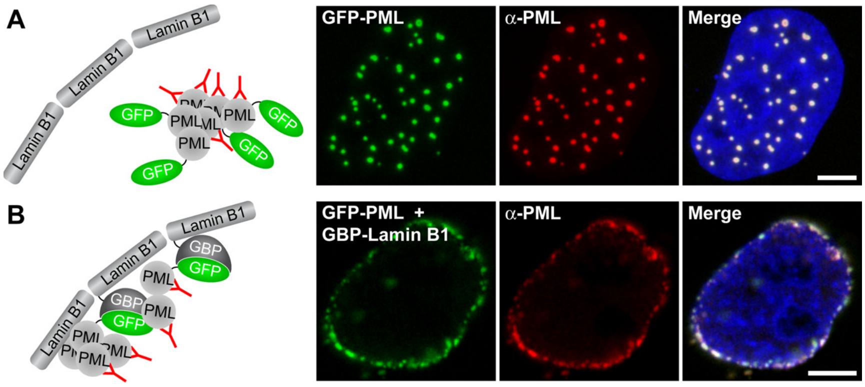

FIG. 6. **Targeted manipulation of nuclear structures with the GFP-nanotrap.** HeLa cells producing GFP-PML either alone or in combination with GBP-Lamin B1 are shown. Illustrating outlines are shown on the *left*. *A*, GFP-PML is assembled into endogenous PML bodies shown by immunofluorescence staining with an anti-PML antibody. *B*, coexpression of the GBP-Lamin B1 together with GFP-PML leads to a depletion of PML bodies from the nuclear interior shown by the absence of PML bodies in the nuclear interior after immunostaining with an anti-PML antibody.

AQ: EE

GFP-nanotrap we detected a preferential binding of HMGA1a at the promoter regions that was far less evident with established anti-GFP antibodies.

In conclusion, this versatile GFP-nanotrap together with the widespread use of fluorescent fusion proteins now enables a fast and direct correlation of the subcellular localization and mobility of fluorescent fusion proteins with their enzymatic activity, interacting factors, and DNA binding properties combining cell biology and biochemistry with mutual benefits. Unlike conventional antibodies, the GFP-nanotrap can also be used for functional studies *in vivo*. We demonstrated that GBP can be fused with cellular proteins to set a GFP-nanotrap at a defined subcellular site to either ectopically recruit GFP fusion proteins and their associated factors or deplete them from their native surroundings. In one example we anchored the GBP at the nuclear lamina to capture nuclear bodies. Multiple other applications are possible because any GFP fusion protein can be combined with any cellular anchor point. The use of GBP as a nanotrap in living cells opens up an entire spectrum of new types of functional studies to probe and manipulate cellular processes and structures.

Acknowledgments—We thank A. Gahl and D. Nowak for excellent technical assistance; A. Jegg, J. Helma, R. Kleinhans, and K. Schmidthals for practical support; G. Längst and K. Dachauer for enzyme activity measurements; and R. Hock for the C2C12 HMGA1a-GFP cell line.

---

* This work was supported by the Center for NanoScience, by Nanosystems Initiative Munich, and by grants from the Deutsche Forschungsgemeinschaft. The costs of publication of this article were defrayed in part by the payment of page charges. This article must therefore be hereby marked "*advertisement*" in accordance with 18 U.S.C. Section 1734 solely to indicate this fact.

S The on-line version of this article (available at http://www.mcponline.org) contains supplemental material.

** To whom correspondence should be addressed. E-mail: h.leonhardt@lmu.de.

REFERENCES

1. Chalfie, M., Tu, Y., Euskirchen, G., Ward, W. W., and Prasher, D. C. (1994) Green fluorescent protein as a marker for gene expression. *Science* **263,** 802–805
2. Misteli, T., and Spector, D. L. (1997) Applications of the green fluorescent protein in cell biology and biotechnology. *Nat. Biotechnol.* **15,** 961–964
3. Tsien, R. Y. (1998) The green fluorescent protein. *Annu. Rev. Biochem.* **67,** 509–544
4. van Roessel, P., and Brand, A. H. (2002) Imaging into the future: visualizing gene expression and protein interactions with fluorescent proteins. *Nat. Cell Biol.* **4,** E15–E20
5. Kellogg, D. R., and Moazed, D. (2002) Protein- and immunoaffinity purification of multiprotein complexes. *Methods Enzymol.* **351,** 172–183
6. Orlando, V., Strutt, H., and Paro, R. (1997) Analysis of chromatin structure by in vivo formaldehyde cross-linking. *Methods* **11,** 205–214
7. Fritze, C. E., and Anderson, T. R. (2000) Epitope tagging: general method for tracking recombinant proteins. *Methods Enzymol.* **327,** 3–16
8. Terpe, K. (2003) Overview of tag protein fusions: from molecular and biochemical fundamentals to commercial systems. *Appl. Microbiol. Biotechnol.* **60,** 523–533
9. Lorkovic, Z. J., Hilscher, J., and Barta, A. (2004) Use of fluorescent protein tags to study nuclear organization of the spliceosomal machinery in transiently transformed living plant cells. *Mol. Biol. Cell* **15,** 3233–3243
10. Cristea, I. M., Williams, R., Chait, B. T., and Rout, M. P. (2005) Fluorescent proteins as proteomic probes. *Mol. Cell. Proteomics* **4,** 1933–1941
11. Hamers-Casterman, C., Atarhouch, T., Muyldermans, S., Robinson, G., Hamers, C., Songa, E. B., Bendahman, N., and Hamers, R. (1993) Naturally occurring antibodies devoid of light chains. *Nature* **363,** 446–448
12. Sheriff, S., and Constantine, K. L. (1996) Redefining the minimal antigen-binding fragment. *Nat. Struct. Biol.* **3,** 733–736
13. Muyldermans, S. (2001) Single domain camel antibodies: current status. *J. Biotechnol.* **74,** 277–302
14. van Koningsbruggen, S., de Haard, H., de Kievit, P., Dirks, R. W., van Remoortere, A., Groot, A. J., van Engelen, B. G., den Dunnen, J. T., Verrips, C. T., Frants, R. R., and van der Maarel, S. M. (2003) Llama-derived phage display antibodies in the dissection of the human disease oculopharyngeal muscular dystrophy. *J. Immunol. Methods* **279,** 149–161
15. Jobling, S. A., Jarman, C., Teh, M. M., Holmberg, N., Blake, C., and Verhoeyen, M. E. (2003) Immunomodulation of enzyme function in plants by single-domain antibody fragments. *Nat. Biotechnol.* **21,** 77–80
16. Groot, A. J., Verheesen, P., Westerlaken, E. J., Gort, E. H., van der Groep, P., Bovenschen, N., van der Wall, E., van Diest, P. J., and Shvarts, A. (2006) Identification by phage display of single-domain antibody fragments specific for the ODD domain in hypoxia-inducible factor 1alpha. *Lab. Investig.* **86,** 345–356
17. Rothbauer, U., Zolghadr, K., Tillib, S., Nowak, D., Schermelleh, L., Gahl, A., Backmann, N., Conrath, K., Muyldermans, S., Cardoso, M. C., and Leonhardt, H. (2006) Targeting and tracing antigens in live cells with fluorescent nanobodies. *Nat. Methods* **3,** 887–889
18. Arbabi Ghahroudi, M., Desmyter, A., Wyns, L., Hamers, R., and Muyldermans, S. (1997) Selection and identification of single domain antibody fragments from camel heavy-chain antibodies. *FEBS Lett.* **414,** 521–526
19. Beaudouin, J., Gerlich, D., Daigle, N., Eils, R., and Ellenberg, J. (2002) Nuclear envelope breakdown proceeds by microtubule-induced tearing of the lamina. *Cell* **108,** 83–96
20. Leonhardt, H., Rahn, H. P., Weinzierl, P., Sporbert, A., Cremer, T., Zink, D., and Cardoso, M. C. (2000) Dynamics of DNA replication factories in living

cells. *J. Cell Biol.* **149,** 271–280

21. Schermelleh, L., Spada, F., Easwaran, H. P., Zolghadr, K., Margot, J. B., Cardoso, M. C., and Leonhardt, H. (2005) Trapped in action: direct visualization of DNA methyltransferase activity in living cells. *Nat. Methods* **2,** 751–756
22. Campbell, R. E., Tour, O., Palmer, A. E., Steinbach, P. A., Baird, G. S., Zacharias, D. A., and Tsien, R. Y. (2002) A monomeric red fluorescent protein. *Proc. Natl. Acad. Sci. U. S. A.* **99,** 7877–7882
23. Shaner, N. C., Campbell, R. E., Steinbach, P. A., Giepmans, B. N., Palmer, A. E., and Tsien, R. Y. (2004) Improved monomeric red, orange and yellow fluorescent proteins derived from Discosoma sp. red fluorescent protein. *Nat. Biotechnol.* **22,** 1567–1572
24. Schepers, A., Ritzi, M., Bousset, K., Kremmer, E., Yates, J. L., Harwood, J., Diffley, J. F., and Hammerschmidt, W. (2001) Human origin recognition complex binds to the region of the latent origin of DNA replication of Epstein-Barr virus. *EMBO J.* **20,** 4588–4602
25. Westphal, M., Jungbluth, A., Heidecker, M., Muhlbauer, B., Heizer, C., Schwartz, J. M., Marriott, G., and Gerisch, G. (1997) Microfilament dynamics during cell movement and chemotaxis monitored using a GFP-actin fusion protein. *Curr. Biol.* **7,** 176–183
26. Daigle, N., Beaudouin, J., Hartnell, L., Imreh, G., Hallberg, E., Lippincott-Schwartz, J., and Ellenberg, J. (2001) Nuclear pore complexes form immobile networks and have a very low turnover in live mammalian cells. *J. Cell Biol.* **154,** 71–84
27. Kanda, T., Sullivan, K. F., and Wahl, G. M. (1998) Histone-GFP fusion protein enables sensitive analysis of chromosome dynamics in living mammalian cells. *Curr. Biol.* **8,** 377–385
28. Easwaran, H. P., Schermelleh, L., Leonhardt, H., and Cardoso, M. C. (2004) Replication-independent chromatin loading of Dnmt1 during G2 and M phases. *EMBO Rep.* **5,** 1181–1186
29. Bustin, M., and Reeves, R. (1996) High-mobility-group chromosomal proteins: architectural components that facilitate chromatin function. *Prog. Nucleic Acids Res. Mol. Biol.* **54,** 35–100
30. Allander, S. V., Durham, S. K., Scheimann, A. O., Wasserman, R. M., Suwanichkul, A., and Powell, D. R. (1997) Hepatic nuclear factor 3 and high mobility group I/Y proteins bind the insulin response element of the insulin-like growth factor-binding protein-1 promoter. *Endocrinology* **138,** 4291–4300
31. Battista, S., Pentimalli, F., Baldassarre, G., Fedele, M., Fidanza, V., Croce, C. M., and Fusco, A. (2003) Loss of Hmga1 gene function affects embryonic stem cell lympho-hematopoietic differentiation. *FASEB J.* **17,** 1496–1498
32. Foti, D., Chiefari, E., Fedele, M., Iuliano, R., Brunetti, L., Paonessa, F., Manfioletti, G., Barbetti, F., Brunetti, A., Croce, C. M., and Fusco, A. (2005) Lack of the architectural factor HMGA1 causes insulin resistance and diabetes in humans and mice. *Nat. Med.* **11,** 765–773
33. Maul, G. G., Negorev, D., Bell, P., and Ishov, A. M. (2000) Review: properties and assembly mechanisms of ND10, PML bodies, or PODs. *J. Struct. Biol.* **129,** 278–287
34. Borden, K. L. (2002) Pondering the promyelocytic leukemia protein (PML) puzzle: possible functions for PML nuclear bodies. *Mol. Cell. Biol.* **22,** 5259–5269
35. Moller, A., Sirma, H., Hofmann, T. G., Rueffer, S., Klimczak, E., Droge, W., Will, H., and Schmitz, M. L. (2003) PML is required for homeodomain-interacting protein kinase 2 (HIPK2)-mediated p53 phosphorylation and cell cycle arrest but is dispensable for the formation of HIPK domains. *Cancer Res.* **63,** 4310–4314
36. Yang, F., Moss, L. G., and Phillips, G. N., Jr. (1996) The molecular structure of green fluorescent protein. *Nat. Biotechnol.* **14,** 1246–1251

ASBMB

SUPPLEMENTAL DATA

EXPERIMENTAL PROCEDURES

Mammalian cell culture and transfection

HeLa, HeLa H2B-GFP (Kanda et al., 1998) and HEK 293T cells were cultured in DMEM containing 50 µg/ml gentamicin supplemented with 10% FCS. HEK 293T cells were transfected with plasmid DNA using TransFectin™ reagent (Bio-Rad Laboratories) according to the manufacturers guidelines and incubated either overnight, 48 h or 72 h before performing immunoprecipitation. Cells grown on coverslips were cotransfected with jetPEI, (Poly Plus Transfection) according to the manufacturer's instructions, 24 h prior to fixation.

C2C12 and C2C12-GFP, a subclone of a mouse myoblast cell line, were cultivated in DMEM, 4.5 g/l glucose, 1% L-Glutamine, and 10 FCS (Blau et al., 1985).

Immunofluorescence

Cells were fixed in 3.7% formaldehyde for 10 min and permeabilized with 0.5% Triton X-100 in PBS. For immunofluorescence an anti-PML (5E10) mouse primary antibody (diluted in PBS containing 2% BSA) was used. For detection a secondary antibody (diluted 1:400 in PBS containing 2% BSA) conjugated to Alexa Fluor 555 (Molecular Probes) was then used. Cells were counterstained with DAPI and mounted in Vectashield (Vector Laboratories).

Confocal Microscopy

Confocal microscopy was carried out with a Leica TCS SP2 AOBS confocal laser scanning microscope equipped with a HCX PL 63x/1.4 NA oil immersion objective. Fluorophores were exited using a 405 nm diode laser line, a 488 nm Ar laser line and a 561 nm diode-pumped solide-state (DPSS) laser line. Confocal image series were typically recorded with a frame size of 512x512 pixels, a pixel sizes between 50 - 100 nm, a typical z-step size of 250 nm and the pinhole opened to 1 Airy unit. A maximum intensity projection of several confocal mid z-sections was then performed using ImageJ (Version 1.37, http://rsb.info.nih.gov/ij/).

Gel filtration

10 µg IMAC purified GBP were loaded on a Superdex-75 column (Amersham Pharmacia Biotech) and chromatographed at a flowrate of 0.5 ml/min in column buffer (1xPBS, 0.5 mM EDTA). BSA (66 kDa), carbonic anhydrase (29.5 kDa) and cytochrome c (12.5 kDa) were used as calibration standards. For complex analysis 2 mg of GBP were incubated for 20 min with 2 mg of purified GFP in 500 µl column buffer and subsequently subjected to gel filtration analysis. Eluted proteins were subjected to SDS-PAGE followed by staining with Coomassie Blue (Invitrogen).

SDS-PAGE and Western blot analysis

Indicated protein fractions were separated on an SDS–PAGE (12% - 15%) or on a 4% – 12% NuPAGE Novex bis-Tris precast gel subsequently stained with Coomassie Blue (Invitrogen) or electrophoretically transferred to nitrocellulose membrane (Bio-Rad Laboratories). The membrane was blocked with 3% milk in PBS containing 0.1% Tween 20 (T-PBS) and incubated for 1 h at RT or overnight at 4°C with the indicated antibodies. After washing with T-PBS the membrane was incubated with secondary antibodies conjugated with horseradish peroxidase (HRP). Immunoreactive bands were visualized with ECL Western Blot Detection Kit (Amersham Biosciences).

Binding assays under high selective condition

The soluble protein extract of HEK 293T cells expressing GFP were adjusted with 5 M NaCl to final concentrations of 150 mM, 0.5 M, 1 M and 2 M NaCl prior adding the GFP-nanotrap. Binding occurs for 10 min at 4°C and constant rotation. After a centrifugation step (2 min, 5000xg, 4°C) the supernatant was removed and 2% was used for SDS-PAGE (referred to as flow through). The bead pellets were washed (2x) in 1 ml dilution buffer containing 300 mM NaCl. Bound proteins were eluted by resuspending the beads in 2x SDS-containing sample buffer and boiling for 10 min at 95°C. For analyzing different temperature conditions immunoprecipitation were carried out as described. After the last washing step the beads pellet was resuspended in 100 µl dilution buffer and incubated at 25°C, 45°C and 65°C respectively for 30 min. Beads were harvested by centrifugation (2 min, 5000xg), the supernatant containing the released protein (R) was removed and 50 µl 3x SDS-containing sample buffer was added. Proteins remaining bound to the beads were eluted as described. To test increasing pH-values the bead pellet was resuspended after immunoprecipitation in dilution buffer adjusted to pH 8, pH 9, pH 10 or pH 11 and incubated for 1 h at room temperature. Subsequently the samples were treated as described. For decreasing pH-conditions, the beads pellet was incubated for 1 min with 0.1 M glycine pH 4.0, 3.2 or 2.5 and subsequently neutralized by adding 2 µl of 1 M Tris-base.

Sequences of oligonucleotides for ChIP experiments

Table 1

oligo name	Sequence	location
IL6 promoter_forward	CCACCCTCCAACAAAGATTTTTATC	1175-1199; acc.: M20572
Il6 promoter_reverse	CTGCCTCACACTCCTCTCTCACAG	1390-1413; acc.: M20572
Il6 control1_forward	AACAAGAAAGACAAAGCCAGAGTCC	6123-6147; acc.: M20572
Il6 control1_reverse	AAACCCCAAAGTAAAACAAAGCAAG	6304-6328; acc.: M20572
Il6 control2_forward	TCTTCCCACAGCCCAGAACAC	7373-7393; acc.: M20572
Il6 control2_reverse	TGGATGGTCTTGGTCCTTAGCC	7535-7556; acc.: M20572
IgfBP1 promoter1_for	GTCGCTTAGGTTTTCTGTGAGCC	2233-2255; acc.: AL607124
IgfBP1 promoter1_rev	TGGGTGGAAGGGGGTAAAGG	2394-2413; acc.: AL607124
IgfBP1 control1 for F11	CAGCAAATAGCCAGGGTCGG	5241-5260; acc.: AL607124
IgfBP1 control1 revB15	TGAGACAGAGCAGGAGCAGCC	5440-5460; acc.: AL607124
IgfBP1 control2 forF285	AAGCAGGAAGGATGGAGGGG	46095-46114; acc.: AL607124
IgfBP1 control2 revB299	TTTTGTGGCTGAATCGGTGTTC	46305-46284; acc.: AL607124

Table1: Sequence and location of oligonucleotides used for quantitative PCR-analysis of ChIP experiments

SUPPLEMENTAL FIGURES

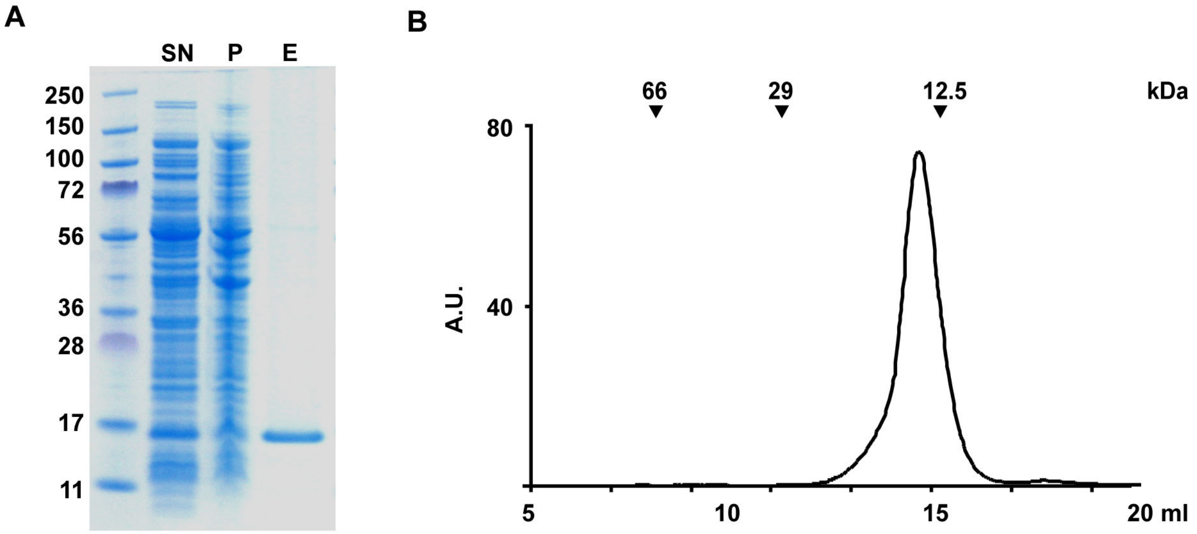

Supplemental Fig. S1. Purification of recombinant GBP by immobilized affinity chromatography (IMAC). (A) Soluble *E.coli* protein extract was subjected to IMAC. Supernatant (SN), pellet (P) and pooled elution fractions (E) were analyzed by SDS-PAGE and coomassie staining. **(B)** Gel filtration analysis of IMAC purified GBP. Purified GBP (10 µg) was subjected to gel filtration on a Superdex-75 column. GBP elutes from the column in peak fractions corresponding to an apparent molecular mass of ~13 kDa. Arrows indicate the elution of calibration standards: BSA (66 kDa), carbonic anhydrase (29.5 kDa) and cytochrome C (12.5 kDa).

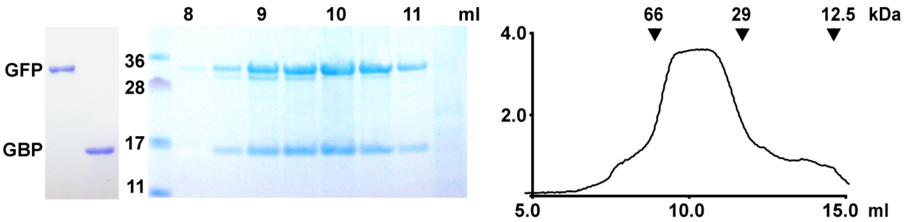

Supplemental Fig. S2. Determination of the native molecular weight of the recombinant GFP-GBP complex. Purified GFP was mixed with GBP in stoichometric amounts, and subjected to gelfiltration analysis on a Superdex-75 column. Elution fractions were subjected to SDS-PAGE and analyzed by Coomassie Blue staining (left panel). The elution profile of the complex is shown in the right panel. Arrows indicate the elution of calibration standards: BSA (66 kDa), carbonic anhydrase (29.5 kDa) and cytochrome C (12.5 kDa).

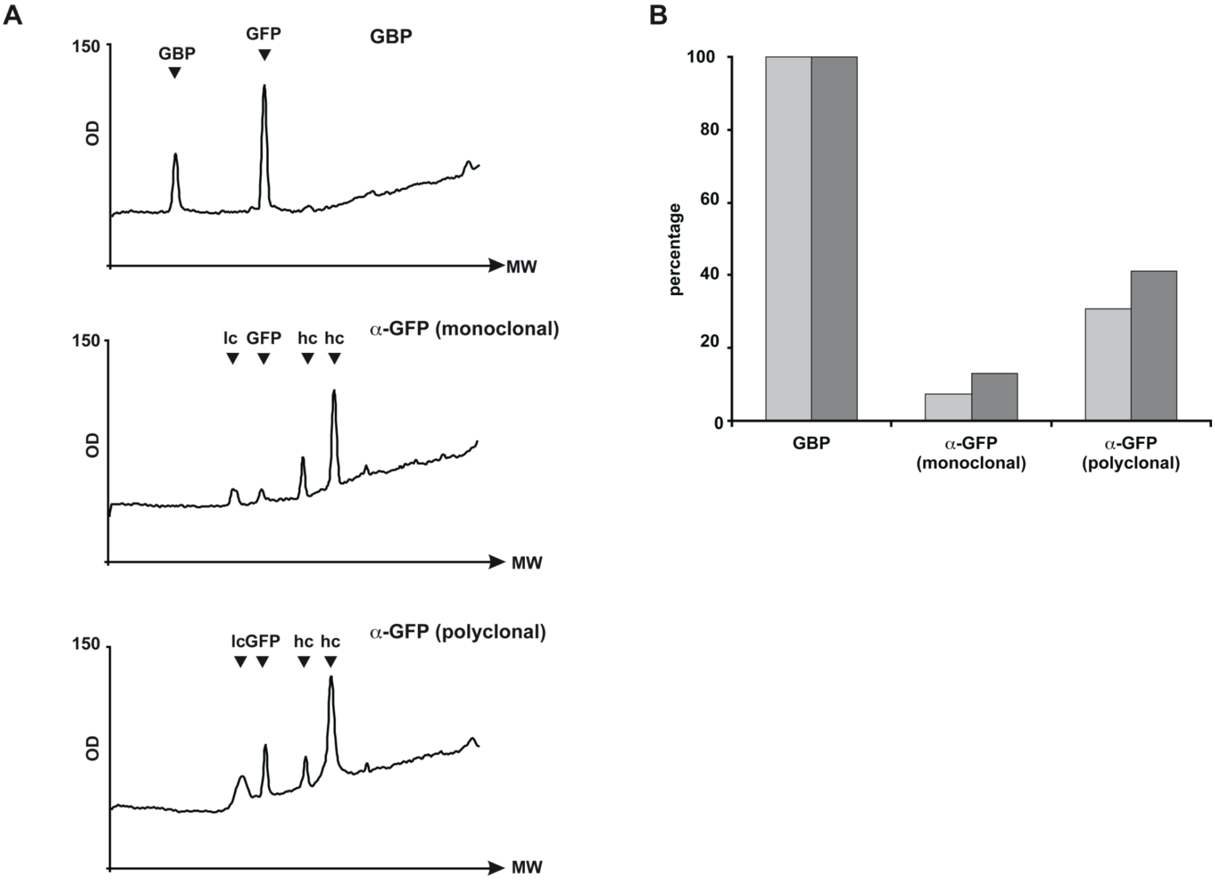

Supplemental Fig. S3. Comparison of GBP with mono- and polyclonal anti-GFP antibodies (A) Intensity profile of bound fractions (B) obtained with GBP, mono- and polyclonal GFP antibodies as shown in **Figure 2A**. Peaks corresponding to GFP, heavy (hc) and light antibody chains (lc) and GBP are indicated. **(B)** Quantification of GFP precipitated with GBP, mono- and polyclonal anti-GFP antibodies. Relative amounts were determined by densitometry of Coomassie Blue stained gels (dark grey bars) and immunostained blots (light grey bars) using ImageJ software (Version 1.34, http://rsb.info.nih.gov.ij/).

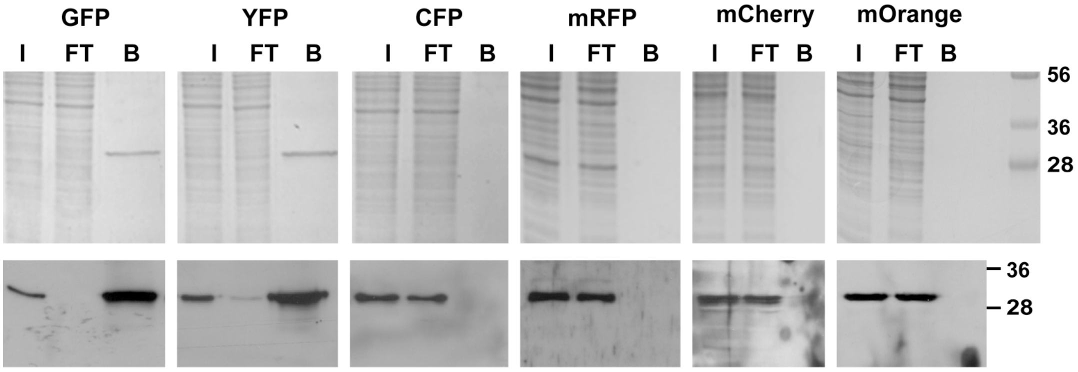
GFP
YFP
CFP
mRFP
mCherry
mOrange
I FT B
I FT B
I FT B
I FT B
I FT B
I FT B
56
36
28
36
28

Supplemental Fig. S4. Specificity of the GFP-nanotrap. Protein extracts of HEK 293T cells expressing either GFP, YFP, CFP, mRFP, mCherry or mOrange were subjected to one-step purification with the GFP-nanotrap. Input (I), flow through (FT) and bound fractions (B) were separated by SDS-PAGE and visualized by Coomassie Blue staining and immunoblotting using an anti-GFP antibody recognizing GFP, YFP, CFP and an anti-mRFP antibody recognizing mRFP, mCherry, mOrange respectively.

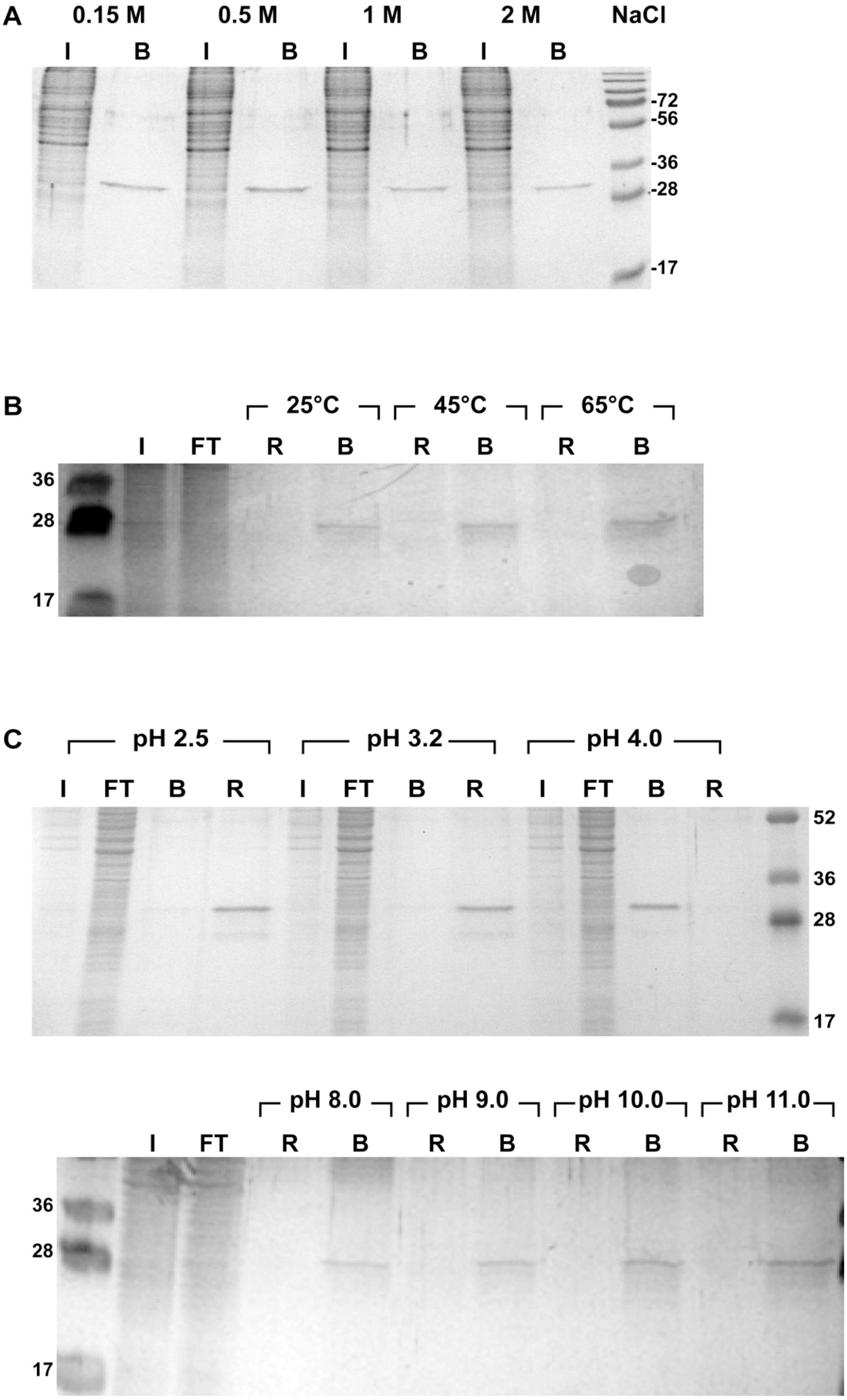
A
0.15 M
0.5 M
1 M
2 M
NaCl
I B I B I B I B
-72
-56
-36
-28
-17
B
25°C
45°C
65°C
I FT R B R B R B
36
28
17
C
pH 2.5
pH 3.2
pH 4.0
I FT B R I FT B R I FT B R
52
36
28
17
pH 8.0
pH 9.0
pH 10.0
pH 11.0
I FT R B R B R B R B
36
28
17

Supplemental Fig. S5. The GFP-nanotrap efficiently binds its epitope even under extreme conditions. Protein extracts of HEK 293T cells expressing GFP were subjected to one-step purification at **(A)** increased NaCl molarity or **(B)** rising temperature or **(C)** different pH conditions. Aliquots of released (R) and bound (B) fractions were separated by SDS-PAGE and visualized by Coomassie Blue staining.

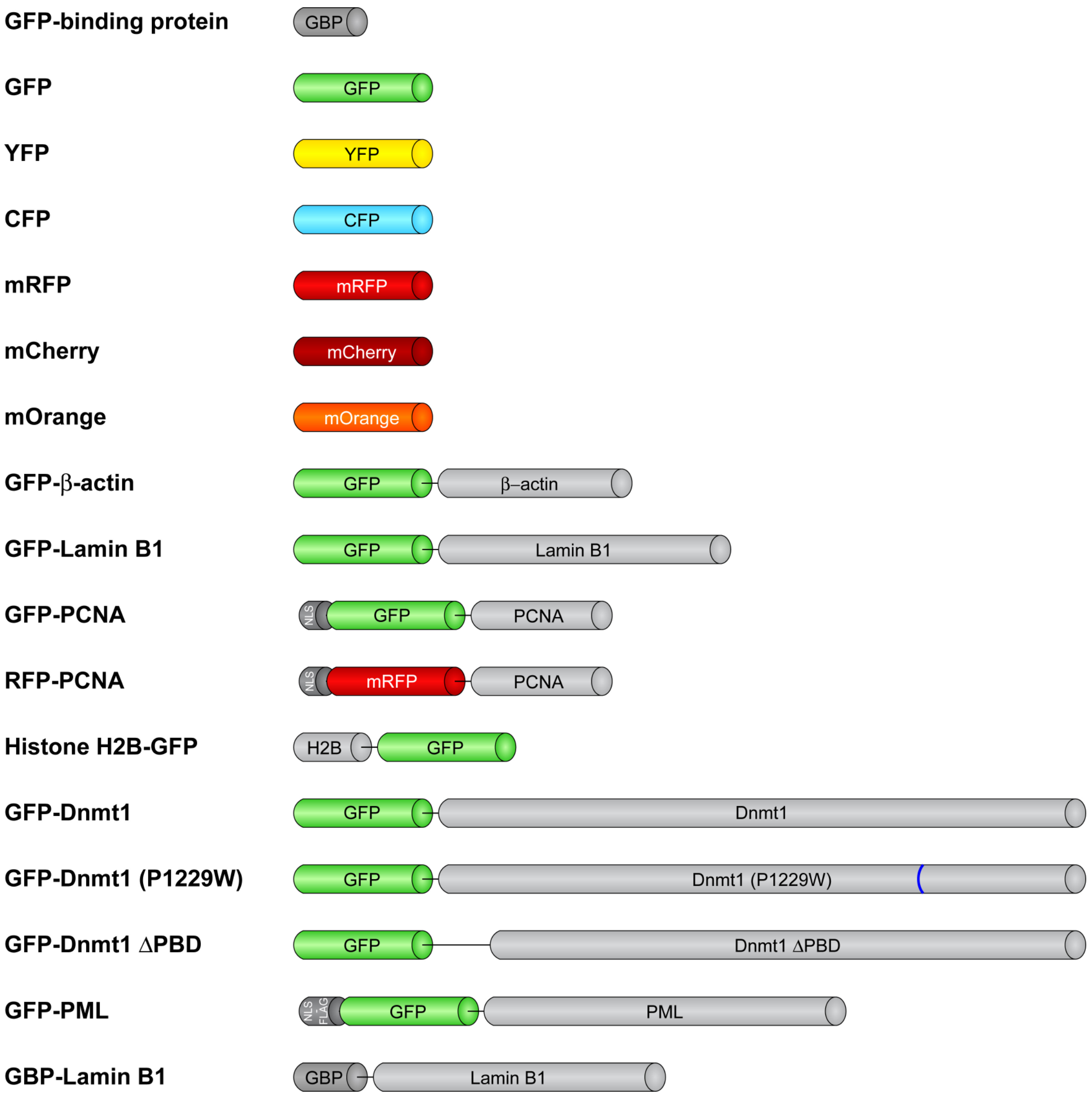
GFP-binding protein
GBP
GFP
GFP
YFP
YFP
CFP
CFP
mRFP
mRFP
mCherry
mCherry
mOrange
mOrange
GFP-β-actin
GFP
β–actin
GFP-Lamin B1
GFP
Lamin B1
GFP-PCNA
NLS
GFP
PCNA
RFP-PCNA
NLS
mRFP
PCNA
Histone H2B-GFP
H2B
GFP
GFP-Dnmt1
GFP
Dnmt1
GFP-Dnmt1 (P1229W)
GFP
Dnmt1 (P1229W)
GFP-Dnmt1 ΔPBD
GFP
Dnmt1 ΔPBD
GFP-PML
NLS
FLAG
GFP
PML
GBP-Lamin B1
GBP
Lamin B1

Supplemental Fig. S6. Schematic representation of all proteins used in this study.

II.4. TRAPPED IN ACTION: DIRECT VISUALIZATION OF DNA METHYLTRANSFERASE ACTIVITY IN LIVING CELLS

© 2005 Nature Publishing Group http://www.nature.com/naturemethods

Trapped in action: direct visualization of DNA methyltransferase activity in living cells

Lothar Schermelleh[1], Fabio Spada[1], Hariharan P Easwaran[2], Kourosh Zolghadr[1], Jean B Margot[2], M Cristina Cardoso[2] & Heinrich Leonhardt[1,2]

DNA methyltransferases have a central role in the complex regulatory network of epigenetic modifications controlling gene expression in mammalian cells. To study the regulation of DNA methylation in living cells, we developed a trapping assay using transiently expressed fluorescent DNA methyltransferase 1 (Dnmt1) fusions and mechanism-based inhibitors 5-azacytidine (5-aza-C) or 5-aza-2′-deoxycytidine (5-aza-dC). These nucleotide analogs are incorporated into the newly synthesized DNA at nuclear replication sites and cause irreversible immobilization, that is, trapping of Dnmt1 fusions at these sites. We measured trapping by either fluorescence bleaching assays or photoactivation of photoactivatable green fluorescent protein fused to Dnmt1 (paGFP-Dnmt1) in mouse and human cells; mutations affecting the catalytic center of Dnmt1 prevented trapping. This trapping assay monitors kinetic properties and activity-dependent immobilization of DNA methyltransferases in their native environment, and makes it possible to directly compare mutations and inhibitors that affect regulation and catalytic activity of DNA methyltransferases in single living cells.

DNA methylation has a central role in the epigenetic control of mammalian gene expression during development and is required for X inactivation, genomic imprinting and silencing of retroviral elements[1,2]. Until now, four DNA methyltransferases, Dnmt1, Dnmt2, Dnmt3a and Dnmt3b, are known in mammals, although the functional significance of the weak activity of Dnmt2 is still unclear[3–7]. Dnmt3a and Dnmt3b are *de novo* methyltransferases implicated in setting up DNA methylation patterns during development[1]. The major mammalian DNA methyltransferase, Dnmt1, maintains the methylation patterns after DNA replication and associates with the replication machinery during S phase[8]. Dnmt1 has been shown to interact with several different proteins including PCNA, HDACs, SUV39H1, HP1, MeCP2, DMAP1, E2F1, pRb and p53 (refs. 9–14). Changes in DNA methylation patterns, that is, general hypomethylation and local hypermethylation, are commonly found in cancerous cells[15], and hypomethylation has been directly shown to cause genome instability and tumors in mice[16]. The regulatory mechanism(s) responsible for these methylation changes are still unknown. Notably, maintenance of methylation patterns has been observed in the human HCT116 colorectal carcinoma cell line after inactivation of both *DNMT1* alleles, indicating possible differences in the regulation of DNA methylation in mouse and human or in transformed cells[17].

The basic enzymatic mechanism of the methylation reaction has been worked out *in vitro* by biochemical studies with purified enzymes[18,19]. The regulation of DNA methylation in mammalian cells, however, is still far from being understood, mostly owing to the fact that multiple methyltransferases are involved that interact with each other as well as with many nuclear factors. Moreover, the substrate itself, the cytosine residue, is embedded in highly dynamic and regulated chromatin structure. Here we describe a method to assay the activity of Dnmt1 in defined chromatin domains of single living cells. The method is based on the ability of Dnmt1 to form a stable covalent complex with the mechanism-based inhibitors 5-aza-C and 5-aza-dC upon their incorporation into DNA during replication. Trapping of GFP-Dnmt1 fusions is measured by fluorescence recovery after photobleaching (FRAP) analysis and reflects the enzymatic activity of the fusion protein. This assay can be used for studying the activity and targeting of Dnmt1 mutants, and for testing candidate catalytic inhibitors in living cells.

RESULTS

Rationale of the DNA methyltransferase trapping assay

To directly test the enzymatic activity of DNA methyltransferases in single living cells we developed an assay based on FRAP measurements in the presence of 5-aza-C and 5-aza-dC. The assay takes advantage of the transient covalent complex formation of the methyltransferase with the C6 position of the cytosine base ring to activate the C5 position for methyl group transfer[20,21]. After methyl group transfer the enzyme is released from the complex by β elimination with the proton at the C5 position (**Fig. 1a**). The DNA methyltransferase inhibitors 5-aza-C and 5-aza-dC are widely used in research and clinical applications as demethylating drugs[22]. Both inhibitors are incorporated during DNA replication instead of cytosine residues throughout the genome including at potential methylation sites. The absence of the proton at the C5 position of the 5-aza analog prevents β elimination, the final step of the methylation reaction, leaving the methyltransferase trapped

---

[1]Ludwig Maximilians University Munich, Department of Biology II, Großhaderner Str. 2, 82152 Planegg-Martinsried, Germany. [2]Max Delbrueck Center for Molecular Medicine, FVK, Wiltbergstr. 50, 13125 Berlin, Germany. Correspondence should be addressed to H.L. (h.leonhardt@lmu.de).

RECEIVED 11 JULY; ACCEPTED 12 AUGUST; PUBLISHED ONLINE 22 SEPTEMBER 2005; DOI:10.1038/NMETH794

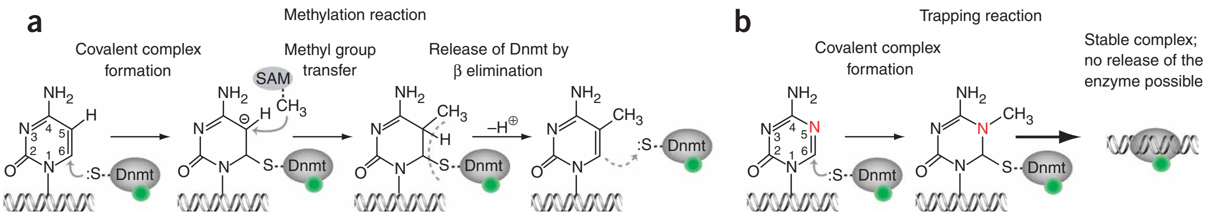
a
Methylation reaction
Covalent complex formation
Methyl group transfer
Release of Dnmt by β elimination
SAM
NH2
H
CH3
–H⊕
:S
Dnmt
b
Trapping reaction
Covalent complex formation
Stable complex; no release of the enzyme possible
N
1 2 3 4 5 6

Figure 1 | Schematic representation of the DNA methylation reaction. (**a**) A covalent complex is formed between the sulfhydryl group of cysteine in the Pro-Cys motif of DNA methyltransferase (Dnmt) and the C6 position of cytosine base ring. Then a methyl group is transferred from *S*-adenosyl-L-methionine (SAM) followed by the release of the enzyme. (**b**) The absence of a proton at the N5 position of the 5-aza-C base ring prevents β elimination and thus causes trapping of the enzyme. Green dots represent GFP fused to the enzyme.

(**Fig. 1b**). Consequently, the free enzyme pool is depleted with progressing S phase, and existing methylation patterns cannot be maintained leading to global genome demethylation.

Direct visualization of DNA methyltransferase trapping

To visualize the distribution and mobility of Dnmt1 in living cells, we constructed a GFP-Dnmt1 fusion comprising the ubiquitously expressed long isoform of the mouse Dnmt1 tagged at the amino terminus with enhanced GFP[23]. GFP-Dnmt1 is catalytically active as it is able to restore cytosine methylation levels when transiently expressed in mouse embryonic stem (ES) cells deficient of Dnmt1 (**Supplementary Fig. 1** online). Coexpression in mouse myoblast cells of GFP-Dnmt1 and proliferating cell nuclear antigen (PCNA) fused to red fluorescent protein (RFP-PCNA) that labels sites of DNA replication[24] showed that the GFP-Dnmt1 localizes at S phase replication foci just like endogenous Dnmt1 (**Fig. 2a** and ref. 23). After bleaching of single or multiple replication foci, we observed nearly complete recovery of the GFP signal within about 90 s indicating a rapid recruitment of new, fluorescent Dnmt1 fusion proteins at these sites. In contrast, the recovery of RFP-PCNA fluorescence was much slower, and the partial recovery after several minutes is likely to be caused by a *de novo* assembly of the trimeric PCNA ring at adjacent replication sites rather than by a constant protein exchange[25]. After the incubation with 5-aza-C, however, we observed no recovery of GFP-Dnmt1 fluorescence at bleached replication foci (**Fig. 2b**) reflecting the depletion of the mobile fraction caused by trapping of the active fusion protein at the newly synthesized DNA. This is consistent with the observation that after incubation with 5-aza-C GFP-Dnmt1 no longer colocalized with RFP-PCNA but seemed to be retained at earlier, adjacent replication sites. These results demonstrate a 5-aza-C–dependent immobilization of GFP-Dnmt1 at sites of DNA replication.

Enzyme trapping depends on catalytic activity

Because 5-aza-C is a mechanism-based inhibitor, immobilization of the GFP-Dnmt1

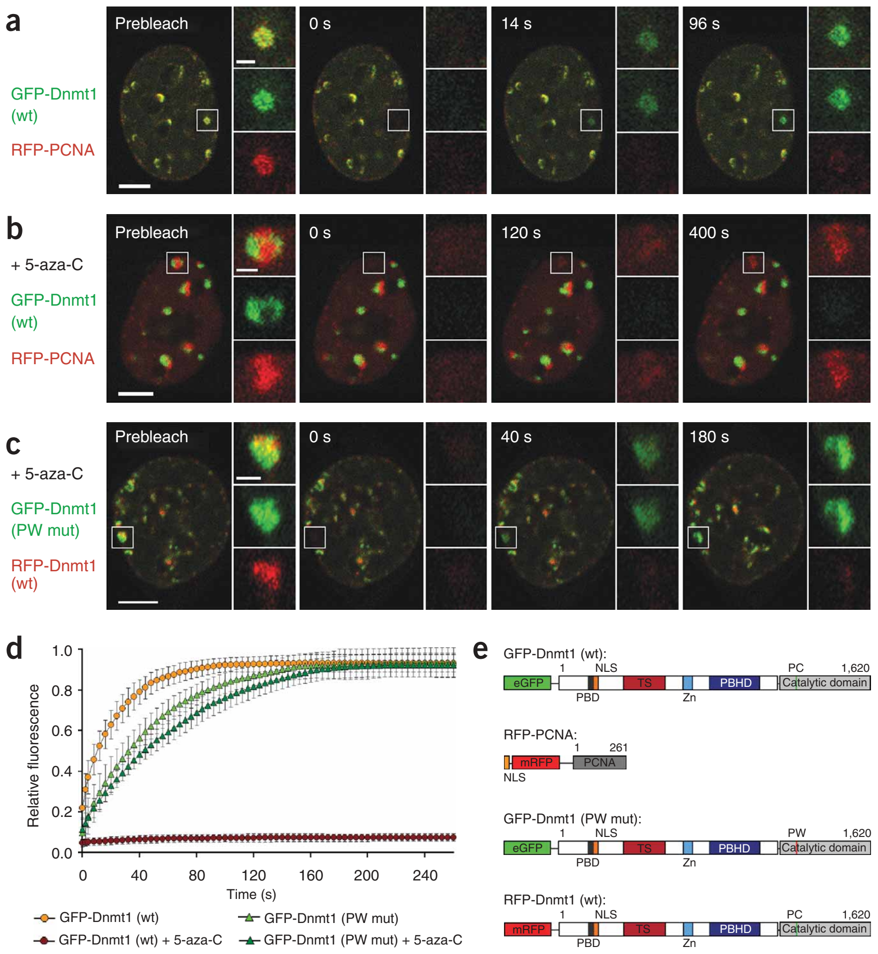
a
GFP-Dnmt1 (wt)
RFP-PCNA
Prebleach
0 s
14 s
96 s
b
+ 5-aza-C
GFP-Dnmt1 (wt)
RFP-PCNA
Prebleach
0 s
120 s
400 s
c
+ 5-aza-C
GFP-Dnmt1 (PW mut)
RFP-Dnmt1 (wt)
Prebleach
0 s
40 s
180 s
d
Relative fluorescence
1.0
0.8
0.6
0.4
0.2
0.0
0
40
80
120
160
200
240
Time (s)
GFP-Dnmt1 (wt)
GFP-Dnmt1 (PW mut)
GFP-Dnmt1 (wt) + 5-aza-C
GFP-Dnmt1 (PW mut) + 5-aza-C
e
GFP-Dnmt1 (wt):
1
NLS
PC
1,620
eGFP
TS
PBHD
Catalytic domain
PBD
Zn
RFP-PCNA:
1
261
mRFP
PCNA
NLS
GFP-Dnmt1 (PW mut):
1
NLS
PW
1,620
eGFP
TS
PBHD
Catalytic domain
PBD
Zn
RFP-Dnmt1 (wt):
1
NLS
PC
1,620
mRFP
TS
PBHD
Catalytic domain
PBD
Zn

Figure 2 | Trapping of active Dnmt1 after 5-aza-C treatment. (**a**) FRAP of GFP-Dnmt1 and RFP-PCNA coexpressed in mouse myoblasts without drug treatment. Late S phase nucleus with GFP-Dnmt1 (green) and RFP-PCNA (red) largely colocalize at replication sites. Inset shows the replication focus. (**b**) Analogous experiment after treatment with 300 μM 5-aza-C for 2 h. (**c**) Comparative FRAP of wild-type RFP-Dnmt1 and the GFP-Dnmt1 PW mutant after treatment with 300 μM 5-aza-C for 2 h. Bars in **a**–**c** represent 5 μm (1 μm in insets). (**d**) Quantitative evaluation of FRAP data showing mean curves. Error bars represent standard deviations. For comparison, only late S phase nuclei were evaluated. (**e**) Schematic representation of the fusion proteins. PBD, PCNA binding domain; NLS, nuclear localization sequence; TS, targeting sequence; Zn, Zn-binding domain; PBHD, poly(bromo) homology domain.

© 2005 Nature Publishing Group http://www.nature.com/naturemethods

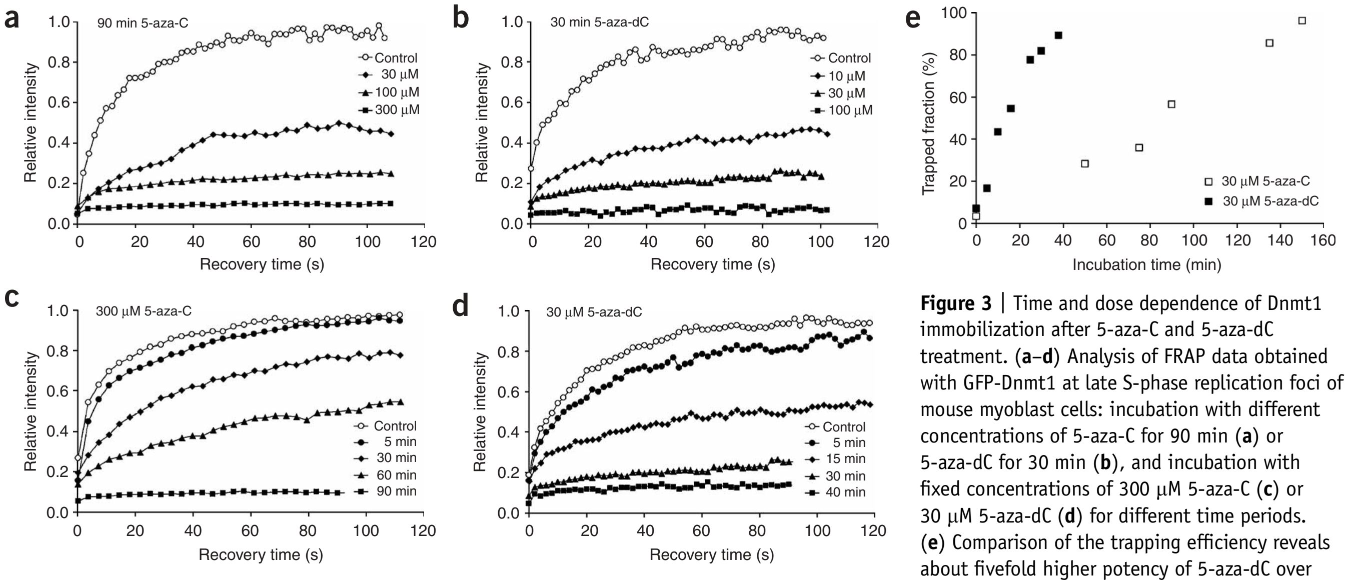

Figure 3 | Time and dose dependence of Dnmt1 immobilization after 5-aza-C and 5-aza-dC treatment. (**a**–**d**) Analysis of FRAP data obtained with GFP-Dnmt1 at late S-phase replication foci of mouse myoblast cells: incubation with different concentrations of 5-aza-C for 90 min (**a**) or 5-aza-dC for 30 min (**b**), and incubation with fixed concentrations of 300 µM 5-aza-C (**c**) or 30 µM 5-aza-dC (**d**) for different time periods. (**e**) Comparison of the trapping efficiency reveals about fivefold higher potency of 5-aza-dC over 5-aza-C, reflecting the higher incorporation rate of the deoxy variant.

© 2005 Nature Publishing Group http://www.nature.com/naturemethods

fusion should be a direct measure of methyltransferase activity. To directly test this, we introduced a site-specific mutation inactivating the catalytic center of Dnmt1. We mutated the conserved Pro-Cys motif, which is involved in the covalent complex formation[21], by exchanging the cysteine for a tryptophan (Dnmt1 C1229W, here referred to as PW mutant). For direct comparison we generated an RFP-tagged wild-type Dnmt1 and cotransfected cells with the wild-type and mutant construct. Both fusion proteins localized at replication foci in S-phase cells as observed for the native protein. In sharp contrast to the wild-type Dnmt1 fusion, the PW mutant did still recover after photobleaching even after 2 h of incubation with 300 µM 5-aza-C (**Fig. 2c**). This indicates that the mutant protein does not form a covalent complex with the DNA, which is consistent with earlier biochemical studies on bacterial DNA (cytosine-5) methyltransferases[26]. In control experiments without 5-aza-C treatment, we determined a mobile fraction of ~90% for both, wild-type Dnmt1 and PW mutant (**Fig. 2d**). After 90–120 min incubation with 5-aza-C, however, the mobile fraction of the active wild-type fusion dropped to ~5%, whereas the mobility of the PW mutant was not affected. Half-times of recovery ($t_{1/2}$) were 15 s and 34 s for wild type and PW mutant, respectively, without 5-aza-C treatment, and 40 s for the PW mutant after 5-aza-C treatment (300 µM, 120 min). The slower recovery of the PW mutant as compared to the wild-type fusion in untreated cells may be due to altered dissociation kinetics of the mutant. The decelerated recovery of the PW mutant in the presence of 5-aza-C is likely due to a general slowdown of the replication and methylation machinery caused by trapping of the endogenous Dnmt1 protein. The fusion proteins are schematically represented in **Figure 2e**. Taken together, the catalytic activity of a Dnmt1 fusion construct can be directly assayed as covalent complex formation rate by FRAP in the presence of 5-aza-C.

Trapping rate is inhibitor-, dose- and time-dependent

To evaluate the trapping assay we compared different incubation times and concentrations of the two widely used demethylating drugs 5-aza-C and 5-aza-dC (**Fig. 3**). In comparison, 5-aza-dC was more potent than 5-aza-C in depleting the nucleoplasmic pool of GFP-Dnmt1. About threefold lower concentrations and threefold shorter incubation times were sufficient to reach the same levels of depletion with 5-aza-dC as compared to 5-aza-C (**Fig. 3a**,**b**). With longer incubation times the nucleoplasmic GFP-Dnmt1 pool became progressively immobilized in cells treated with 300 µM 5-aza-C or 30 µM 5-aza-dC, until complete depletion was reached after about 90 min or 40 min, respectively (**Fig. 3c**,**d** and **Supplementary Video 1** online). Direct comparison of the same concentration of the two inhibitors showed that 5-aza-dC is about fivefold more potent than 5-aza-C in depleting the nucleoplasmic pool of GFP-Dnmt1 (**Fig. 3e**). This is consistent with the fact that 5-aza-dC is directly incorporated into DNA, whereas 5-aza-C has to be modified before incorporation and can also be incorporated into RNA[27,28]. These results demonstrate that the assay is sensitive to the type of inhibitor, its dose and incubation time.

Experiments with human DNMT1 fused to GFP expressed in human neuroblastoma cells also showed trapping of the fusion protein upon treatment with 5-aza-dC, thus demonstrating the general applicability of the trapping assay not only in mouse but also in human cells (**Supplementary Fig. 2** online).

Direct visualization of trapping with paGFP-Dnmt1

For further dynamic studies we fused Dnmt1 to photoactivatable GFP (paGFP-Dnmt1) and coexpressed with RFP-PCNA to mark replication sites. Photoactivatable GFP has a low initial absorbance at 488 nm, which increases ~100-fold by photoconversion after excitation with ~400-nm light[29]. Photoactivation of paGFP-Dnmt1 at replication sites in an untreated control cell revealed rapid dissociation of paGFP-Dnmt1 (**Fig. 4a**). Upon treatment with 5-aza-dC we observed no dissociation of paGFP-Dnmt1, directly showing the trapping of the enzyme (**Fig. 4b**). In contrast, local activation of paGFP-Dnmt1 in a G1 nucleus was followed by a quick redistribution throughout the entire nucleus as no incorporation of 5-aza-dC can take place at this cell cycle stage (**Fig. 4c**).

© 2005 Nature Publishing Group http://www.nature.com/naturemethods

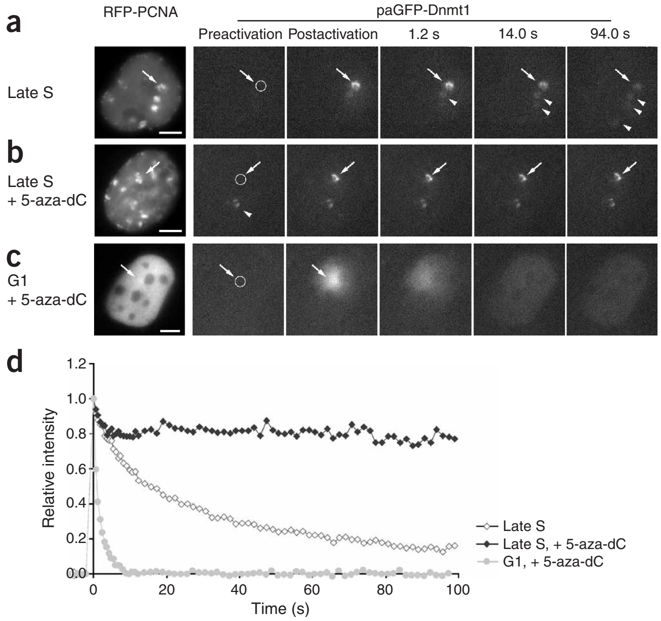

Figure 4 | Direct visualization of trapping by photoactivation of paGFP-Dnmt1. (**a**–**c**) Mouse myoblast cells were cotransfected with RFP-PCNA to identify cell cycle stage and replication sites of S-phase cells. Photoactivated paGFP-Dnmt1 dissociates from the irradiated site (indicated by arrows) and associates with neighboring replication sites (indicated by arrowheads) until a new equilibrium is reached (94 s; **a**). Upon treatment with 30 μM 5-aza-dC for 1 h, no dissociation of paGFP-Dnmt1 is observed (arrow; **b**). The arrowhead indicates a replication focus irradiated a few minutes earlier. Note that fluorescence intensity of trapped paGFP-Dnmt1 at this site also does not change during the time course. Local activation of paGFP-Dnmt1 (arrow) in a G1 nucleus is followed by a quick redistribution throughout the entire nucleus, as no incorporation of 5-aza-dC can take place in this cell cycle stage (**c**). (**d**) Quantitative evaluation of the fluorescence activation experiments shown in **a**–**c**.

These fundamental differences in Dnmt1 dissociation kinetics are underscored by the quantitative evaluation (**Fig. 4d**). Without treatment paGFP-Dnmt1 dissociates with a $t_{1/2}$ of ~12 s to reach a level of ~15% at the end of the observation period. After 5-aza-dC treatment fluorescence levels drop to ~80% of the initial fluorescence and then remain constant during the rest of the observation period. In G1 nuclei, paGFP-Dnmt1 shows a very rapid dissociation to 0% with a $t_{1/2}$ of ~0.5 s. This application of paGFP is the first direct demonstration of the action of mechanism-based inhibitors and covalent complex formation with DNA methyltransferases in living cells.

DISCUSSION

We owe most of our basic knowledge about DNA methylation to classical biochemical approaches, which cannot reproduce the complexity of living, mammalian cells. Recent biochemical studies of DNA methyltransferase activity involved detection of either lowered DNA methyltransferase levels in nuclear extracts[30,31] or of elevated levels of DNA methyltransferase–DNA adducts in genomic DNA extracts after 5-aza-dC treatment in both cases by immunoblotting analysis[32]. The trapping assay described here makes it possible for the first time to study Dnmt1 in its natural environment with its natural substrate in the context of dynamic chromatin structures and simultaneously ongoing DNA replication. Both activity and subnuclear targeting of DNA methyltransferases can be analyzed *in situ* at different cell cycle stages in single living cells.

The basic principle of the trapping assay and its application to test catalytic mutants and potential inhibitors of the catalytic domain is illustrated in **Figure 5**. The method takes advantage of the covalent complex formation of DNA methyltransferases with cytosine residues during catalysis. By using a catalytic mutant of Dnmt1 we show that trapping depends on catalytic activity, providing direct evidence that the technique can be used to monitor DNA methyltransferases actively engaged in the methylation reaction. Comparing different concentrations and incubation times of known DNA methyltransferase inhibitors, 5-aza-C and 5-aza-dC, we demonstrate the sensitivity of this assay.

The assay can be applied to all DNA (cytosine-5) methyltransferases that form a covalent complex with cytosine residues and have a mobile nuclear distribution. Here we focus on Dnmt1 as it is of major clinical relevance. Unlike *de novo* methyltransferases, Dnmt1 is ubiquitously expressed in proliferating cells in which it

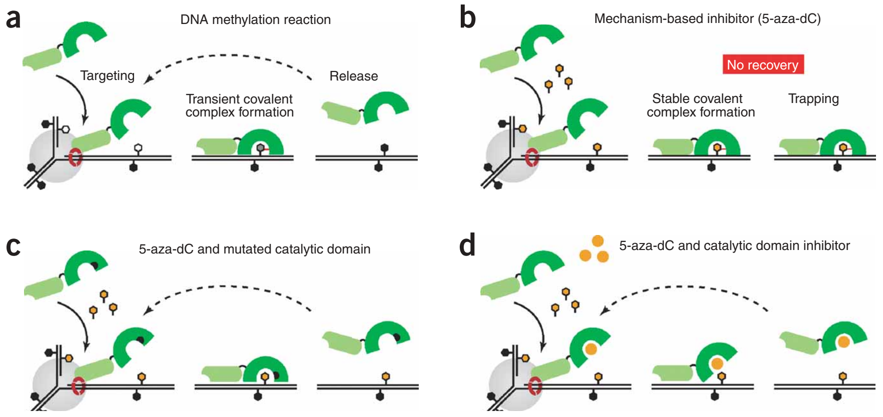

Figure 5 | Postreplicative action of Dnmt1 and rationale of the trapping assay. (**a**) Regulatory and catalytic domains of Dnmt1 are in lighter and darker shades of green, respectively. For simplicity only events at the leading strand are shown. Methylated and nonmethylated cytosines are depicted as black and white hexagons, respectively. The trimeric PCNA ring (red) is shown as part of the replication complex (grey circle). Dnmt1 transiently interacts with PCNA at the replication site, binds to CpG sites and forms a transient covalent complex with the cytosine residue (red line). After methyl group transfer the enzyme is released and becomes available for another round of methylation (dotted arrow). (**b**) Mechanism-based inhibitors (orange hexagons) are incorporated into DNA during S phase. Dnmt1 forms a stable complex with these inhibitors and becomes trapped. (**c**) In contrast, trapping is eliminated if the catalytic domain of Dnmt1 is mutated (black dot). (**d**) Likewise, blocking the catalytic site of Dnmt1 with new types of small-molecule inhibitors (filled orange circles) would prevent covalent complex formation.

© 2005 Nature Publishing Group http://www.nature.com/naturemethods

maintains normal as well as aberrant methylation patterns through DNA replication. In cancer cells tumor-suppressor genes are frequently silenced by methylation. Thus, pharmaceutical strategies aim at transient inhibition of Dnmt1 to reactivate such epigenetically silenced genes and re-establish normal cell cycle and growth control[22]. Mechanism-based inhibitors presently under clinical trials, however, generate Dnmt1-DNA adducts that may lead to cytotoxic effects[33]. Therefore, small-molecule inhibitors targeting the catalytic domain of Dnmt1 are actively sought after, and candidate molecules can now be directly tested by their ability to prevent 5-aza-dC–mediated trapping of GFP-Dnmt1 (**Fig. 5d**). It should be noted that some compounds may affect cell cycle progression or DNA replication, which would reduce the incorporation of 5-aza-dC and thus indirectly prevent trapping of DNA methyltransferases. Such unspecific cell cycle progression effects can, however, be identified using the changing subnuclear GFP-Dnmt1 and RFP-PCNA patterns to monitor cell cycle progression[23,34]. In any case, newly identified compounds need to be further characterized *in vitro* with additional biochemical DNA methyltransferase activity assays.

In summary, the mechanism-based trapping assay provides a new approach to directly study the regulation of DNA methylation and to test the effect of mutations and interacting factors in living cells. In addition, this method now makes it possible to directly investigate the cellular effects of demethylating drugs like 5-aza-dC that are widely used in basic research and in cancer therapy and offers an approach to test new types of DNA methyltransferase inhibitors.

METHODS

Cell culture and transfections. We cultured mouse C2C12 myoblast cells in DMEM containing 25 mM HEPES and supplemented with 20% fetal calf serum and 50 μg/ml gentamycin. We grew cells to 30–40% confluence on Lab-Tek chamber slides (Nunc) and then cotransfected them with the indicated expression constructs by standard Ca_2PO_4 DNA coprecipitation followed by a glycerol shock[35], or using TransFectin transfection reagent (Bio-Rad) according to the manufacturer's instructions. We then incubated cells overnight before performing drug treatment and live-cell analysis. For culture, transfection and 5-methylcytosine staining of mouse ES and human cell lines, see **Supplementary Methods** online.

Expression constructs. We visualized replication sites using a red fluorescent fusion with full-length human PCNA (RFP-PCNA)[36]. To generate GFP-Dnmt1 (previously referred to as GMT1L) we cloned the full-length mouse cDNA of the long Dnmt1 isoform in the pEGFP-C1 vector (Clontech)[23]. To generate RFP-Dnmt1 and paGFP-Dnmt1 we replaced the sequence encoding GFP with those encoding mRFP1[37] and paGFP[29], respectively. We introduced the C1229W mutation (PW mutant) into the Dnmt1 cDNA by site-directed mutagenesis (QuikChange Kit, Stratagene) and confirmed it by DNA sequencing. We tested all fusion constructs by expression in COS-7 or 293T cells and subsequent western blot analysis[34].

Live-cell microscopy, FRAP analysis and photoactivation. We added 5-Aza-C or 5-aza-dC (Sigma) at indicated final concentrations and incubated cells as indicated before starting live-cell observations. We performed FRAP experiments using a Zeiss LSM 510 confocal laser scanning microscope with a 63×, 1.4 NA Plan-Apochromat oil immersion objective. We excited fluorophores with a 488-nm Ar laser and a 543-nm HeNe laser. We typically recorded confocal image series with a frame size of 256 × 256 pixels and a pixel size of 70–90 nm. The laser power was typically set to 1–5% transmission with the pinhole opened to 2 Airy units. For FRAP analysis, we selected a region of interest and photobleached it by an intense 488-nm Ar laser beam (laser set to maximum power at 100% transmission) for 1 s. Before and after bleaching, we recorded confocal image series at 2–5 s intervals (typically 6 prebleach and 50–100 postbleach frames). Mean fluorescence intensities of the bleached region were corrected for background and for total nuclear loss of fluorescence over the time course, and normalized to the mean of the last 4 prebleach values. For the quantitative evaluation of FRAP experiments, we averaged data of 4–6 nuclei, calculated the mean curve as well as the standard deviation and displayed these using GraphPad Prism 4.01 software. We calculated the $t_{1/2}$ of recovery from the average curves.

We performed photoactivation experiments using a DeltaVision widefield epifluorescence microscope system (Applied Precision) equipped with a 60×, 1.4 NA Plan-Apochromat objective and appropriate filter sets. Photoactivatable GFP was activated using a 405 nm diode laser coupled into the light path of the microscope. After laser photoactivation for 1 s (100% transmission), we acquired epifluorescence time series at 0.6-s intervals. For quantitative evaluation, we corrected the mean fluorescence intensities of the activated area for background and for the increase of fluorescence in a nonirradiated nuclear control region, and then normalized it to the value of the first time point after activation.

Note: Supplementary information is available on the Nature Methods website.

ACKNOWLEDGMENTS

We thank R.Y. Tsien for providing mRFP1 cDNA, J. Lippincott-Schwartz for providing paGFP cDNA, E. Li for mutant *Dnmt1* ES cells and P. Vertino for the human *DNMT1* cDNA. We thank M. Grohmann for sharing expression constructs. We are grateful to I. Grunewald and A. Gahl for technical assistance. This work was supported by grants from the Deutsche Forschungsgemeinschaft and the Max Delbrück Center to H.L. and M.C.C.

COMPETING INTERESTS STATEMENT

The authors declare that they have no competing financial interests.

Published online at http://www.nature.com/naturemethods/
Reprints and permissions information is available online at http://npg.nature.com/reprintsandpermissions/

1. Li, E. Chromatin modification and epigenetic reprogramming in mammalian development. *Nat. Rev. Genet.* **3**, 662–673 (2002).
2. Jaenisch, R. & Bird, A. Epigenetic regulation of gene expression: how the genome integrates intrinsic and environmental signals. *Nat. Genet.* **33** (Suppl.), 245–254 (2003).
3. Bestor, T.H. The DNA methyltransferases of mammals. *Hum. Mol. Genet.* **9**, 2395–2402 (2000).
4. Robertson, K.D. DNA methylation and chromatin—unraveling the tangled web. *Oncogene* **21**, 5361–5379 (2002).
5. Tang, L.Y. *et al.* The eukaryotic *DNMT2* genes encode a new class of cytosine-5 DNA methyltransferases. *J. Biol. Chem.* **278**, 33613–33616 (2003).
6. Hermann, A., Schmitt, S. & Jeltsch, A. The human Dnmt2 has residual DNA-(cytosine-C5) methyltransferase activity. *J. Biol. Chem.* **278**, 31717–31721 (2003).
7. Kunert, N., Marhold, J., Stanke, J., Stach, D. & Lyko, F.A. Dnmt2-like protein mediates DNA methylation in *Drosophila*. *Development* **130**, 5083–5090 (2003).
8. Leonhardt, H., Page, A.W., Weier, H.U. & Bestor, T.H. A targeting sequence directs DNA methyltransferase to sites of DNA replication in mammalian nuclei. *Cell* **71**, 865–873 (1992).
9. Chuang, L.S. *et al.* Human DNA-(cytosine-5) methyltransferase-PCNA complex as a target for p21WAF1. *Science* **277**, 1996–2000 (1997).

© 2005 Nature Publishing Group http://www.nature.com/naturemethods

10. Rountree, M.R., Bachman, K.E. & Baylin, S.B. DNMT1 binds HDAC2 and a new co-repressor, DMAP1, to form a complex at replication foci. *Nat. Genet.* **25**, 269–277 (2000).
11. Robertson, K.D. *et al.* DNMT1 forms a complex with Rb, E2F1 and HDAC1 and represses transcription from E2F-responsive promoters. *Nat. Genet.* **25**, 338–342 (2000).
12. Fuks, F., Hurd, P.J., Deplus, R. & Kouzarides, T. The DNA methyltransferases associate with HP1 and the SUV39H1 histone methyltransferase. *Nucleic Acids Res.* **31**, 2305–2312 (2003).
13. Kimura, H. & Shiota, K. Methyl-CpG-binding protein, MeCP2, is a target molecule for maintenance DNA methyltransferase, Dnmt1. *J. Biol. Chem.* **278**, 4806–4812 (2003).
14. Esteve, P.O., Chin, H.G. & Pradhan, S. Human maintenance DNA (cytosine-5)-methyltransferase and p53 modulate expression of p53-repressed promoters. *Proc. Natl. Acad. Sci. USA* **102**, 1000–1005 (2005).
15. Jones, P.A. & Baylin, S.B. The fundamental role of epigenetic events in cancer. *Nat. Rev. Genet.* **3**, 415–428 (2002).
16. Gaudet, F. *et al.* Induction of tumors in mice by genomic hypomethylation. *Science* **300**, 489–492 (2003).
17. Rhee, I. *et al.* CpG methylation is maintained in human cancer cells lacking DNMT1. *Nature* **404**, 1003–1007 (2000).
18. Cheng, X. & Roberts, R.J. AdoMet-dependent methylation, DNA methyltransferases and base flipping. *Nucleic Acids Res.* **29**, 3784–3795 (2001).
19. Bestor, T.H. & Verdine, G.L. DNA methyltransferases. *Curr. Opin. Cell Biol.* **6**, 380–389 (1994).
20. Santi, D.V., Garrett, C.E. & Barr, P.J. On the mechanism of inhibition of DNA-cytosine methyltransferases by cytosine analogs. *Cell* **33**, 9–10 (1983).
21. Chen, L. *et al.* Direct identification of the active-site nucleophile in a DNA (cytosine-5)-methyltransferase. *Biochemistry* **30**, 11018–11025 (1991).
22. Christman, J.K. 5-Azacytidine and 5-aza-2′-deoxycytidine as inhibitors of DNA methylation: mechanistic studies and their implications for cancer therapy. *Oncogene* **21**, 5483–5495 (2002).
23. Easwaran, H.P., Schermelleh, L., Leonhardt, H. & Cardoso, M.C. Replication-independent chromatin loading of Dnmt1 during G2 and M phases. *EMBO Rep.* **5**, 1181–1186 (2004).
24. Leonhardt, H. *et al.* Dynamics of DNA replication factories in living cells. *J. Cell Biol.* **149**, 271–280 (2000).
25. Sporbert, A., Gahl, A., Ankerhold, R., Leonhardt, H. & Cardoso, M.C. DNA polymerase clamp shows little turnover at established replication sites but sequential *de novo* assembly at adjacent origin clusters. *Mol. Cell* **10**, 1355–1365 (2002).
26. Wyszynski, M.W., Gabbara, S. & Bhagwat, A.S. Substitutions of a cysteine conserved among DNA cytosine methylases result in a variety of phenotypes. *Nucleic Acids Res.* **20**, 319–326 (1992).
27. Jones, P.A. & Taylor, S.M. Cellular differentiation, cytidine analogs and DNA methylation. *Cell* **20**, 85–93 (1980).
28. Cihak, A. Biological effects of 5-azacytidine in eukaryotes. *Oncology* **30**, 405–422 (1974).
29. Patterson, G.H. & Lippincott-Schwartz, J. A photoactivatable GFP for selective photolabeling of proteins and cells. *Science* **297**, 1873–1877 (2002).
30. Robert, M.F. *et al.* DNMT1 is required to maintain CpG methylation and aberrant gene silencing in human cancer cells. *Nat. Genet.* **33**, 61–65 (2003).
31. Weisenberger, D.J. *et al.* Role of the DNA methyltransferase variant DNMT3b3 in DNA methylation. *Mol. Cancer Res.* **2**, 62–72 (2004).
32. Liu, K., Wang, Y.F., Cantemir, C. & Muller, M.T. Endogenous assays of DNA methyltransferases: Evidence for differential activities of DNMT1, DNMT2, and DNMT3 in mammalian cells *in vivo*. *Mol. Cell. Biol.* **23**, 2709–2719 (2003).
33. Juttermann, R., Li, E. & Jaenisch, R. Toxicity of 5-aza-2′-deoxycytidine to mammalian cells is mediated primarily by covalent trapping of DNA methyltransferase rather than DNA demethylation. *Proc. Natl. Acad. Sci. USA* **91**, 11797–11801 (1994).
34. Easwaran, H.P., Leonhardt, H. & Cardoso, M.C. Cell cycle markers for live cell analyses. *Cell Cycle* **4**, 453–455 (2005).
35. Cardoso, M.C. *et al.* Mapping and use of a sequence that targets DNA ligase I to sites of DNA replication *in vivo*. *J. Cell Biol.* **139**, 579–587 (1997).
36. Sporbert, A., Domaing, P., Leonhardt, H. & Cardoso, M.C. PCNA acts as a stationary loading platform for transiently interacting Okazaki fragment maturation proteins. *Nucleic Acids Res.* **33**, 3521–3528 (2005).
37. Campbell, R.E. *et al.* A monomeric red fluorescent protein. *Proc. Natl. Acad. Sci. USA* **99**, 7877–7882 (2002).

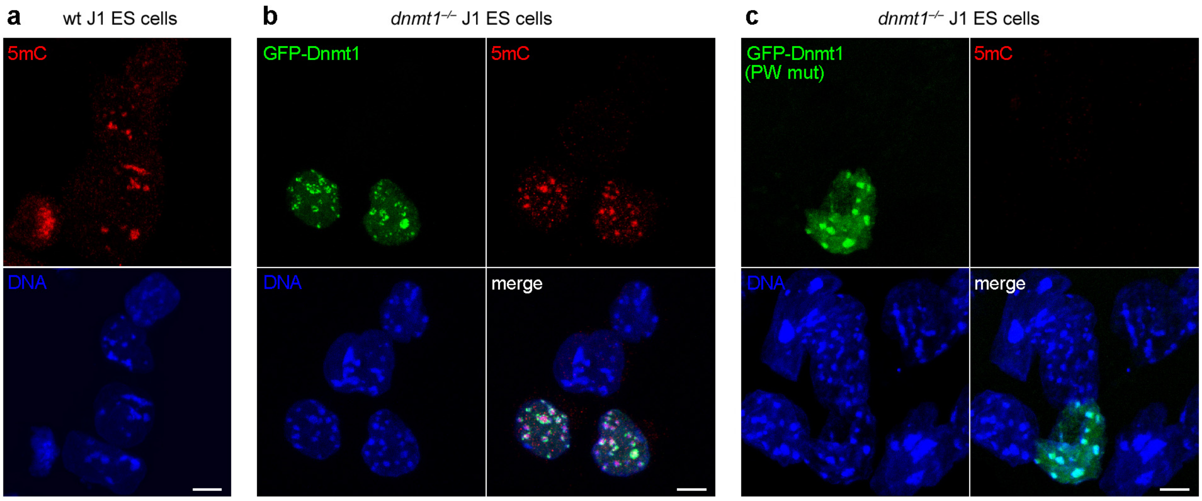

Supplementary Figure 1. GFP-Dnmt1 fusion protein restores methylation at chromocenters in *dnmt1*$^{-/-}$ ES cells. Mouse minor and major satellite sequences are heavily methylated in wild type cells and severely hypomethylated in *dnmt1*$^{-/-}$ ES cells[1]. These sequences can be visualised *in situ* as DAPI-bright chromocenters that are heavily stained with an antibody to 5-methylcytosine (5mC) in wild type cells (**a**), but not in *dnmt1*$^{-/-}$ ES cells (**b**, **c**). The latter cells were transiently transfected with constructs driving the expression of GFP-Dnmt1 wild type (**b**) and PW mutant (**c**). 60 hours after transfection cells were stained with the 5mC antibody (red) and DAPI (blue) and imaged by confocal microscopy. Cells expressing GFP-Dnmt1 showed a clear increase in 5mC staining at chromocenters compared to non transfected cells, indicating that the fusion protein is functional *in vivo*. As a control, cells expressing the catalytically inactive PW mutant did not show any increase of 5mC staining. Shown are projections of optical sections. Bars: 5 μm.

1. Lei, H. et al. De novo DNA cytosine methyltransferase activities in mouse embryonic stem cells. *Development* **122**, 3195-3205 (1996).

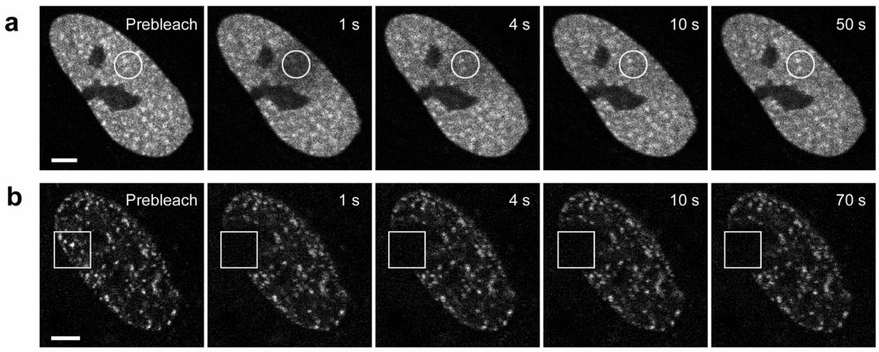

Supplementary Figure 2. Trapping of DNMT1 after 5-aza-dC treatment in human SH-EP N14 neuroblastoma cells. S phase cell nuclei with a replication pattern typical for early to mid S phase are shown. (**a**) FRAP of transiently expressed human DNMT1 fused to GFP without drug treatment. After photobleaching full recovery of GFP-DNMT1 can be observed within less then 50 sec. (**b**) No recovery can be observed over the time course after bleaching of GFP-DNMT1 in cells incubated 2.5 hours with 30 µM 5-aza-dC. Bars: 5 µm.

Supplementary Methods

The fusion of the human DNMT1 to GFP was generated by cloning the full length human cDNA of the long isoform[1] (kindly provided by P. Vertino) in the pEGFP-C1 vector (Clontech). SH-EP N14 neuroblastoma cells were cultured in RPMI 1640 medium supplemented with 10% FCS and 50 µg/ml gentamycine and transfected with JetPEI (Polyplus-Transfection). *Dnmt1*$^{s/s}$ J1 ES cells[2] were cultured on gelatin coated plastic dishes with 1000 U/ml of LIF and were transfected with FuGene6 (Roche) according to the manufacturer's instructions. 48 hours after transfection cells were seeded on gelatin coated coverslips and 12 hours later they were fixed with 3.7% formaldehyde for 10 min at RT. Cells were then permeabilized with 0.5% Triton X-100 for 5 min at RT and 5mC was exposed by digestion with 10 mU/ml of DNase I for 1hr at 37°C in PBS containing 0.1% Tween 20, 3% BSA and 5 mM $MgCl_2$. After extensive washing with PBS containing 0.1% Tween 20 and 1 mM EDTA 5mC was detected with a specific mouse monoclonal antibody (Eurogentec) and an anti-mouse secondary antibody conjugated with rhodamine Red-X (Jackson Immunoresearch Laboratories). Samples were stained with DAPI and mounted in Vectashield (Vector Labs).

1. Yoder, J. A., Yen, R. W., Vertino, P. M., Bestor, T. H. & Baylin, S. B. New 5' regions of the murine and human genes for DNA (cytosine-5)-methyltransferase. *J Biol Chem* **271**, 31092-31097 (1996).
2. Lei, H. et al. De novo DNA cytosine methyltransferase activities in mouse embryonic stem cells. *Development* **122**, 3195-3205 (1996).

II.5. REGULATION OF DNA METHYLTRANSFERASE 1

3B2v8.06a/w (Dec 5 2003).51c
+model
JAER : 407
Prod.Type:COM
pp.1–11(col.fig.:NIL)
ED:SreejaGA
PAGN:gopal SCAN:oliver

ARTICLE IN PRESS

ELSEVIER
Advan. Enzyme Regul. ▮ (▮▮▮▮) ▮▮▮–▮▮▮
ADVANCES IN ENZYME REGULATION
www.elsevier.com/locate/advenzreg

Regulation of DNA methyltransferase 1

Fabio Spada, Ulrich Rothbauer, Kourosh Zolghadr,
Lothar Schermelleh, Heinrich Leonhardt*

Biocenter, Department of Biology II, Ludwig Maximilians University Munich, Germany

UNCORRECTED PROOF

Introduction

Although essentially all cells of a mammalian organism contain the same genetic information they may differ dramatically in form and function. This cellular differentiation is established during development by cascades of transcription factors driving the expression of cell-type specific sets of genes. These cell type specific gene expression patterns are established, maintained and changed in conjunction with epigenetic mechanisms including DNA methylation, histone modification and chromatin structure. The most tangible epigenetic mark is DNA methylation, a postreplicative modification, which in vertebrates is mainly catalyzed by DNA methyltransferases (Dnmts: EC 2.1.1.37) 1, 3a and 3b at palindromic CpG sites. The DNA methylation pattern changes along with cellular differentiation and is generally inversely correlated with transcriptional activity. Over the past decade, several functional links between DNA methylation, histone modification, chromatin structure and transcriptional regulation have been discovered.

In mammalian cells Dnmt1 is the major and ubiquitously expressed Dnmt. By direct and indirect interactions Dnmt1 plays a central role in the epigenetic networks controlling gene expression in development and disease. We will outline results and open questions concerning the regulation of Dnmt1 and discuss novel approaches to study Dnmts in living cells.

---

*Corresponding author. Department of Biology II, Ludwig Maximilians University Munich, Grosshadernerstr. 2, 82152 Planegg-Martinsried, Germany. Tel.: +49 89 218074232; fax: +49 89 218074236.

E-mail addresses: h.leonhardt@lmu.de, geoweber@iupui.edu (H. Leonhardt).

0065-2571/$ - see front matter © 2006 Published by Elsevier Ltd.
doi:10.1016/j.advenzreg.2006.01.011

Regulation of Dnmt1 and its effects on DNA methylation patterns

The importance of Dnmt1 in maintaining genomic methylation is underscored by studies on cell lines and mice carrying *dnmt1* homozygous null mutations. Dnmt1 null ES cells have reduced but stable levels of DNA methylation and are impaired in their differentiation potential, while the corresponding null mice die prior to the 8-somite stage (Lei et al., 1996). In addition, somatic cells with conditional homozygous *dnmt1* null mutations display genomic hypomethylation and die by apoptosis within 5–6 days (Jackson-Grusby et al., 2001). These data indicate that de novo methylation activity mainly provided by the Dnmt3a and b enzymes is sufficient for survival of undifferentiated ES cells, while proper differentiation and survival of differentiated cells requires maintenance of DNA methylation patterns by Dnmt1. This is consistent with the concept that differential DNA methylation patterns in differentiated cells contribute to their specific gene expression programs. Although de novo methyltransferases are necessary for the establishment of genomic methylation patterns, setup and maintenance of specific expression programs depend on maintenance of DNA methylation patterns.

Given the central role of DNA methylation in the epigenetic control of gene expression it is to be expected that the activity and cellular levels of Dnmt1 are strictly regulated. The postreplicative maintenance of methylation patterns in a large part of the genome is mediated and secured by recruitment of Dnmt1 to replication foci (Chuang et al., 1997; Leonhardt et al., 1992). This major role of Dnmt1 is mostly restricted to the S phase of the cell cycle suggesting that Dnmt1 levels could cycle in a way similar to that observed for replication factors like PCNA. Indeed, evidence for cell cycle-dependent control of Dnmt1 levels comes from the observations that Dnmt1 transcript levels correlate positively with normal cell proliferation and that the *dnmt1* promoter is under control of the Rb/E2F pathway (Bestor and Ingram, 1985; Kimura et al., 2003; McCabe et al., 2005; Robertson et al., 2000a, b). Consistent with these data, both Dnmt1 transcript and protein levels were shown to be minimal in quiescent cells (G0) and peak during S phase in human cells (Robertson et al., 2000a, b; Tatematsu et al., 2000). However, in mouse cells Dnmt1 was also detected at (peri-)centromeric heterochromatin from late S-phase till M and early G1 phase (Easwaran et al., 2004). Consistent with this, Dnmt1 transcript levels were shown to increase steadily through S to G2 in synchronized mouse cells (Kimura H. et al., 2003). Interestingly, Dnmt1 protein levels comparable to those present in proliferating cells were found in postmitotic neurons indicating the presence of cell-type specific regulatory mechanisms (Inano et al., 2000). The general theme, however, seems to be a proliferation-dependent expression of Dnmt1 and two independent mechanisms for subnuclear recruitment to replication sites and (peri-)centromeric heterochromatin to secure efficient maintenance of DNA methylation patterns (Fig. 1).

In contrast, a special situation with respect to Dnmt1 levels, subcellular localization and genomic methylation levels is found in mammalian oocytes and preimplantation embryos. In the mouse zygote there is a drastic decrease of DNA methylation in the paternal genome within a few hours after fertilization (active demethylation) and both the maternal and paternal genomes undergo progressive demethylation during segmentation stages (Mayer et al., 2000; Oswald et al., 2000; Rougier et al., 1998; Santos et al., 2002). At these stages only the 118 amino acids shorter, maternal Dnmt1 isoform can be detected, which is present in large amounts but is sequestered in the cytoplasm. As the short Dnmt1 enters embryonic nuclei only transiently at the 8-cell stage it is believed that its retention in the

UNCORRECTED PROOF

ARTICLE IN PRESS

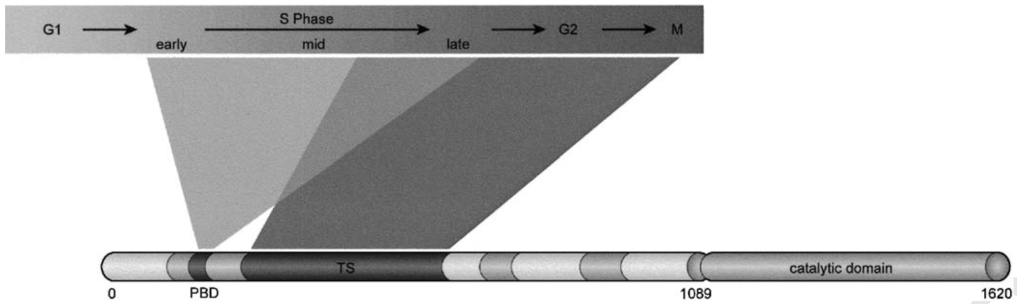

Fig. 1. PBD and TS-mediated association of Dnmt1 with chromatin during the cell cycle. PBD directs association of Dnmt1 with replication foci throughout the S phase and TS mediates association with (peri-)centromeric heterochromatin from mid/late S till M phase.

cytoplasm of preimplantation embryos prevents maintenance of gamete-specific methylation patterns (passive demethylation) and thus contributes to epigenetic reprogramming of the embryo (Cardoso and Leonhardt, 1999; Carlson et al., 1992; Grohmann et al., 2005; Mertineit et al., 1998). Also, it has been proposed that the presence of the long Dnmt1 isoform in donor somatic nuclei used in animal cloning would result in defective epigenetic reprogramming, thus explaining the low survival rates of cloned embryos (Chung et al., 2003). However, it is far from clear how methylation patterns at imprinted loci, transposable elements and satellite sequences are maintained throughout mouse preimplantation development and how Dnmt1 levels and subcellular localization are regulated in mammalian species with little passive demethylation during early embryonic development (Young and Beaujean, 2004).

Alterations of DNA methylation patterns are a general feature of cancer cells (Jones and Baylin, 2002). Typically, both tumors and cancer cell lines display a global reduction of genomic methylation and at the same time local hypermethylation of selected CpG islands. Local hypermethylation often involves regulatory regions of tumor-suppressor genes and effects their silencing. This epigenetic alteration may thus contribute to tumorigenesis by disturbing the balance of growth control. Dnmt1 is an obvious candidate for a role in this epigenetic deregulation. Indeed, overexpression of Dnmt1 resulted in increased CpG island methylation in human cells (Vertino et al., 1996) and increased global methylation and oncogenic transformation of NIH3T3 cells (Wu et al., 1993). Also, elevated levels of Dnmt1 have frequently been found in tumors and cancer cell lines compared to the respective normal tissues (Choi et al., 2003; Fang et al., 2003; Kanai et al., 2001; Li et al., 2003; Mizuno et al., 2001; Nagai et al., 2003; Patra et al., 2002; Saito et al., 2001) and correlated with progression of pancreatic carcinoma (Peng et al., 2005). However, this correlation does not seem to be consistent for a given type of tumor cell and alterations of Dnmt1 abundance often do not correlate with variations in DNA methylation levels in the same cancerous tissue (Eads et al., 1999; Kimura F. et al., 2003; Li et al., 2003; Saito et al., 2001). In addition, homozygous deletion of the *DNMT1* locus in the human colorectal cancer cell line HCT116 led to a surprisingly minor reduction in DNA methylation levels, apparently involving only classical satellite 2 and 3 sequences. Interestingly, a drastic reduction of genomic methylation was observed only after additional ablation of *DNMT3b* (Rhee et al., 2000; Rhee et al., 2002). Although these data suggest an unexpected level of cooperativity between the two methyltransferases, it should be noted that the starting cell

UNCORRECTED PROOF

type used in these studies was already a transformed one and that functional knock out of DNMT1 in other types of cancer cell lines led to more substantial alteration of methylation patterns. This suggests that the effects of DNMT1 ablation depend on the specific genetic and epigenetic background (Leu et al., 2003; Suzuki et al., 2004).

Besides local hypermethylation most tumors show a general hypomethylation. To test also whether lowered levels of Dnmt1 may contribute to oncogenic transformation, mice carrying a hypomorphic *dnmt1* allele were generated, reducing Dnmt1 expression to about 10% of wild-type levels. These mice have substantially reduced genomic methylation levels, develop aggressive T-cell lymphomas and show chromosomal instability (Eden et al., 2003; Gaudet et al., 2003). These effects are likely due to the mobilization of endogenous retroviral elements normally silenced by DNA methylation (Gaudet et al., 2004) and to instability of hypomethylated satellite sequences (Chen et al., 1998; Eden et al., 2003; Gaudet et al., 2003; Kim et al., 2004). Thus, model studies on altered Dnmt1 expression levels demonstrate that both alterations of DNA methylation patterns commonly found in spontaneous tumors, i.e. global hypomethylation and local hypermethylation, can contribute to oncogenic transformation. However, it is not yet clear how either increased or lowered Dnmt1 levels found in tumors may simultaneously cause the establishment of global hypomethylation and local hypermethylation.

Nevertheless, methyltransferase inhibitors like 5-aza-2'-deoxycytidine are actively pursued as anti-cancer treatment. The hope of such treatments is that transient inhibition of methyltransferase activity would lead to demethylation and consequent reactivation of silenced tumor-suppressor genes, although this has actually been documented in very few cases (Brueckner and Lyko, 2004; Brueckner et al., 2005). These demethylating drugs are highly cytotoxic and, although they have been used in numerous clinical trials, promising results were obtained with low and repeated doses only in leukemia patients. Studies employing Dnmt1 deficient ES cells and mice support the idea that their cytotoxic effects are mainly due to covalent complex formation of Dnmt1 with the DNA substrate rather than to the consequent global demethylation (Juttermann et al., 1994). This and the frequent occurrence of tumors and chromosomal rearrangements in hypomethylated animal models mentioned above have raised concern about the long-term exposure to such agents. For these reasons alternative small molecule inhibitors of Dnmts that lack the undesired cytotoxic effects of cytosine analogs are intensively sought after (Brueckner et al., 2005).

Interactions controlling Dnmt1 activity

These findings that changes in DNA methylation patterns may have severe consequences for human health have raised strong interest in the regulation of the activity of Dnmt1. In vitro assays with purified Dnmt1 showed a preference for hemi-methylated CpG sites, which on one hand led to its classification as the maintenance methyltransferase (Bestor et al., 1988; Leonhardt and Bestor, 1993), but on the other hand can hardly explain the faithful inheritance of epigenetic information over countless cell division cycles throughout the lifespan of an organism.

Dnmt1 is composed of a large N-terminal, regulatory domain and a C-terminal, catalytic domain that is closely related to the bacterial C5-methyltransferases (Bestor et al., 1988; Bestor, 1992; Leonhardt and Bestor, 1993). The regulatory domain is essential for the complex regulation of Dnmt1 in the context of a dividing cell. Despite its striking

UNCORRECTED PROOF

homology to prokaryotic methyltransferases, the catalytic portion of Dnmt1 alone is not sufficient for the enzymatic activity. Methyltransferase activity could only be observed in the presence of a substantial part of the N-terminal domain (Fatemi et al., 2001; Margot et al., 2000; Zimmermann et al., 1997). Consistent with these data a physical interaction between the N- and the C-terminus could be detected (Fatemi et al., 2001; Margot et al., 2003). It is assumed that intramolecular interactions induce a conformational change of the catalytic domain leading to an allosteric activation of the enzyme. In this context it was suggested, that upon binding to hemimethylated DNA the zinc binding domain (aa 613–748) interacts with the catalytic domain and stimulates DNA methylation (Fatemi et al., 2001). However, the precise mechanism through which the regulatory domain can activate the enzymatic process remains unknown.

The preference of Dnmt1 for hemi-methylated CpG sites, which are produced by semi-conservative DNA replication, is matched by its subnuclear localization at replication foci throughout S phase (Leonhardt et al., 1992). In addition, live cell microscopy using fluorescent fusion constructs recently revealed an association with (peri-)centromeric heterochromatin (Easwaran et al., 2004). This complex and cell cycle dependent localization of Dnmt1 is mediated by two independent domains within the N-terminus of Dnmt1 (Fig. 1). The association with replication sites during S phase is mediated by the PCNA binding domain (PBD, aa 158–171) while prolonged binding to heterochromatin from late S phase through mitosis is mediated by the targeting sequence (TS, aa 256–629; Chuang et al., 1997; Leonhardt et al., 1992; Easwaran et al., 2004). Therefore, substrate specificity and subcellular localization are both likely to contribute to the faithful, postreplicative maintenance of genomic methylation patterns in mammalian cells. This cell cycle dependent localization of fluorescent Dnmt1 fusion proteins has also been used to distinguish cell cycle phases in living cells (Easwaran et al., 2005).

The binding of Dnmt1 to late replicating heterochromatin beyond S phase may either represent an additional mechanism to ensure complete maintenance of the dense methylation in these genomic regions and/or point to a novel role of Dnmt1 in the maintenance of transcriptionally repressed chromatin (Easwaran et al., 2004). In this context it is interesting to note that the N-terminal portion of Dnmt1 has been shown to interact with a range of chromatin-associated proteins including pRb, DMAP1, HDAC 1/2, MeCP2, SUV39H1 and HP1β and the nucleolar chromatin remodelling complex Tip5/Snf2h (Fuks et al., 2000; Fuks et al., 2003; Geiman et al., 2004a, b; Kimura and Shiota, 2003; Robertson et al., 2004; Robertson et al., 2000a, b; Santoro et al., 2002). A summary of interacting factors and their reported binding sites is outlined in Fig. 2. These interactions indicate several independent mechanisms by which Dnmt1 could cause transcriptional repression. First, Dnmt1 interacts with the retinoblastoma (Rb) tumor-suppressor gene product, a cell cycle regulator protein that represses transcription by recruiting the histone deacetylase HDAC1 (Pradhan and Kim, 2002; Robertson et al., 2000a, b). The Dnmt1-Rb complex also associates with the transcription factor E2F1 (Robertson et al., 2000a, b), resulting in transcriptional repression of E2F1-responsive promoters. Second, Dnmt1 is reported to establish transcriptional repression by a direct interaction with DMAP1 (DNMT1-associated protein) and the histone deactetylase HDAC2 (Rountree et al., 2000). DMAP1 has an intrinsic silencing activity and binds to the transcriptional co-repressor TSG101 and the transcriptional co-regulator Daxx (Muromoto et al., 2004). In contrast to DMAP1, which associates with Dnmt1 throughout S phase, the interaction of HDAC2 with Dnmt1 occurs specifically at replication foci in

UNCORRECTED PROOF

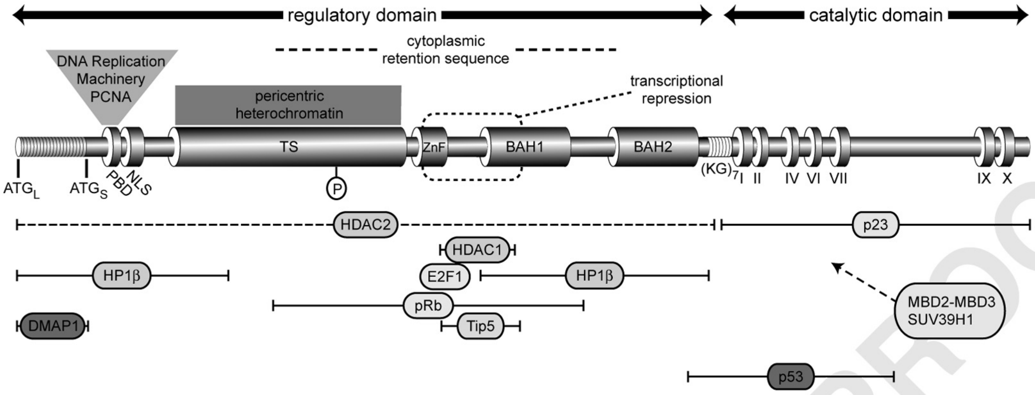

Fig. 2. Structure and interacting factors of Dnmt1. Dnmt1 contains a C-terminal domain including the ten conserved sequence motifs of pro- and eukaryotic C5-cytosine methyltransferases. The N-terminal, regulatory domain exists in two variants generated by alternative transcriptional start sites and translation initiation at either ATG-L (long isoform) or ATG-S (short isoform). Several functional domains have been mapped including a Zn binding region (ZnF), a nuclear localization sequence (NLS), a targeting sequence (TS), a phosphorylation site, two bromo homology domains (BAH), a transcriptional repression domain and a cytoplasmic localization sequence. Several proteins reported to interact with Dnmt1 and their mapped interaction domains are indicated. See text for further details.

late S phase. It was proposed that Dnmt1 mediates recruitment of HDACs to (peri-)centromeric heterochromatin and thus supports deacetylation of histones assembled onto newly replicated DNA (Rountree et al., 2000). Third, Dnmt1 directly interacts with methyl CpG binding proteins such as MBD2, MBD3 and MeCP2 (Kimura and Shiota, 2003; Tatematsu et al., 2000) which may then recruit HDACs. Binding to MeCP2 could also contribute to the recognition of hemi-methylated DNA by the MeCP2-Dnmt1 complex and play a role in maintenance of DNA methylation. Fourth, Dnmt1 is also described to interact with the histone methyltransferase SUV39H1 and the heterochromatin-binding protein HP1*β* (Fuks et al., 2003). Importantly, the TS domain-mediated loading of Dnmt1 onto late replicating heterochromatin is independent of HP1*β* and SUV39H1 which could indicate a pathway for heterochromatin formation and/or maintenance that is independent of histone H3K9 tri-methylation (Easwaran et al., 2004).

The C-terminal portion of Dnmt1, contains the 10 conserved motifs including the catalytical center, which are characteristic for C5 cytosine methyltransferases (Leonhardt and Bestor, 1993). In contrast to the N-terminus only two proteins are reported to interact with the C-terminus of Dnmt1. One is the molecular chaperone p23, which localizes to genomic response elements in a hormone-dependent manner, disrupting receptor-mediated transcriptional activation (Freeman and Yamamoto, 2002; Zhang and Verdine, 1996). Whether p23 modulates the catalytic activity of Dnmt1 and/or contributes to transcriptional repression by disrupting transcription complexes remains to be investigated. Finally, also the tumor suppressor protein p53 was reported to interact with the catalytic domain of Dnmt1. It is proposed that the DNMT1-p53 interaction is essential for

UNCORRECTED PROOF

the regulation of the *survivin* gene by stabilizing the HDAC1–DNMT1–p53 complex on the *survivin* promotor leading to a hypermethylation of its CpG sites (Esteve et al., 2005).

In summary, the sheer number of all reported Dnmt1 interactions makes it clear that not all of them may occur at all times. It is now necessary to establish which of them occur when and what their functional consequences are. A common theme of these interactions is transcriptional repression and involves different types of proteins ranging from transcription factors to histone methyltransferases. These observations place Dnmt1 at the center of a complex network connecting two epigenetic pathways, DNA methylation and histone modification which result in the establishment and maintenance of transcriptionally inactive chromatin.

Analysis of Dnmt1 activity and regulation in living cells

The fact that Dnmt1 interacts with numerous cellular protein, shows a cell cycle and development specific subcellular localization and—last but not least—works on a substrate as complex and dynamic as DNA packaged into chromatin clearly indicates that any real understanding of its regulation will require in vivo studies. The basic enzymatic mechanism of the methylation reaction is shared by all eukaryotic and prokaryotic C5-cytosine methyltransferases and has been worked out in vitro with purified enzymes (Bestor and Verdine, 1994; Cheng and Roberts, 2001). These assays, however, miss most, if not all, interacting factors and are carried out with 'naked' and often artificial DNA substrates.

As outlined above, the control of DNA methylation in the context of highly regulated and dynamic chromatin in mammals is extraordinarily complex and far from being understood. The establishment and maintenance of genomic methylation in mammals is accomplished by multiple methyltransferases, which interact with each other as well as with numerous nuclear factors via their regulatory domains. Even though many interaction partners and subdomains within the regulatory domains of methyltransferases have been described, it is still largely unknown how they control and modulate the enzymatic activity during cell cycle and development.

As in vitro assays do not reproduce the complexity of living cells it would be ideal to directly study the regulation of DNA methyltransferases in their natural environment. Unfortunately, the methylation reaction is not suited for chromogenic substrates that could provide an optical readout of enzyme activities.

To overcome this limitation a novel in vivo assay was recently developed that utilizes fluorescent GFP-Dnmt1 fusions (or mutants thereof) in combination with a mechanism-based inhibitor (Schermelleh et al., 2005). The assay takes advantage of the rather complex catalytic mechanism of C5-methyltransferases which form a transient, covalent complex with the base ring to facilitate methyl group transfer.

The mechanism-based inhibitor, the cytosine analogue 5-aza-2'-deoxycytidine (5-aza-dC), gets incorporated into DNA during replication just like deoxycytidine itself and Dnmts form a covalent complex but cannot be released due to the nitrogen substitution in the base ring. In other words the enzyme gets trapped as a result of its enzymatic activity (Fig. 3). The time dependent immobilization of Dnmt1 (trapping) can be measured by fluorescence recovery after photobleaching (FRAP) analysis and reflects the enzymatic activity of the fusion protein. This assay makes it now possible to study the regulation of Dnmts in situ at different cell cycle stages and to directly study the effect of mutations and interacting factors in its natural environment with its natural substrate in the context of

UNCORRECTED PROOF

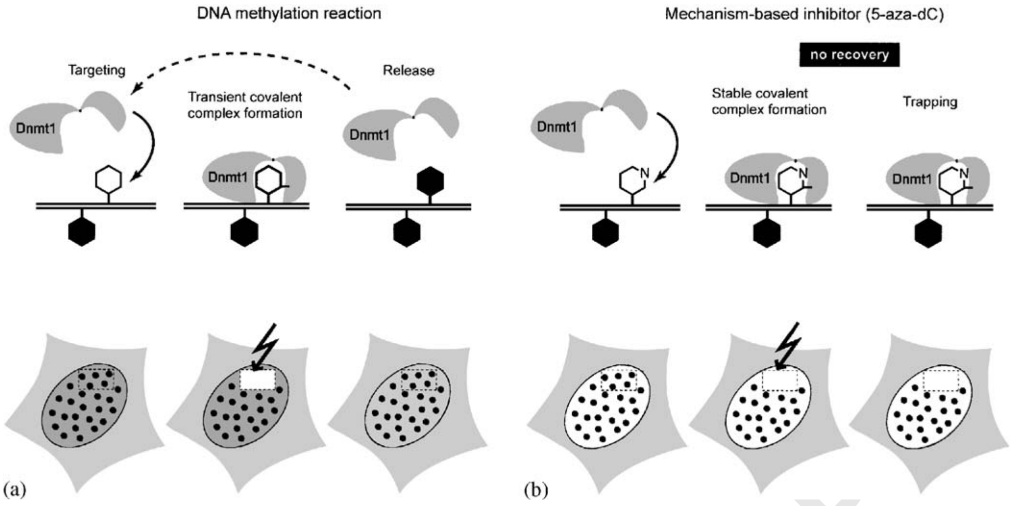
DNA methylation reaction
Targeting
Transient covalent complex formation
Release
Dnmt1
Mechanism-based inhibitor (5-aza-dC)
no recovery
Stable covalent complex formation
Trapping
N
(a)
(b)

Fig. 3. Postreplicative action of Dnmt1 and rational of the trapping assay. Methylated and non-methylated cytosines are depicted as black and white hexagons, respectively. Dnmt1 is depicted in gray shade. (a) Dnmt1 binds to hemimethylated CpG sites produced during DNA replication and forms a transient covalent complex with the cytosine residue (gray line). After methyl group transfer the enzyme is released and becomes available for another round of methylation (dotted arrow), which is visualized as fluorescence recovery after photobleaching of GFP-Dnmt1 in the outlined region (bottom row). (b) Mechanism-based inhibitors such as 5-aza-dC (hexagons with N at position 5) are incorporated into DNA during S phase. Dnmt1 forms a stable covalent complex with 5-aza-dC (black line) and becomes trapped. Immobilization of GFP-Dnmt1 is detected as lack of recovery after photobleaching (bottom row).

dynamic chromatin remodelling and ongoing DNA replication. In addition, this method offers a novel approach to test new types of small molecule inhibitors targeting the catalytic domain of Dnmt1 by their ability to prevent 5-aza-dC-mediated trapping of GFP-Dnmt1. Such inhibitors are actively sought after as transient blocking of the catalytic activity of Dnmt1 is expected to reactivate epigenetically silenced tumor-suppressor genes (Brueckner et al., 2005).

UNCORRECTED PROOF

Summary

DNA methylation plays a central role in the control of gene expression, chromatin condensation and genome stability. In mammalian cells DNA methylation patterns are established and maintained by DNA methyltransferases 1, 3a and 3b. The regulation of DNA methylation by these enzymes requires interactions with other cellular factors involved in histone modification, chromatin structure and transcription and interference with either of these DNA methyltransferases severely impairs viability and development. Although hypo- and hypermethylation have both been linked with cancer, very little is known about the regulation of DNA methylation during development and disease.

The best system to study this complex regulation should be living cells and organisms where both the native substrate and all potential interaction partners are available.

References

Bestor TH. Activation of mammalian DNA methyltransferase by cleavage of a Zn binding regulatory domain. EMBO J 1992;11:2611–7.

Bestor TH, Ingram VM. Growth-dependent expression of multiple species of DNA methyltransferase in murine erythroleukemia cells. Proc Natl Acad Sci USA 1985;82:2674–8.

Bestor TH, Verdine GL. DNA methyltransferases. Curr Opin Cell Biol 1994;6:380–9.

Bestor T, Laudano A, Mattaliano R, Ingram V. Cloning and sequencing of a cDNA encoding DNA methyltransferase of mouse cells. The carboxyl-terminal domain of the mammalian enzymes is related to bacterial restriction methyltransferases. J Mol Biol 1988;203:971–83.

Brueckner B, Lyko F. DNA methyltransferase inhibitors: old and new drugs for an epigenetic cancer therapy. Trends Pharmacol Sci 2004;25:551–4.

Brueckner B, Boy RG, Siedlecki P, Musch T, Kliem HC, Zielenkiewicz P, et al. Epigenetic reactivation of tumor suppressor genes by a novel small-molecule inhibitor of human DNA methyltransferases. Cancer Res 2005;65:6305–11.

Cardoso MC, Leonhardt H. DNA methyltransferase is actively retained in the cytoplasm during early development. J Cell Biol 1999;147:25–32.

Carlson LL, Page AW, Bestor TH. Properties and localization of DNA methyltransferase in preimplantation mouse embryos: implications for genomic imprinting. Genes Dev 1992;6:2536–41.

Chen RZ, Pettersson U, Beard C, Jackson-Grusby L, Jaenisch R. DNA hypomethylation leads to elevated mutation rates. Nature 1998;395:89–93.

Cheng X, Roberts RJ. Adomet-dependent methylation, DNA methyltransferases and base flipping. Nucl Acids Res 2001;29:3784–95.

Choi MS, Shim Y-H, Hwa JY, Lee SK, Ro JY, Kim J-S, et al. Expression of DNA methyltransferases in multistep hepatocarcinogenesis. Hum Pathol 2003;34:11–7.

Chuang LS-H, Ian H-I, Koh T-W, Ng H-H, Xu G, Li BFL. Human DNA-(cytosine-5) methyltransferase-PCNA complex as a target for p21WAF1. Science 1997;277:1996–2000.

Chung YG, Ratnam S, Chaillet JR, Latham KE. Abnormal regulation of DNA methyltransferase expression in cloned mouse embryos. Biol Reprod 2003;69:146–53.

Eads CA, Danenberg KD, Kawakami K, Saltz LB, Danenberg PV, Laird PW. CpG island hypermethylation in human colorectal tumors is not associated with DNA methyltransferase overexpression. Cancer Res 1999;59:2302–6.

Easwaran HP, Schermelleh L, Leonhardt H, Cardoso MC. Replication-independent chromatin loading of Dnmt1 during G2 and M phases. EMBO Rep 2004;5:1181–6.

Easwaran HP, Leonhardt H, Cardoso MC. Cell cycle markers for live cell analyses. Cell Cycle 2005;4:453–5.

Eden A, Gaudet F, Waghmare A, Jaenisch R. Chromosomal instability and tumors promoted by DNA hypomethylation. Science 2003;300:455.

Esteve PO, Chin HG, Pradhan S. Human maintenance DNA (cytosine-5)-methyltransferase and p53 modulate expression of p53-repressed promoters. Proc Natl Acad Sci USA 2005;102:1000–5.

Fang JY, Lu J, Chen YX, Yang L. Effects of DNA methylation on expression of tumor suppressor genes and proto-oncogene in human colon cancer cell lines. World J Gastroenterol 2003;9:1976–80.

Fatemi M, Hermann A, Pradhan S, Jeltsch A. The activity of the murine DNA methyltransferase Dnmt1 is controlled by interaction of the catalytic domain with the N-terminal part of the enzyme leading to an allosteric activation of the enzyme after binding to methylated DNA. J Mol Biol 2001;309:1189–99.

Freeman BC, Yamamoto KR. Disassembly of transcriptional regulatory complexes by molecular chaperones. Science 2002;296:2232–5.

Fuks F, Burgers WA, Brehm A, Hughes-Davies L, Kouzarides T. DNA methyltransferase Dnmt1 associates with histone deacetylase activity. Nat Genet 2000;24:88–91.

Fuks F, Hurd PJ, Deplus R, Kouzarides T. The DNA methyltransferases associate with HP1 and the SUV39H1 histone methyltransferase. Nucl Acids Res 2003;31:2305–12.

Gaudet F, Hodgson JG, Eden A, Jackson-Grusby L, Dausman J, Gray JW, et al. Induction of tumors in mice by genomic hypomethylation. Science 2003;300:489–92.

Gaudet F, Rideout III WM, Meissner A, Dausman J, Leonhardt H, Jaenisch R. Dnmt1 expression in pre- and postimplantation embryogenesis and the maintenance of IAP silencing. Mol Cell Biol 2004;24:1640–8.

UNCORRECTED PROOF

Geiman TM, Sankpal UT, Robertson AK, Chen Y, Mazumdar M, Heale JT, et al. Isolation and characterization of a novel DNA methyltransferase complex linking DNMT3b with components of the mitotic chromosome condensation machinery. Nucl Acids Res 2004a;32:2716–29.

Geiman TM, Sankpal UT, Robertson AK, Zhao Y, Robertson KD. DNMT3b interacts with hSNf2H chromatin remodeling enzyme, HDACS 1 and 2, and components of the histone methylation system. Biochem Biophys Res Commun 2004b;318:544–55.

Grohmann M, Spada F, Schermelleh L, Alenina N, Bader M, Cardoso MC, et al. Restricted mobility of Dnmt1 in preimplantation embryos: Implications for epigenetic reprogramming. BMC Dev Biol 2005;5:18–24.

Inano K, Suetake I, Ueda T, Miyake Y, Nakamura M, Okada M, et al. Maintenance-type DNA methyltransferase is highly expressed in post-mitotic neurons and localized in the cytoplasmic compartment. J Biochem (Tokyo) 2000;128:315–21.

Jackson-Grusby L, Beard C, Possemato R, Tudor M, Fambrough D, Csankovszki G, et al. Loss of genomic methylation causes p53-dependent apoptosis and epigenetic deregulation. Nat Genet 2001;27:31–9.

Jones PA, Baylin SB. The fundamental role of epigenetic events in cancer. Nat Rev Genet 2002;3:415–28.

Juttermann R, Li E, Jaenisch R. Toxicity of 5-aza-2'-deoxycytidine to mammalian cells is mediated primarily by covalent trapping of DNA methyltransferase rather than DNA demethylation. Proc Natl Acad Sci USA 1994;91:11797–801.

Kanai Y, Ushijima S, Kondo Y, Nakanishi Y, Hirohashi S. DNA methyltransferase expression and DNA methylation of CpG islands and peri-centromeric satellite regions in human colorectal and stomach cancers. Int J Cancer 2001;91:205–12.

Kim M, Trinh BN, Long TI, Oghamian S, Laird PW. Dnmt1 deficiency leads to enhanced microsatellite instability in mouse embryonic stem cells. Nucl Acids Res 2004;32:5742–9.

Kimura F, Seifert H-H, Florl AR, Santourlidis S, Steinhoff C, Swiatkowski S, et al. Decrease of DNA methyltransferase 1 expression relative to cell proliferation in transitional cell carcinoma. Int J Cancer 2003;104:568–78.

Kimura H, Shiota K. Methyl-CpG-binding protein, MeCP2, is a target molecule for maintenance DNA methyltransferase, Dnmt1. J Biol Chem 2003;278:4806–12.

Kimura H, Nakamura T, Ogawa T, Tanaka S, Shiota K. Transcription of mouse DNA methyltransferase 1 (Dnmt1) is regulated by both E2F-Rb-HDAC-dependent and -independent pathways. Nucl Acids Res 2003;31:3101–13.

Lei H, Oh S, Okano M, Juttermann R, Goss K, Jaenisch R, et al. De novo DNA cytosine methyltransferase activities in mouse embryonic stem cells. Development 1996;122:3195–205.

Leonhardt H, Bestor TH. Structure, function and regulation of mammalian DNA methyltransferase. Exs 1993;64:109–19.

Leonhardt H, Page AW, Weier HU, Bestor TH. A targeting sequence directs DNA methyltransferase to sites of DNA replication in mammalian nuclei. Cell 1992;71:865–73.

Leu Y-W, Rahmatpanah F, Shi H, Wei SH, Liu JC, Yan PS, et al. Double RNA interference of DNMT3b and DNMT1 enhances DNA demethylation and gene reactivation. Cancer Res 2003;63:6110–5.

Li S, Chiang T-c, Richard-Davis G, Barrett JC, Mclachlan JA. DNA hypomethylation and imbalanced expression of DNA methyltransferases (DNMT1, 3a, and 3b) in human uterine leiomyoma. Gynecol Oncol 2003;90:123–30.

Margot JB, Aguirre-Arteta AM, Di Giacco BV, Pradhan S, Roberts RJ, Cardoso MC, et al. Structure and function of the mouse DNA methyltransferase gene: Dnmt1 shows a tripartite structure. J Mol Biol 2000;297:293–300.

Margot JB, Ehrenhofer-Murray AE, Leonhardt H. Interactions within the mammalian DNA methyltransferase family. BMC Mol Biol 2003;4:7–15.

Mayer W, Niveleau A, Walter J, Fundele R, Haaf T. Demethylation of the zygotic paternal genome. Nature 2000;403:501–2.

McCabe MT, Davis JN, Day ML. Regulation of DNA methyltransferase 1 by the pRb/E2F1 pathway. Cancer Res 2005;65:3624–32.

Mertineit C, Yoder JA, Taketo T, Laird DW, Trasler JM, Bestor TH. Sex-specific exons control DNA methyltransferase in mammalian germ cells. Development 1998;125:889–97.

Mizuno S-i, Chijiwa T, Okamura T, Akashi K, Fukumaki Y, Niho Y, et al. Expression of DNA methyltransferases DNMT1, 3a, and 3b in normal hematopoiesis and in acute and chronic myelogenous leukemia. Blood 2001;97:1172–9.

UNCORRECTED PROOF

Muromoto R, Sugiyama K, Takachi A, Imoto S, Sato N, Yamamoto T, et al. Physical and functional interactions between Daxx and DNA methyltransferase 1-associated protein, DMAP1. J Immunol 2004;172:2985–93.

Nagai M, Nakamura A, Makino R, Mitamura K. Expression of DNA (5-cytosin)-methyltransferases (DNMTs) in hepatocellular carcinomas. Hepatol Res 2003;26:186–91.

Oswald J, Engemann S, Lane N, Mayer W, Olek A, Fundele R, et al. Active demethylation of the paternal genome in the mouse zygote. Curr Biol 2000;10:475–8.

Patra SK, Patra A, Zhao H, Dahiya R. DNA methyltransferase and demethylase in human prostate cancer. Mol Carcinog 2002;33:163–71.

Peng DF, Kanai Y, Sawada M, Ushijima S, Hiraoka N, Kosuge T, et al. Increased DNA methyltransferase 1 (DNMT1) protein expression in precancerous conditions and ductal carcinomas of the pancreas. Cancer Sci 2005;96:403–8.

Pradhan S, Kim GD. The retinoblastoma gene product interacts with maintenance human DNA (cytosine-5) methyltransferase and modulates its activity. EMBO J 2002;21:779–88.

Rhee I, Jair KW, Yen RW, Lengauer C, Herman JG, Kinzler KW, et al. CpG methylation is maintained in human cancer cells lacking DNMT1. Nature 2000;404:1003–7.

Rhee I, Bachman KE, Park BH, Jair KW, Yen RW, Schuebel KE, et al. DNMT1 and DNMT3b cooperate to silence genes in human cancer cells. Nature 2002;416:552–6.

Robertson AK, Geiman TM, Sankpal UT, Hager GL, Robertson KD. Effects of chromatin structure on the enzymatic and DNA binding functions of DNA methyltransferases DNMT1 and Dnmt3a in vitro. Biochem Biophys Res Commun 2004;322:110–8.

Robertson KD, Ait-Si-Ali S, Yokochi T, Wade PA, Jones PL, Wolffe AP. DNMT1 forms a complex with Rb, E2F1 and HDAC1 and represses transcription from E2F-responsive promoters. Nat Genet 2000a;25:338–42.

Robertson KD, Keyomarsi K, Gonzales FA, Velicescu M, Jones PA. Differential mRNA expression of the human DNA methyltransferases (DNMTs) 1, 3a and 3b during the G(0)/G(1) to S phase transition in normal and tumor cells. Nucl Acids Res 2000b;28:2108–13.

Rougier N, Bourc'his D, Gomes DM, Niveleau A, Plachot M, Paldi A, Viegas-Pequignot E. Chromosome methylation patterns during mammalian preimplantation development. Genes Dev 1998;12:2108–13.

Rountree MR, Bachman KE, Baylin SB. DNMT1 binds HDAC2 and a new co-repressor, DMAP1, to form a complex at replication foci. Nat Genet 2000;25:269–77.

Saito Y, Kanai Y, Sakamoto M, Saito H, Ishii H, Hirohashi S. Expression of mRNA for DNA methyltransferases and methyl-CpG-binding proteins and DNA methylation status on CpG islands and pericentromeric satellite regions during human hepatocarcinogenesis. Hepatology 2001;33:561–8.

Santoro R, Li J, Grummt I. The nucleolar remodeling complex NoRC mediates heterochromatin formation and silencing of ribosomal gene transcription. Nat Genet 2002;32:393–6.

Santos F, Hendrich B, Reik W, Dean W. Dynamic reprogramming of DNA methylation in the early mouse embryo. Dev Biol 2002;241:172–82.

Schermelleh L, Spada F, Easwaran HP, Zolghadr K, Margot JB, Cardoso MC, et al. Trapped in action: direct visualization of DNA methyltransferase activity in living cells. Nat Methods 2005 in press.

Suzuki M, Sunaga N, Shames DS, Toyooka S, Gazdar AF, Minna JD. RNA interference-mediated knockdown of DNA methyltransferase 1 leads to promoter demethylation and gene re-expression in human lung and breast cancer cells. Cancer Res 2004;64:3137–43.

Tatematsu KI, Yamazaki T, Ishikawa F. MBD2-MBD3 complex binds to hemi-methylated DNA and forms a complex containing DNMT1 at the replication foci in late S phase. Genes Cells 2000;5:677–88.

Vertino PM, Yen RW, Gao J, Baylin SB. De novo methylation of CpG island sequences in human fibroblasts overexpressing DNA (cytosine-5-)-methyltransferase. Mol Cell Biol 1996;16:4555–65.

Wu J, Issa JP, Herman J, Bassett Jr. DE, Nelkin BD, Baylin SB. Expression of an exogenous eukaryotic DNA methyltransferase gene induces transformation of NIH 3T3 cells. Proc Natl Acad Sci USA 1993;90:8891–5.

Young LE, Beaujean N. DNA methylation in the preimplantation embryo: the differing stories of the mouse and sheep. Anim Reprod Sci 2004;82-83:61–78.

Zhang X, Verdine GL. Mammalian DNA cytosine-5 methyltransferase interacts with p23 protein. FEBS Lett 1996;392:179–83.

Zimmermann C, Guhl E, Graessmann A. Mouse DNA methyltransferase (MTase) deletion mutants that retain the catalytic domain display neither de novo nor maintenance methylation activity in vivo. Biol Chem 1997;378:393–405.

UNCORRECTED PROOF

CHAPTER III. DISCUSSION

In the course of this work presented here we designed and improved new cell biological assays to analyze protein interactions, function and mobility in their natural environment. We developed versatile tools and techniques to visualize and manipulate endogenous proteins in living cells and to isolate proteins together with their interacting partners for biochemical approaches. The results were presented in three articles that are accepted for publication in peer-review scientific journals until now. A fourth manuscript presenting a new fluorescent protein-protein interaction assay was also submitted to a peer-review journal and is prepared to be accepted with minor revisions. An additional publication is a review article subsuming the current state of the regulation of DNA methyltransferase 1 (Dnmt1) at that time. In principle, we designed the new assays and tools to study proteins promoting DNA methylation particularly Dnmt1. The ultimate goal is to combine and integrate *in vivo* and *in vitro* data to gain a deep insight into the regulation of DNA methylation in living cells.

III.1. A NEW ASSAY TO VISUALIZE PROTEIN-PROTEIN INTERACTIONS *IN VIVO*

The substantial importance of protein interactions and complex protein networks for almost all cellular processes has driven the development of numerous technologies to monitor such interactions. These technologies range from biochemical approaches to measure protein binding to genetic tools such as the yeast two-hybrid assay or fluorescent-based approaches to analyze protein associations within a living cell. Despite the broad assortment of assays, work in this field is constrained by the fact that virtually all methods require some perturbation or manipulation of the physiological situation to allow assessment of interaction. As fluorescent proteins are being constantly improved microscopic techniques encounter increasing popularity and more and more methods are developed. Still, they are often not generally applicable since mostly expensive instrumentation or advanced technical expertise is required.

As an alternative to present methods we designed a simple fluorescent two-hybrid (F2H) assay based on the immobilization of a fluorescently labeled bait protein at a distinct subcellular structure. This enables the detection of protein-protein interactions as co-localization of signal of a differently labeled prey protein at this defined structure in real-time (Fig. 10a). In case the analyzed proteins do not interact, the prey protein fluorescence remains dispersed throughout the nucleus without being enrichment at that structure (Fig. 10b). In the work presented here we took advantage of cell lines with 200-1000 copies of a *lac* operator array stably integrated at one chromosomal site to which the bait protein binds (Janicki et al., 2004; Tsukamoto et al., 2000).

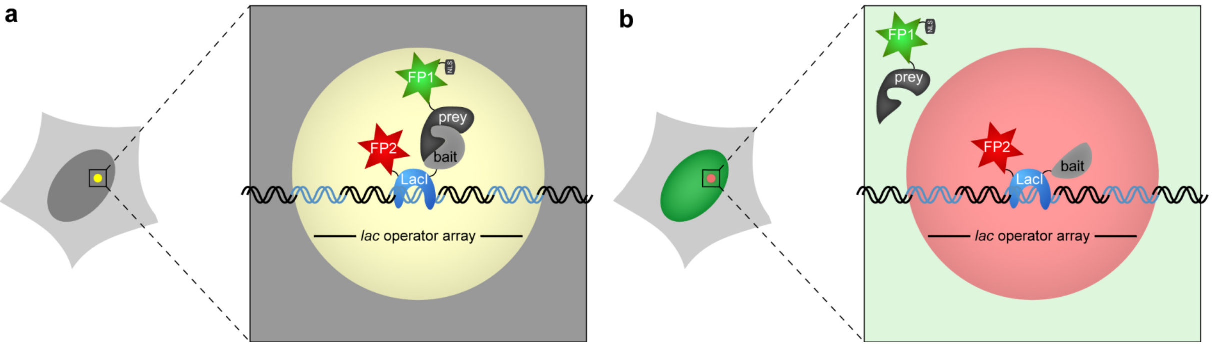

Fig. 10 | Schematic outline of the fluorescent two-hybrid (F2H) assay. (a) The bait-protein binds to the chromosomally integrated *lac* operator array, which is visible as a red fluorescent spot in the nucleus. In case of interaction of the differentially labeled prey protein (green) with the bait it becomes enriched at the same spot resulting in co-localization of fluorescent signals at the *lac* operator (visible as yellow spot in the overlay image). (b) If the prey does not interact with the bait protein, it remains dispersed in the nucleus (green) and the *lac* operator array is only visualized by the bait protein (red spot).

We have demonstrated the reliability of the assay by testing and visualizing protein-protein interactions from different cellular compartments such as the nucleus, the cytoplasm or the mitochondria. The F2H assay allows detection of interactions in real-time and is independent of dynamic processes the studied proteins are involved in such as DNA replication, DNA repair or mitochondrial import. Furthermore, we were able to analyze specific disruptions of protein-protein interactions by deletions of dedicated domains or single point mutations. With the F2H assay we investigated more than 20 protein-protein interactions from different subcellular compartments. Notably, we obtained in all cases corresponding results as previously described with other genetic or biochemical methods. The interactions could be detected independently of the combination of the used fluorescent proteins (GFP/RFP; YFP/RFP; GFP/mCherry). Furthermore, the F2H assay could successfully be applied irrespectively of the order of the individual protein parts in the bait vector (bait-LacI-FP or FP-LacI-bait). Consequently, we could demonstrate that the interaction between Dnmt1 and PCNA is exclusively mediated through the PCNA binding domain (of Dnmt1) and occurs also outside S phase (and is therefore replication independent). However, in rare cases the prey protein may bind to the anchoring structure by itself. Such prey proteins can quickly be identified with an initial screen without the presence of the bait protein. Analyzing those proteins as baits only easily circumvents this limitation.

Our results demonstrate the simplicity, reliability and versatility of the F2H assay and make it therefore generally interesting to study protein-protein interactions. The only prerequisite of the assay is a simple fluorescent microscope equipped with a filter set good enough to distinguish two fluorescent proteins e.g. GFP and RFP and basic experience in cell culture and transfections. The simple co-localization read out of the F2H assay could be automated in the future and applied in cell-based high-throughput protein-protein interaction screens.

III.2. A NEW ANTIBODY-FORMAT TO FOLLOW ENDOGENOUS ANTIGENS IN LIVING CELLS

There are two very common methods to analyze proteins inside cells: either to label them with a fluorescent protein or to stain them with specific antibodies. Fluorescent protein-fusions can only be N- or C-terminal. This might cause the masking of an important domain or a general dysfunction of the studied protein. In addition, the artificial introduction of the expression plasmid into cells can lead to un-physiological overexpression of the encoded protein. A major drawback of fluorescent fusion proteins is the lack of any information about their conformational state or important post-translational modifications.

In comparison, antibodies are ideal tools to detect proteins and their post-translational modifications but only in fixed and permeabilized cells. Our goal was to combine the versatility of antibodies with the live cell applications of fluorescent proteins. We therefore took advantage of heavy-chain antibodies derived from *Camelidae*, more precisely alpacas (*Lama pacos*). We isolated the repertoire of antigen-binding fragments (V_HH), selected specific V_HHs by phage display and combined them with a fluorescent protein. According to their chimeric nature we termed these fluorescent antigen-binding molecules “chromobodies”.

With chromobodies we could target and trace endogenous antigens in living cells with minimal perturbation. Our results demonstrate that chromobodies efficiently recognize and bind their epitope in different structures such as the cytoskeleton, the replication machinery, the chromatin or the nuclear envelope as well as in different subcellular compartments like the cytoplasm or nucleus. We generated chromobodies with different binding affinities and could demonstrate that even transient binding was sufficient for visualization of cellular structures.

Since low affinity binding of chromobodies to the protein of interest is likely to be less harmful than a permanent fusion of the studied protein with a fluorescent protein we aim to modulate chromobody affinities through directed *in vitro* mutagenesis and maturation. As the entire antigen surface is available for chromobody selection not only chromobodies with different binding/recognition sites can be identified but also chromobodies against post-translational modifications can be selected (Fig. 11a). In principle, different conformational states of proteins could be distinguished. Moreover, induced gene expression as a cellular response to external stimuli could be monitored as spontaneous accumulation of chromobodies at distinct sites or overall altered fluorescent intensity distribution. Antigens have not necessarily to be only proteins but also could be non-protein components of cells like methylated DNA respectively 5-methylcytosine. Chromobodies can also be generated by coupling purified V_HHs to a chemical dye (e.g. Cy5) or directly fusing a V_HH to a chromogenic enzyme e.g. horseradish peroxidase (HRP) (Fig. 11b).

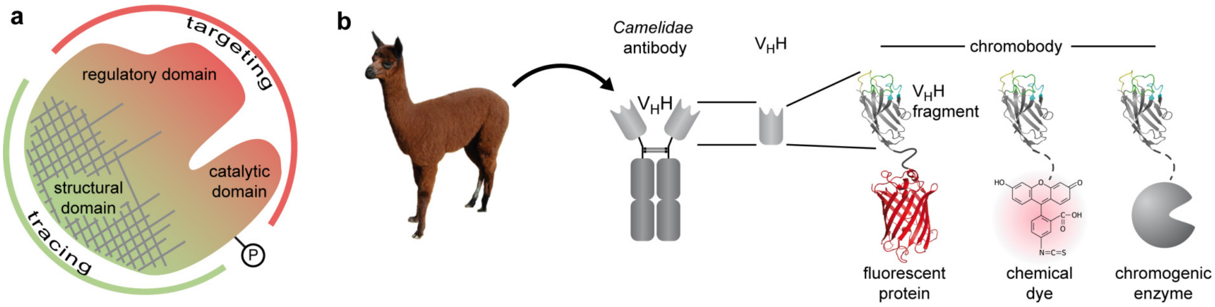
a
targeting
regulatory domain
catalytic domain
structural domain
tracing
P
b
Camelidae antibody
V_HH
chromobody
V_HH fragment
fluorescent protein
chemical dye
chromogenic enzyme

Fig. 11 | (a) Visualization (tracing) and inhibition (targeting) of proteins with chromobodies. (b) Illustration of the conjugated types of chromobodies

Chromobodies open up new opportunities to specifically and reversibly knocking out protein function without depleting the protein from the cellular context. Simultaneously, the chromobody would visualize the targeted protein. Other methods such as the use of siRNA (small interfering RNA) does not lead to a complete gene knock-out but only to a knock-down with largely reduced protein amount and residual activity (Fig. 12). In addition, siRNA down-regulates gene expression often with unknown off-target or side effects. Alternatively, target inhibition with small molecule inhibitors (SMI) usually only blocks catalytic centers of proteins without visualizing them (Fig. 12). In summary, chromobodies combine the wide target range of antibodies with live cell capabilities of fluorescent protein fusions and thus allow tracing of any cellular epitope including endogenous proteins, their post-translational modifications and conformational states as well as non-protein components *in vivo*.

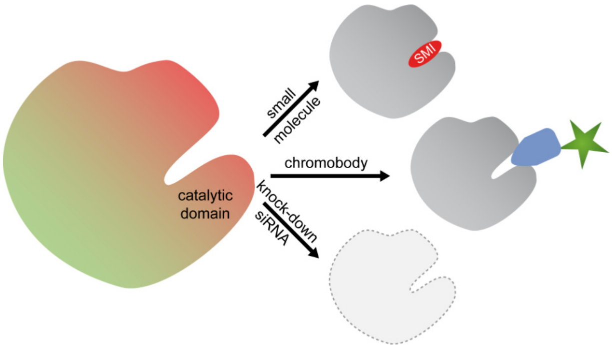
SMI
small molecule
chromobody
catalytic domain
knock-down siRNA

Fig. 12 | Different strategies of protein inhibition and knock-down: small molecule inhibitors (SMI) directed against catalytic centers of proteins; down-regulation of protein expression with siRNA; chromobodies to simultaneously inhibit protein function and visualize the endogenous protein.

III.3. A GFP-BINDING PROTEIN FOR BIOCHEMICAL AND FUNCTIONAL STUDIES

In recent years green fluorescent protein (GFP) and spectral variants thereof became popular tools to study protein localization, interaction and in combination with fluorescence photobleaching techniques, provided unique information on protein dynamics in living cells. Necessary further information on DNA binding, enzymatic activity and complex formation of the studied proteins can be obtained with various biochemical techniques. These methods, however, are often hampered by the limited availability of specific antibodies. A common way to bypass that limitation are fusions of the protein of interest to specific epitope- or protein-tags including HA, c-Myc, FLAG or GST (Terpe, 2003). Curiously, GFP, the most widely used labeling tag in cell biology, is rarely used for biochemical analyses (Cristea et al., 2005; Lorkovic et al., 2004).

We have now engineered a novel tool to isolate GFP, based on the antigen-binding V_HH domain derived from an alpaca heavy-chain antibody, referred to as the GFP-binding protein (GBP). This GBP can easily be produced in bacteria in unlimited quantities and reproducible quality and coupled to matrices (referred to as the GFP-nanotrap). The GFP-nanotrap resembles the versatile link between cell biological and biochemical approaches where GFP fusion proteins can first be studied *in vivo* and thereafter be easily isolated for *in vitro* analyses. The high affinity of the GFP-nanotrap allows short (5 – 30 min) time incubations to quantitatively precipitate GFP fusion proteins with minimized unspecific binding. Furthermore, it entirely avoids contamination by heavy and light chains of conventional antibodies (50 and 25 kDa) that normally interfere with subsequent analyses. We took advantage of the GFP-nanotrap to isolate GFP-labeled wild-type and mutant Dnmt1 for comparison of enzymatic activity or interactions assays after having analyzed the distribution of the proteins in cells.

In an additional approach, we demonstrated that the GFP-nanotrap could be fused with structural proteins, like lamins to ectopically capture GFP fusion proteins and their interacting endogenous partners to a defined region inside living cells. The use of this intracellular nanotrap opens up an entire spectrum of new types of functional studies to probe and manipulate cellular processes and structures. Currently we aim to target specific gene loci to heterochromatic or euchromatic domains in the nucleus. This would enable direct studies on the role and organization of nuclear architecture, in particular the effects of nuclear localization of genes on their transcriptional activity. Additionally we try to implement a “switch” in the GFP-nanotrap to reversibly induce directed translocations.

III.4. DIRECT VISUALIZATION OF ENZYME-ACTIVITY IN LIVING CELLS

Faithful replication of genetic and epigenetic information is crucial to ensure the integrity and identity of proliferating cells. We owe part of our basic knowledge about DNA methylation to classical biochemical approaches, which cannot reflect the complexity of living, mammalian cells.

The trapping assay described in chapter II.4 allows to study Dnmt1 for the first time in its physiological environment with its natural substrate in the context of dynamic chromatin structures and simultaneously ongoing DNA replication. The method is based on the formation of a covalent complex of DNA methyltransferases with cytosine residues during the methylation reaction. After the methylation reaction the enzyme is released from DNA by β-elimination and available for another round of methylation. This mobility of the enzyme can be measured in FRAP experiments with fluorescently labeled Dnmt1 as fluorescence recovery when bleaching replication foci (Fig. 13a). Incubation of cells with normal growth medium containing the cytosine analog 5-aza-2'-deoxycitidine (5-aza-dC) leads to incorporation of 5-aza-dC into newly replicated DNA. The subsequent methylation of 5-aza-dC results in a covalent nucleotide/protein complex, which cannot be disassembled due to the lack of a proton at carbon 5 of the base ring. This trapping of Dnmt1 at the DNA can be visualized since no fluorescence of GFP-Dnmt1 at bleached replication sites recovers (Fig. 13b).

With this trapping assay both, activity and subnuclear targeting of Dnmts can be analyzed *in situ* at different cell cycle stages in single living cells. We show that this technique can be used to monitor any fluorescently labeled DNA methyltransferase actively engaged in the methylation reaction with a mobile nuclear distribution. In addition, we demonstrate that the trapping assay is a new approach to directly test the effects of mutations of Dnmts in living cells on account of different fluorescence recovery rates, which reflect the enzymatic activity of the fusion proteins (Fig. 13c). Furthermore, this method now enables a direct analysis of the consequences of other demethylating drugs than 5-aza-dC, like zebularine (1-(β-D-ribofuranosyl)-1,2-dihydropyrimidin-2-one) (Cheng et al., 2003; Zhou et al., 2002) or procainamide (Lin et al., 2001; Scheinbart et al., 1991), which are widely used in basic research and in cancer therapy. The trapping assay also offers an approach to test new types of target inhibition of Dnmts including treatment with small molecule inhibitors to specifically block the catalytic center (Fig. 13d).

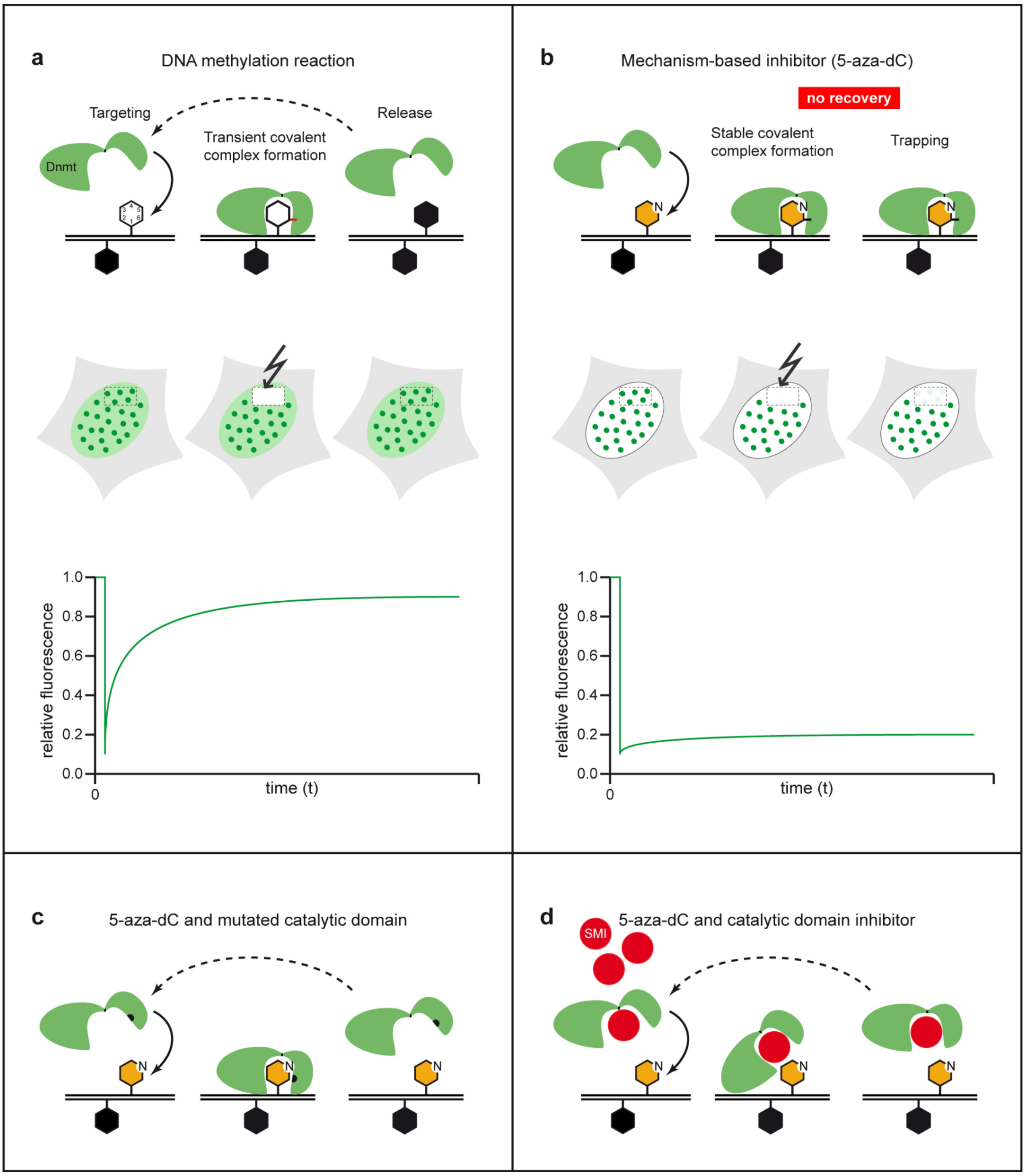
a
DNA methylation reaction
Targeting
Transient covalent complex formation
Release
Dnmt
relative fluorescence
1.0
0.8
0.6
0.4
0.2
0.0
0
time (t)
b
Mechanism-based inhibitor (5-aza-dC)
no recovery
Stable covalent complex formation
Trapping
N
relative fluorescence
1.0
0.8
0.6
0.4
0.2
0.0
0
time (t)
c
5-aza-dC and mutated catalytic domain
d
5-aza-dC and catalytic domain inhibitor
SMI

Fig. 13 | Rational of the trapping assay. (a) Dnmt1 binds to hemimethylated CpG sites (black and white hexagons) and forms a transient covalent complex with the cytosine residue (red line). After methyl group transfer the enzyme is released and becomes available for another round of methylation (dotted arrow), which is visualized as fluorescence recovery after photobleaching of GFP-Dnmt1. (b) Mechanism based inhibitors such as 5-aza-dC (orange hexagons) are incorporated into DNA during S phase. Dnmt1 forms a stable covalent complex with 5-aza-dC and becomes trapped. Immobilization of GFP-Dnmt1 is detected as lack of recovery after photobleaching. (c) In contrast, fluorescence recovery is observed if the catalytic function of Dnmt1 is eliminated by a mutation (black dot in the catalytic domain). (d) Likewise, blocking the catalytic site of Dnmt1 with small molecule inhibitors (SMI) would prevent covalent complex formation again resulting in fluorescence recovery after photobleaching.

III.5. COMBINATORIAL APPROACHES AND OUTLOOK

After the development of several new powerful methods and tools to investigate protein localization, distribution, dynamics, interactions and function the next challenge is now to optimize, expand, automate, integrate and combine them.

First, to generate new chromobodies, large libraries of potential V_HHs have to be screened to isolate antigen-recognizing chromobodies. This is classically done with the phage display technology followed by an enzyme-linked immunosorbent assay (ELISA). *In vitro* identified chromobodies then have to be tested *in vivo* where they can have divergent properties on account of the natively folded antigen. Instead, high-throughput screening of chromobody-libraries with the F2H assay in living cells would directly identify "true" chromobodies and could also provide data about binding affinities to the antigen by FRAP analysis. By presenting either a denatured antigen in the classical systems or an antigen that is properly folded inside eukaryotic cells, different chromobodies with different binding properties for different applications could be identified.

Second, generating a chromobody-based target inhibitor specifically directed against the catalytic center of Dnmt1 while simultaneously visualizing the endogenous protein and testing its ability to prevent 5-aza-dC–mediated trapping is yet another challenge, since in cancer cells tumor-suppressor genes are frequently silenced by erroneous methylation. Pharmaceutical strategies aim at transient inhibition of Dnmts to reactivate such epigenetically silenced genes and re-establish normal cell cycle and growth control (Christman, 2002). Mechanism-based inhibitors such as 5-aza-dC presently under clinical trials, generate irreversible Dnmt1-DNA adducts that may lead to cytotoxic side-effects (Juttermann et al., 1994). Therefore, our goal is to isolate chromobodies recognizing Dnmt1 and identify with the trapping assay those that are potentially inhibiting their target. In a subsequent step candidate inhibitors can be further analyzed with the F2H assay to exclude those chromobodies that are perturbing any protein-protein interaction.

Third, the GFP-binding protein (GBP) - taken advantage of in the GFP-nanotrap - can be introduced in a non-fluorescent F2H-bait vector replacing protein X in the bait construct. Expressed in living cells, this fusion protein will bind to its associated distinct cellular structure. The GBP part of the protein will then immobilize GFP-fusion proteins at the defined structure, thus indirectly highlighting that structure. Other proteins labeled with a different fluorescence either co-localize at that anchoring structure, in case of interaction with the GFP fusion protein or show no local enrichment. With this, essentially any GFP labeled protein can be analyzed for interaction with any red fluorescent fusion protein, rendering this GBP-coupled F2H assay a versatile, highly flexible method. In initial experiments we have successfully tested the feasibility of this approach. We will optimize the assay to screen new chromobody-libraries and to study internal and external interactions of Dnmts, mutant Dnmts or isolated domains. In a similar approach we targeted GFP labeled Dnmt1 and mutants thereof to the anchoring structure. Preliminary experiments indicate a TS-domain (see Fig. 8) mediated DNA decondensation at the locus. This unexpected observation has to be validated and further analyzed. In general, this demonstrates that the GBP-based F2H assay can also be used to investigate protein-DNA interactions.

The cell biological applications developed during this work are in principle applicable for *in vivo* high-throughput screenings. However, designing and optimizing large-scale transfection methods and engineering a microscopic set-up for high-resolution live cell imaging with fluorescence dynamics techniques, i.e. FRAP is a further challenge. Current screening stations mostly are based on wide-field fluorescence microscopy, imaging with relatively low-resolution air objectives through thick (~1mm) plastic bottom multiwell dishes. Such acquisition settings are necessary to gain data from hundreds of thousands of cells on thousands of images. At the same time, the image quality is sufficient to discriminate between cytoplasmic and nuclear localization of a reporter protein, which is presently a common assay. For a more detailed analysis of many cells a confocal or confocal-like illumination with high magnification through glass bottom plates with optical properties would be preferable. Currently we are collaborating with manufacturers of live cell dishes for high-resolution microscopy. Furthermore we will improve large-scale transfection methods. A potential automated On-Chip transfection assay is outlined in Fig. 14. A transfection mix containing the expression plasmids is spotted on an *in vivo* imaging chamber and cells are seeded on top of the dried DNA spots. Cells growing on one of these spots take up the corresponding DNA, express the protein and will be imaged in high resolution through the optical bottom dish. The next step will be a collaboration with developer of high-content imaging systems to implement dynamic live-cell applications.

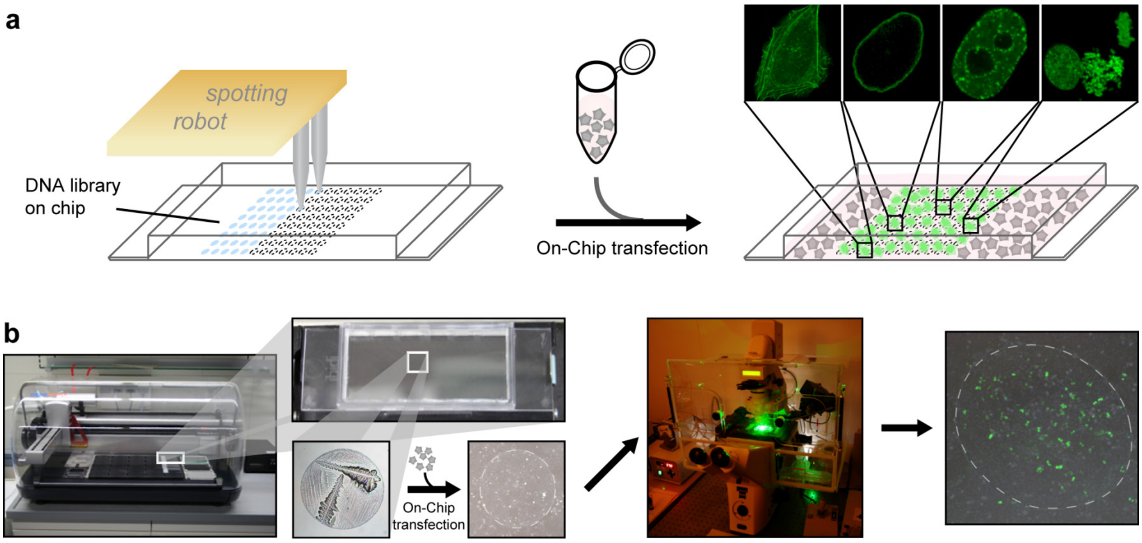

Fig. 14 | (a) Exemplary illustration of a cell-biological high-content analysis with On-Chip transfection. Automated spotting of the DNA-transfection reagent-mix at defined positions on a live cell chamber with optical bottom (transfection-chip). When dried, cells are seeded on top and incubated. Those growing in one of the spots specifically take up the DNA and express the corresponding fusion protein. (b) From left to right: spotting robot with enlarged transfection-chip, magnification of a dried transfection spot with cells seeded on top, a live cell imaging station imaging transfected cells in a DNA spot.

Further projects will involve the direct transduction of the chromobody-protein into cells using e.g. chemical compounds. An alternative method is based on chromobody fusion to viral proteins and small peptides that have the ability to transduce or travel through biological membranes. At present, we are developing chromobodies for immunofluorescent methods. In initial experiments we could demonstrate that purified chromobodies - directly coupled to a chemical dye - when applied in immunofluorescent stainings in fixed cells, do detect their antigen. They do so equally efficient as conventional antibodies without the necessity of amplifying the signal intensity with secondary antibodies (Fig. 15).

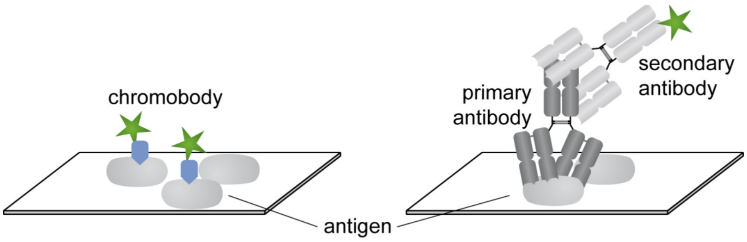

Fig. 15 | Principle comparison between immunofluorescence staining with chromobodies and conventional antibody-detection.

In summary, during this thesis we developed novel, simple, versatile and efficient methods and tools to gain a better understanding of the regulation and function of cellular processes such as DNA methylation by direct detection of protein-protein interaction, tracing of endogenous proteins, targeted translocation of proteins and visualization of DNA methyltransferase activity all in living cells in real-time. These tools are now the basis for intriguing applications and further developments.

CHAPTER IV. ANNEX

IV.1. ABBREVIATIONS

5-aza-dC: 5-aza-2'-deoxycitidine

5mC: 5-methylcytosine

AD: activator domain

B2H: bacterial two-hybrid

BiFC: bimolecular fluorescence complementation

CDR: complementarity-determining region

CFP: enhanced cyan fluorescent protein

ChIP: chromatin immunoprecipitation

Co-IP: co-immunoprecipitation

COBRA: combined bisulfite restriction analysis

CpG: cytosine-guanine dinucleotide

DAPI: 4',6-diamidino-2-phenylindole

DB: DNA-binding domain

DDP1: deafness dystonia peptide 1

Dnmt: DNA methyltransferase

DPSS: Diode-Pumped Solid-State

ELISA: enzyme-linked immunosorbent assay

F2H: fluorescent two-hybrid

Fab: fragment antigen binding

FCS: fluorescence correlation spectroscopy

FCCS: fluorescence cross-correlation spectroscopy

FLIP: fluorescence loss in photobleaching

FP: fluorescent protein

FRAP: fluorescence recovery after photobleaching

FRET: fluorescent resonance energy transfer / Förster radius energy transfer

Gadd: growth arrest and DNA-damage-inducible protein

GBP: GFP binding protein

GFP: enhanced green fluorescent protein

GST: glutathione S-transferase

H2B: histone H2B

HDAC: histone deacetylase

HEK: human embryonic kidney cell line

HMGA1a : mobility group protein A1a

HPLC: high-performance liquid chromatography

HRP: horseradish peroxidase

IMS: intermembrane space

Igf: Insulin growth factor

IgG: Immunoglobulin G

IP: immunoprecipitation

kDa: kilodalton

LacI: Lac repressor

methyl-DIP: methylated DNA immunoprecipitation

MeCP: methyl CpG binding protein

NHS: N-hydroxysuccinimide

NLS: nuclear localization signal

PBD: PCNA binding domain

PA: photoactivation

PARP: Poly (ADP-ribose) polymerase

PBHD: polybromo homology domain

PC: photoconversion / proline-cysteine

PCNA: proliferating cell nuclear antigen

PML: promyelocytic leukemia protein

RFP: monomeric red fluorescent protein 1

SAH: S-adenosyl homocysteine

SAM: S-adenosyl methionine

scFv: single chain variable fragment

siRNA: small interfering RNA

SMI: small molecule inhibitor

SMT: single molecule tracking

SUMO3: small ubiquitin-related modifier 3

TS: targeting sequence (of Dnmt1)

V_HH: variable domain of heavy-chain antibody

Vim: Vimentin

XRCC1: X-ray repair cross-complementing protein 1

Y2H: yeast two-hybrid

YFP: enhanced yellow fluorescent protein

ZnF: Zn2+-binding region

IV.2. CONTRIBUTIONS

IV.2.1. DECLARATIONS OF CONTRIBUTIONS TO II.1

Heinrich Leonhardt, Cristina Cardoso and me developed the method, conceived the study laid and out the project aims. I generated most of the expression constructs and performed corresponding experiments. Oliver Mortusewicz generated the XRCC1-LacI-RFP and PCNA-LacI-RFP expression constructs and analyzed the respective data together with Regina Kleinhans. Ulrich Rothbauer provided cDNA for the mitochondrial proteins while Heike Göhler from the laboratory of Erich Wanker provided the Huntington's disease related cDNAs. Together with Heinrich Leonhardt, Oliver Mortusewicz and Ulrich Rothbauer I prepared the manuscript and the figures.

IV.2.2. DECLARATIONS OF CONTRIBUTIONS TO II.2

The project was started as a collaboration with the laboratory of Serge Muyldermans, where Natalija Backmann and Katja Conrath isolated the corresponding V_HH. Ulrich Rothbauer designed and generated all chromobody expression constructs as well as the molecular biological experiments. Sergei Tillib provided anti-Lamin and anti-Cytokeratin8-V_HHs. Danny Nowak and Anja Gahl from the group of Cristina Cardoso purified GFP and provided several expression constructs. I designed, performed and analyzed the cell biological experiments: expressing chromobodies in living cells, performing long term live cell microscopy and FRAP analysis of binding properties of chromobodies. I prepared the figures and help writing the manuscript.

IV.2.3. DECLARATIONS OF CONTRIBUTIONS TO II.3

Ulrich Rothbauer and Heinrich Leonhardt developed the method and conceived the study. Ulrich Rothbauer performed all molecular biological experiments. Serge Muyldermans generated the anti-GFP V_HH. Aloys Schepers performed ChIP experiments for Figure 4. All fluorescently labeled Dnmt1 and PCNA fusions were provided by Cristina Cardoso. I designed and conducted the Lamin-GBP experiments, prepared all figures and helped writing the manuscript.

IV.2.4. DECLARATIONS OF CONTRIBUTIONS TO II.4

Heinrich Leonhardt and Lothar Schermelleh laid out the project aims and conceived the study. Fabio Spada designed and performed the methylation analysis in *dnmt1*$^{-/-}$ ES cells for supplementary Figure 1. Hariharan Easwaran, Jean Margot from the laboratory of Cristina Cardoso provided all fluorescently labeled Dnmt1 and PCNA fusions. I performed the experiment for supplementary Figure 2 and analyzed the data for Figures 2d and 3 together with Lothar Schermelleh and helped setting up the microscopy for the photoactivation experiment. In addition, I prepared the Figures 1 and 5 and helped writing the manuscript.

IV.2.5. DECLARATIONS OF CONTRIBUTIONS TO II.5

Fabio Spada wrote most of the manuscript. I prepared the figures, discussed and helped writing the manuscript together with Ulrich Rothbauer, Lothar Schermelleh and Heinrich Leonhardt.

IV.2.6. DECLARATION ACCORDING TO THE "PROMOTIONSORDNUNG DER LMU MÜNCHEN FÜR DIE FAKULTÄT BIOLOGIE"

Betreuung: Hiermit erkläre ich, dass die vorgelegte Arbeit an der LMU von Herrn Prof. Dr. Heinrich Leonhardt betreut wurde (Gemäß §5 Abs. (1) 5. Promotionsordnung der LMU)

Anfertigung: Hiermit versichere ich ehrenwörtlich, dass die Dissertation selbstständig und ohne unerlaubte Hilfsmittel angefertigt wurde. Über Beiträge, die im Rahmen der kumulativen Dissertation in Form von Manuskripten in der Dissertation enthalten sind, wurde im Kapitel IV.2 Rechenschaft abgelegt und die eigenen Leistungen wurden aufgelistet. (Gemäß §5 Abs. (1) 6. Promotionsordnung der LMU)

Prüfung: Hiermit erkläre ich, dass die Dissertation weder als ganzes noch in Teilen an einem anderen Ort einer Prüfungskommission vorgelegt wurde. Weiterhin habe ich weder an einem anderen Ort eine Promotion angestrebt oder angemeldet oder versucht eine Doktorprüfung abzulegen. (Gemäß §5 Abs. (1) 7. & 8. Promotionsordnung der LMU)

IV.3. ACKNOWLEDGEMENTS

First, I would like to thank Prof. Heinrich Leonhardt for the unique opportunity to conduct my PhD research under his supervision, with his support and to give me the freedom to participate in the chromobody-project. This provided me a highly informative insight into a world apart from daily laboratory life of basic research and opened up promising future prospects. It was a great inspiration to work in his group with all his ideas for new experiments, projects and future plans.

Next, I would like to acknowledge Prof. Harry MacWilliams for accepting to be second referee for my thesis.

Many thanks also to Cristina Cardoso for all the interesting discussions, advices and suggestions especially during my trips to Berlin and at our "Illuminati"-meetings. For kindly providing me with a lot of reagents essential for a great part of my work I am also grateful to the people in Cristina´s lab; particularly Robert Martin for a lot of interesting scientific discussions (and non-scientific ones, too!) wherever we met and his hospitality.

Back in Munich, the nice and friendly atmosphere in Heinrich's lab really made me enjoy the last four years of my PhD project. Going hiking and sledging or to the Wies'n with the people from the lab was always very much fun! Thank you all for that! I would like to express my gratitude towards Anja Gahl for keeping the lab running, managed and safe (very important for me, clumsy fellow)! Furthermore I like to thank Ulrich Rothbauer and Oliver Mortusewicz not only for their very helpful scientific comments and discussions, but also for them becoming good friends, neighbors (home / office) and Schnappauf! Uli: Thank you for "kicking my ..." and let's get the chromobodies successfully running! Oli: You still have an unredeemed concert voucher; by the way when is the next poster karaoke?

For very helpful and instructive discussions I owe many thanks to Lothar Schermelleh and Fabio Spada. I also want to thank Katrin Schmidthals and Anna-Maria Jegg for the good and successful teamwork. Of course I must also thank all other members of the Department of Anthropology and Human Genetics, i.e. the Cremer group. Everybody has been very kind, helpful and exquisitely taking care of my stomach. I want to explicitly mention Daniela Köhler who gave me a fabulous shelter with great housemates and Hilmar Strickfaden for stimulating discussions and his overwhelming helpfulness.

Last, but certainly not least, I would like to thank my parents for their ongoing support, patience and believe in me throughout all these years. Baba, Mama, kheli mamnoun baraye komake shoma, hoseleh ba man wa etminanetoun be man hameh in salha. Omidwaram, man tounestam shomaro razi bokonam. But actually most of all I would like to thank the person who was always able to turn my bad moods into good moods, made me laugh and happy but does not want to be namely mentioned.

IV.4. REFERENCES

Abbe, E. 1873. Beiträge zur Theorie des Mikroskops und der mikroskopischen Wahrnehmung. *Arch. Mikrosk. Anat.* 9:413-468.

Bacolla, A., S. Pradhan, R.J. Roberts, and R.D. Wells. 1999. Recombinant human DNA (cytosine-5) methyltransferase. II. Steady-state kinetics reveal allosteric activation by methylated dna. *J Biol Chem*. 274:33011-9.

Barreto, G., A. Schafer, J. Marhold, D. Stach, S.K. Swaminathan, V. Handa, G. Doderlein, N. Maltry, W. Wu, F. Lyko, and C. Niehrs. 2007. Gadd45a promotes epigenetic gene activation by repair-mediated DNA demethylation. *Nature*. 445:671-5.

Baylin, S., and T.H. Bestor. 2002. Altered methylation patterns in cancer cell genomes: cause or consequence? *Cancer Cell*. 1:299-305.

Beard, C., E. Li, and R. Jaenisch. 1995. Loss of methylation activates Xist in somatic but not in embryonic cells. *Genes Dev*. 9:2325-34.

Berger, S.L. 2007. The complex language of chromatin regulation during transcription. *Nature*. 447:407-412.

Bestor, T., A. Laudano, R. Mattaliano, and V. Ingram. 1988. Cloning and sequencing of a cDNA encoding DNA methyltransferase of mouse cells. The carboxyl-terminal domain of the mammalian enzymes is related to bacterial restriction methyltransferases. *J Mol Biol*. 203:971-83.

Bestor, T.H. 1988. Cloning of a mammalian DNA methyltransferase. *Gene*. 74:9-12.

Bestor, T.H. 2000. The DNA methyltransferases of mammals. *Hum Mol Genet*. 9:2395-402.

Bestor, T.H., and V.M. Ingram. 1983. Two DNA methyltransferases from murine erythroleukemia cells: purification, sequence specificity, and mode of interaction with DNA. *Proc Natl Acad Sci U S A*. 80:5559-63.

Bestor, T.H., and V.M. Ingram. 1985. Growth-dependent expression of multiple species of DNA methyltransferase in murine erythroleukemia cells. *Proc Natl Acad Sci U S A*. 82:2674-8.

Bestor, T.H., and G.L. Verdine. 1994. DNA methyltransferases. *Curr Opin Cell Biol*. 6:380-9.

Bird, A. 2002. DNA methylation patterns and epigenetic memory. *Genes Dev*. 16:6-21.

Bird, A. 2007. Perceptions of epigenetics. *Nature*. 447:396-8.

Bird, A.P. 1986. CpG-rich islands and the function of DNA methylation. *Nature*. 321:209-13.

Bird, A.P., and A.P. Wolffe. 1999. Methylation-induced repression--belts, braces, and chromatin. *Cell*. 99:451-4.

Bostick, M., J.K. Kim, P.O. Esteve, A. Clark, S. Pradhan, and S.E. Jacobsen. 2007. UHRF1 plays a role in maintaining DNA methylation in mammalian cells. *Science*. 317:1760-4.

Bourc'his, D., G.L. Xu, C.S. Lin, B. Bollman, and T.H. Bestor. 2001. Dnmt3L and the establishment of maternal genomic imprints. *Science*. 294:2536-9.

Brown, K.D., and K.D. Robertson. 2007. DNMT1 knockout delivers a strong blow to genome stability and cell viability. *Nat Genet*. 39:289-90.

Cardinale, A., I. Filesi, S. Mattei, and S. Biocca. 2004. Intracellular targeting and functional analysis of single-chain Fv fragments in mammalian cells. *Methods*. 34:171-8.

Cardoso, M.C., and H. Leonhardt. 1999. DNA methyltransferase is actively retained in the cytoplasm during early development. *J Cell Biol*. 147:25-32.

Carlson, L.L., A.W. Page, and T.H. Bestor. 1992. Properties and localization of DNA methyltransferase in preimplantation mouse embryos: implications for genomic imprinting. *Genes Dev*. 6:2536-41.

Chedin, F., M.R. Lieber, and C.L. Hsieh. 2002. The DNA methyltransferase-like protein DNMT3L stimulates de novo methylation by Dnmt3a. *Proc Natl Acad Sci U S A*. 99:16916-21.

Chen, L., A.M. MacMillan, W. Chang, K. Ezaz-Nikpay, W.S. Lane, and G.L. Verdine. 1991. Direct identification of the active-site nucleophile in a DNA (cytosine-5)-methyltransferase. *Biochemistry*. 30:11018-25.

Cheng, J.C., C.B. Matsen, F.A. Gonzales, W. Ye, S. Greer, V.E. Marquez, P.A. Jones, and E.U. Selker. 2003. Inhibition of DNA methylation and reactivation of silenced genes by zebularine. *J Natl Cancer Inst*. 95:399-409.

Cheng, X., and R.J. Roberts. 2001. AdoMet-dependent methylation, DNA methyltransferases and base flipping. *Nucleic Acids Res*. 29:3784-95.

Chiang, P.K., R.K. Gordon, J. Tal, G.C. Zeng, B.P. Doctor, K. Pardhasaradhi, and P.P. McCann. 1996. S-Adenosylmethionine and methylation. *Faseb J*. 10:471-80.

Cho, S., S.G. Park, D.H. Lee, and B.C. Park. 2004. Protein-protein interaction networks: from interactions to networks. *J Biochem Mol Biol*. 37:45-52.

Christman, J.K. 2002. 5-Azacytidine and 5-aza-2'-deoxycytidine as inhibitors of DNA methylation: mechanistic studies and their implications for cancer therapy. *Oncogene*. 21:5483-95.

Chuang, L.S., H.I. Ian, T.W. Koh, H.H. Ng, G. Xu, and B.F. Li. 1997. Human DNA-(cytosine-5) methyltransferase-PCNA complex as a target for p21WAF1. *Science*. 277:1996-2000.

Craig, J.M., and W.A. Bickmore. 1994. The distribution of CpG islands in mammalian chromosomes [see comments] [published erratum appears in Nat Genet 1994 Aug;7(4):551]. *Nat Genet*. 7:376-82.

Cristea, I.M., R. Williams, B.T. Chait, and M.P. Rout. 2005. Fluorescent proteins as proteomic probes. *Mol Cell Proteomics*. 4:1933-41.

Davies, J., and L. Riechmann. 1995. Antibody VH domains as small recognition units. *Biotechnology (N Y)*. 13:475-9.

Deane, C.M., L. Salwinski, I. Xenarios, and D. Eisenberg. 2002. Protein interactions: two methods for assessment of the reliability of high throughput observations. *Mol Cell Proteomics*. 1:349-56.

Desmyter, A., K. Decanniere, S. Muyldermans, and L. Wyns. 2001. Antigen specificity and high affinity binding provided by one single loop of a camel single-domain antibody. *J Biol Chem*. 276:26285-90.

Desmyter, A., T.R. Transue, M.A. Ghahroudi, M.H. Thi, F. Poortmans, R. Hamers, S. Muyldermans, and L. Wyns. 1996. Crystal structure of a camel single-domain VH antibody fragment in complex with lysozyme. *Nat Struct Biol*. 3:803-11.

Doherty, A.S., M.S. Bartolomei, and R.M. Schultz. 2002. Regulation of stage-specific nuclear translocation of Dnmt1o during preimplantation mouse development. *Dev Biol*. 242:255-66.

Durfee, T., K. Becherer, P.L. Chen, S.H. Yeh, Y. Yang, A.E. Kilburn, W.H. Lee, and S.J. Elledge. 1993. The retinoblastoma protein associates with the protein phosphatase type 1 catalytic subunit. *Genes Dev*. 7:555-69.

Easwaran, H.P., L. Schermelleh, H. Leonhardt, and M.C. Cardoso. 2004. Replication-independent chromatin loading of Dnmt1 during G2 and M phases. *EMBO Rep*. 5:1181-6.

Eden, A., F. Gaudet, A. Waghmare, and R. Jaenisch. 2003. Chromosomal instability and tumors promoted by DNA hypomethylation. *Science*. 300:455.

Ehrlich, M., M.A. Gama-Sosa, L.H. Huang, R.M. Midgett, K.C. Kuo, R.A. McCune, and C. Gehrke. 1982. Amount and distribution of 5-methylcytosine in human DNA from different types of tissues of cells. *Nucleic Acids Res*. 10:2709-21.

Erlanson, D.A., L. Chen, and G.L. Verdine. 1993. DNA Methylation through a Locally Unpaired Intermediate. *J Am Chem Soc*. 115:12583-4.

Esteve, P.O., H.G. Chin, A. Smallwood, G.R. Feehery, O. Gangisetty, A.R. Karpf, M.F. Carey, and S. Pradhan. 2006. Direct interaction between DNMT1and G9a coordinates DNA and histone methylation during replication. *Genes Dev*.

Fields, S., and O. Song. 1989. A novel genetic system to detect protein-protein interactions. *Nature*. 340:245-6.

Frommer, M., L.E. McDonald, D.S. Millar, C.M. Collis, F. Watt, G.W. Grigg, P.L. Molloy, and C.L. Paul. 1992. A genomic sequencing protocol that yields a positive display of 5-methylcytosine residues in individual DNA strands. *Proc Natl Acad Sci U S A*. 89:1827-31.

Fuks, F., W.A. Burgers, A. Brehm, L. Hughes-Davies, and T. Kouzarides. 2000. DNA methyltransferase Dnmt1 associates with histone deacetylase activity. *Nat Genet*. 24:88-91.

Fuks, F., P.J. Hurd, R. Deplus, and T. Kouzarides. 2003. The DNA methyltransferases associate with HP1 and the SUV39H1 histone methyltransferase. *Nucleic Acids Res*. 31:2305-12.

Gardiner-Garden, M., and M. Frommer. 1987. CpG islands in vertebrate genomes. *J Mol Biol*. 196:261-82.

Gaudet, F., J.G. Hodgson, A. Eden, L. Jackson-Grusby, J. Dausman, J.W. Gray, H. Leonhardt, and R. Jaenisch. 2003. Induction of tumors in mice by genomic hypomethylation. *Science*. 300:489-92.

Gaudet, F., W.M. Rideout, 3rd, A. Meissner, J. Dausman, H. Leonhardt, and R. Jaenisch. 2004. Dnmt1 expression in pre- and postimplantation embryogenesis and the maintenance of IAP silencing. *Mol Cell Biol*. 24:1640-8.

Gaudet, F., D. Talbot, H. Leonhardt, and R. Jaenisch. 1998. A short DNA methyltransferase isoform restores methylation in vivo. *J Biol Chem*. 273:32725-9.

Geiman, T.M., U.T. Sankpal, A.K. Robertson, Y. Chen, M. Mazumdar, J.T. Heale, J.A. Schmiesing, W. Kim, K. Yokomori, Y. Zhao, and K.D. Robertson. 2004a. Isolation and characterization of a novel DNA methyltransferase complex linking DNMT3B with components of the mitotic chromosome condensation machinery. *Nucleic Acids Res*. 32:2716-29.

Geiman, T.M., U.T. Sankpal, A.K. Robertson, Y. Zhao, Y. Zhao, and K.D. Robertson. 2004b. DNMT3B interacts with hSNF2H chromatin remodeling enzyme, HDACs 1 and 2, and components of the histone methylation system. *Biochem Biophys Res Commun*. 318:544-55.

Goll, M.G., and T.H. Bestor. 2005. Eukaryotic cytosine methyltransferases. *Annu Rev Biochem*. 74:481-514.

Goll, M.G., F. Kirpekar, K.A. Maggert, J.A. Yoder, C.L. Hsieh, X. Zhang, K.G. Golic, S.E. Jacobsen, and T.H. Bestor. 2006. Methylation of tRNAAsp by the DNA methyltransferase homolog Dnmt2. *Science*. 311:395-8.

Grohmann, M., F. Spada, L. Schermelleh, N. Alenina, M. Bader, M.C. Cardoso, and H. Leonhardt. 2005. Restricted mobility of Dnmt1 in preimplantation embryos: implications for epigenetic reprogramming. *BMC Dev Biol*. 5:18.

Gruenbaum, Y., R. Stein, H. Cedar, and A. Razin. 1981. Methylation of CpG sequences in eukaryotic DNA. *FEBS Lett*. 124:67-71.

Grunwald, D., B. Spottke, V. Buschmann, and U. Kubitscheck. 2006. Intranuclear binding kinetics and mobility of single native U1 snRNP particles in living cells. *Mol Biol Cell*. 17:5017-27.

Hamers-Casterman, C., T. Atarhouch, S. Muyldermans, G. Robinson, C. Hamers, E.B. Songa, N. Bendahman, and R. Hamers. 1993. Naturally occurring antibodies devoid of light chains. *Nature*. 363:446-8.

Hanahan, D., and R.A. Weinberg. 2000. The hallmarks of cancer. *Cell*. 100:57-70.

Harmsen, M.M., and H.J. De Haard. 2007. Properties, production, and applications of camelid single-domain antibody fragments. *Appl Microbiol Biotechnol*. 77:13-22.

Harmsen, M.M., R.C. Ruuls, I.J. Nijman, T.A. Niewold, L.G. Frenken, and B. de Geus. 2000. Llama heavy-chain V regions consist of at least four distinct subfamilies revealing novel sequence features. *Mol Immunol*. 37:579-90.

Hata, K., M. Okano, H. Lei, and E. Li. 2002. Dnmt3L cooperates with the Dnmt3 family of de novo DNA methyltransferases to establish maternal imprints in mice. *Development*. 129:1983-93.

Haustein, E., and P. Schwille. 2007. Fluorescence correlation spectroscopy: novel variations of an established technique. *Annu Rev Biophys Biomol Struct*. 36:151-69.

Hellman, A., and A. Chess. 2007. Gene body-specific methylation on the active X chromosome. *Science*. 315:1141-3.

Horton, J.R., G. Ratner, N.K. Banavali, N. Huang, Y. Choi, M.A. Maier, V.E. Marquez, A.D. MacKerell, Jr., and X. Cheng. 2004. Caught in the act: visualization of an intermediate in the DNA base-flipping pathway induced by HhaI methyltransferase. *Nucleic Acids Res*. 32:3877-86.

Howard, G., R. Eiges, F. Gaudet, R. Jaenisch, and A. Eden. 2007. Activation and transposition of endogenous retroviral elements in hypomethylation induced tumors in mice. *Oncogene*.

Howell, C.Y., T.H. Bestor, F. Ding, K.E. Latham, C. Mertineit, J.M. Trasler, and J.R. Chaillet. 2001. Genomic imprinting disrupted by a maternal effect mutation in the Dnmt1 gene. *Cell*. 104:829-38.

Howlett, S.K., and W. Reik. 1991. Methylation levels of maternal and paternal genomes during preimplantation development. *Development*. 113:119-27.

Hsieh, C.L. 1999. In vivo activity of murine de novo methyltransferases, Dnmt3a and Dnmt3b. *Mol Cell Biol*. 19:8211-8.

Hu, C.D., Y. Chinenov, and T.K. Kerppola. 2002. Visualization of interactions among bZIP and Rel family proteins in living cells using bimolecular fluorescence complementation. *Mol Cell*. 9:789-98.

Hu, J.C., M.G. Kornacker, and A. Hochschild. 2000. Escherichia coli one- and two-hybrid systems for the analysis and identification of protein-protein interactions. *Methods*. 20:80-94.

Jach, G., M. Pesch, K. Richter, S. Frings, and J.F. Uhrig. 2006. An improved mRFP1 adds red to bimolecular fluorescence complementation. *Nat Methods*. 3:597-600.

Jackson, D.A., and A. Pombo. 1998. Replicon clusters are stable units of chromosome structure: evidence that nuclear organization contributes to the efficient activation and propagation of S phase in human cells. *J Cell Biol*. 140:1285-95.

Jaenisch, R., and A. Bird. 2003. Epigenetic regulation of gene expression: how the genome integrates intrinsic and environmental signals. *Nat Genet*. 33 Suppl:245-54.

Janicki, S.M., T. Tsukamoto, S.E. Salghetti, W.P. Tansey, R. Sachidanandam, K.V. Prasanth, T. Ried, Y. Shav-Tal, E. Bertrand, R.H. Singer, and D.L. Spector. 2004. From silencing to gene expression: real-time analysis in single cells. *Cell*. 116:683-98.

Jia, D., R.Z. Jurkowska, X. Zhang, A. Jeltsch, and X. Cheng. 2007. Structure of Dnmt3a bound to Dnmt3L suggests a model for de novo DNA methylation. *Nature*. 449:248-51.

Jones, P.A., and S.B. Baylin. 2002. The fundamental role of epigenetic events in cancer. *Nat Rev Genet*. 3:415-28.

Jones, P.A., W.M. Rideout, 3rd, J.C. Shen, C.H. Spruck, and Y.C. Tsai. 1992. Methylation, mutation and cancer. *Bioessays*. 14:33-6.

Jones, P.A., and D. Takai. 2001. The role of DNA methylation in mammalian epigenetics. *Science*. 293:1068-70.

Jones, P.L., G.J. Veenstra, P.A. Wade, D. Vermaak, S.U. Kass, N. Landsberger, J. Strouboulis, and A.P. Wolffe. 1998. Methylated DNA and MeCP2 recruit histone deacetylase to repress transcription. *Nat Genet*. 19:187-91.

Joung, J.K., E.I. Ramm, and C.O. Pabo. 2000. A bacterial two-hybrid selection system for studying protein-DNA and protein-protein interactions. *Proc Natl Acad Sci U S A*. 97:7382-7.

Juttermann, R., E. Li, and R. Jaenisch. 1994. Toxicity of 5-aza-2'-deoxycytidine to mammalian cells is mediated primarily by covalent trapping of DNA methyltransferase rather than DNA demethylation. *Proc Natl Acad Sci U S A*. 91:11797-801.

Kaneda, M., M. Okano, K. Hata, T. Sado, N. Tsujimoto, E. Li, and H. Sasaki. 2004. Essential role for de novo DNA methyltransferase Dnmt3a in paternal and maternal imprinting. *Nature*. 429:900-3.

Kass, S.U., D. Pruss, and A.P. Wolffe. 1997. How does DNA methylation repress transcription? *Trends Genet*. 13:444-9.

Kerppola, T.K. 2006a. Complementary methods for studies of protein interactions in living cells. *Nat Methods*. 3:969-71.

Kerppola, T.K. 2006b. Visualization of molecular interactions by fluorescence complementation. *Nat Rev Mol Cell Biol*. 7:449-56.

Keshet, I., Y. Schlesinger, S. Farkash, E. Rand, M. Hecht, E. Segal, E. Pikarski, R.A. Young, A. Niveleau, H. Cedar, and I. Simon. 2006. Evidence for an instructive mechanism of de novo methylation in cancer cells. *Nat Genet*. 38:149-53.

Kim, J.Y., O.G. Park, J.W. Lee, and Y.C. Lee. 2007. One plus two-hybrid system: a novel yeast genetic selection for specific missense mutations disrupting protein-protein interactions. *Mol Cell Proteomics*.

Kimura, H., and K. Shiota. 2003. Methyl-CpG-binding protein, MeCP2, is a target molecule for maintenance DNA methyltransferase, Dnmt1. *J Biol Chem*. 278:4806-12.

Kirber, M.T., K. Chen, and J.F. Keaney, Jr. 2007. YFP photoconversion revisited: confirmation of the CFP-like species. *Nat Methods*. 4:767-8.

Klimasauskas, S., S. Kumar, R.J. Roberts, and X. Cheng. 1994. HhaI methyltransferase flips its target base out of the DNA helix. *Cell*. 76:357-69.

Laird, P.W., and R. Jaenisch. 1994. DNA methylation and cancer. *Hum Mol Genet*. 3 Spec No:1487-95.

Lei, H., S.P. Oh, M. Okano, R. Juttermann, K.A. Goss, R. Jaenisch, and E. Li. 1996. De novo DNA cytosine methyltransferase activities in mouse embryonic stem cells. *Development*. 122:3195-205.

Leonhardt, H., and T.H. Bestor. 1993. Structure, function and regulation of mammalian DNA methyltransferase. *Exs*. 64:109-19.

Leonhardt, H., and M.C. Cardoso. 2000. DNA methylation, nuclear structure, gene expression and cancer. *J Cell Biochem Suppl*. Suppl:78-83.

Leonhardt, H., A.W. Page, H.U. Weier, and T.H. Bestor. 1992. A targeting sequence directs DNA methyltransferase to sites of DNA replication in mammalian nuclei. *Cell*. 71:865-73.

Li, E. 2002. Chromatin modification and epigenetic reprogramming in mammalian development. *Nat Rev Genet*. 3:662-73.

Li, E., C. Beard, and R. Jaenisch. 1993. Role for DNA methylation in genomic imprinting. *Nature*. 366:362-5.

Li, E., T.H. Bestor, and R. Jaenisch. 1992. Targeted mutation of the DNA methyltransferase gene results in embryonic lethality. *Cell*. 69:915-26.

Lin, X., K. Asgari, M.J. Putzi, W.R. Gage, X. Yu, B.S. Cornblatt, A. Kumar, S. Piantadosi, T.L. DeWeese, A.M. De Marzo, and W.G. Nelson. 2001. Reversal of GSTP1 CpG island hypermethylation and reactivation of pi-class glutathione S-transferase (GSTP1) expression in human prostate cancer cells by treatment with procainamide. *Cancer Res*. 61:8611-6.

Lippincott-Schwartz, J., N. Altan-Bonnet, and G.H. Patterson. 2003. Photobleaching and photoactivation: following protein dynamics in living cells. *Nat Cell Biol*. Suppl:S7-14.

Lock, L.F., D.W. Melton, C.T. Caskey, and G.R. Martin. 1986. Methylation of the mouse hprt gene differs on the active and inactive X chromosomes. *Mol Cell Biol*. 6:914-24.

Lorkovic, Z.J., J. Hilscher, and A. Barta. 2004. Use of fluorescent protein tags to study nuclear organization of the spliceosomal machinery in transiently transformed living plant cells. *Mol Biol Cell*. 15:3233-43.

Magde, D., E.L. Elson, and W.W. Webb. 1974. Fluorescence correlation spectroscopy. II. An experimental realization. *Biopolymers*. 13:29-61.

Magliery, T.J., C.G. Wilson, W. Pan, D. Mishler, I. Ghosh, A.D. Hamilton, and L. Regan. 2005. Detecting protein-protein interactions with a green fluorescent protein fragment reassembly trap: scope and mechanism. *J Am Chem Soc*. 127:146-57.

Margot, J.B., A.E. Ehrenhofer-Murray, and H. Leonhardt. 2003. Interactions within the mammalian DNA methyltransferase family. *BMC Mol Biol*. 4:7.

Mc Intyre, J., E.G. Muller, S. Weitzer, B.E. Snydsman, T.N. Davis, and F. Uhlmann. 2007. In vivo analysis of cohesin architecture using FRET in the budding yeast Saccharomyces cerevisiae. *Embo J*. 26:3783-93.

Mertineit, C., J.A. Yoder, T. Taketo, D.W. Laird, J.M. Trasler, and T.H. Bestor. 1998. Sex-specific exons control DNA methyltransferase in mammalian germ cells. *Development*. 125:889-97.

Miyawaki, A., J. Llopis, R. Heim, J.M. McCaffery, J.A. Adams, M. Ikura, and R.Y. Tsien. 1997. Fluorescent indicators for Ca2+ based on green fluorescent proteins and calmodulin. *Nature*. 388:882-7.

Mortusewicz, O., L. Schermelleh, J. Walter, M.C. Cardoso, and H. Leonhardt. 2005. Recruitment of DNA methyltransferase I to DNA repair sites. *Proc Natl Acad Sci U S A*. 102:8905-9.

Muyldermans, S. 2001. Single domain camel antibodies: current status. *J Biotechnol*. 74:277-302.

Muyldermans, S., T. Atarhouch, J. Saldanha, J.A. Barbosa, and R. Hamers. 1994. Sequence and structure of VH domain from naturally occurring camel heavy chain immunoglobulins lacking light chains. *Protein Eng*. 7:1129-35.

Muyldermans, S., and M. Lauwereys. 1999. Unique single-domain antigen binding fragments derived from naturally occurring camel heavy-chain antibodies. *J Mol Recognit*. 12:131-40.

Muyldermans, S., and A.A. Travers. 1994. DNA sequence organization in chromatosomes. *J Mol Biol*. 235:855-70.

Nan, X., H.H. Ng, C.A. Johnson, C.D. Laherty, B.M. Turner, R.N. Eisenman, and A. Bird. 1998. Transcriptional repression by the methyl-CpG-binding protein MeCP2 involves a histone deacetylase complex. *Nature*. 393:386-9.

O'Gara, M., R.J. Roberts, and X. Cheng. 1996. A structural basis for the preferential binding of hemimethylated DNA by HhaI DNA methyltransferase. *J Mol Biol*. 263:597-606.

Okano, M., D.W. Bell, D.A. Haber, and E. Li. 1999. DNA methyltransferases Dnmt3a and Dnmt3b are essential for de novo methylation and mammalian development. *Cell*. 99:247-57.

Okano, M., S. Xie, and E. Li. 1998a. Cloning and characterization of a family of novel mammalian DNA (cytosine-5) methyltransferases. *Nat Genet*. 19:219-20.

Okano, M., S. Xie, and E. Li. 1998b. Dnmt2 is not required for de novo and maintenance methylation of viral DNA in embryonic stem cells. *Nucleic Acids Res*. 26:2536-40.

Oswald, J., S. Engemann, N. Lane, W. Mayer, A. Olek, R. Fundele, W. Dean, W. Reik, and J. Walter. 2000. Active demethylation of the paternal genome in the mouse zygote. *Curr Biol*. 10:475-8.

Panning, B., and R. Jaenisch. 1996. DNA hypomethylation can activate Xist expression and silence X-linked genes. *Genes Dev*. 10:1991-2002.

Paulmurugan, R., Y. Umezawa, and S.S. Gambhir. 2002. Noninvasive imaging of protein-protein interactions in living subjects by using reporter protein complementation and reconstitution strategies. *Proc Natl Acad Sci U S A*. 99:15608-13.

Periasamy, A. 2001. Fluorescence resonance energy transfer microscopy: a mini review. *J Biomed Opt*. 6:287-91.

Phair, R.D., and T. Misteli. 2001. Kinetic modelling approaches to in vivo imaging. *Nat Rev Mol Cell Biol*. 2:898-907.

Pradhan, S., A. Bacolla, R.D. Wells, and R.J. Roberts. 1999. Recombinant human DNA (cytosine-5) methyltransferase. I. Expression, purification, and comparison of de novo and maintenance methylation. *J Biol Chem*. 274:33002-10.

Reale, A., G.D. Matteis, G. Galleazzi, M. Zampieri, and P. Caiafa. 2005. Modulation of DNMT1 activity by ADP-ribose polymers. *Oncogene*. 24:13-9.

Reik, W. 2007. Stability and flexibility of epigenetic gene regulation in mammalian development. *Nature*. 447:425-32.

Reik, W., W. Dean, and J. Walter. 2001. Epigenetic reprogramming in mammalian development. *Science*. 293:1089-93.

Remy, I., and S.W. Michnick. 2006. A highly sensitive protein-protein interaction assay based on Gaussia luciferase. *Nat Methods*. 3:977-9.

Robertson, A.K., T.M. Geiman, U.T. Sankpal, G.L. Hager, and K.D. Robertson. 2004. Effects of chromatin structure on the enzymatic and DNA binding functions of DNA methyltransferases DNMT1 and Dnmt3a in vitro. *Biochem Biophys Res Commun*. 322:110-8.

Robertson, K.D. 2002. DNA methylation and chromatin - unraveling the tangled web. *Oncogene*. 21:5361-79.

Robertson, K.D., S. Ait-Si-Ali, T. Yokochi, P.A. Wade, P.L. Jones, and A.P. Wolffe. 2000a. DNMT1 forms a complex with Rb, E2F1 and HDAC1 and represses transcription from E2F-responsive promoters. *Nat Genet*. 25:338-42.

Robertson, K.D., K. Keyomarsi, F.A. Gonzales, M. Velicescu, and P.A. Jones. 2000b. Differential mRNA expression of the human DNA methyltransferases (DNMTs) 1, 3a and 3b during the G(0)/G(1) to S phase transition in normal and tumor cells. *Nucleic Acids Res*. 28:2108-13.

Robertson, K.D., E. Uzvolgyi, G. Liang, C. Talmadge, J. Sumegi, F.A. Gonzales, and P.A. Jones. 1999. The human DNA methyltransferases (DNMTs) 1, 3a and 3b: coordinate mRNA expression in normal tissues and overexpression in tumors. *Nucleic Acids Res*. 27:2291-8.

Robertson, K.D., and A.P. Wolffe. 2000. DNA methylation in health and disease. *Nat Rev Genet*. 1:11-9.

Rougier, N., D. Bourc'his, D.M. Gomes, A. Niveleau, M. Plachot, A. Paldi, and E. Viegas-Pequignot. 1998. Chromosome methylation patterns during mammalian preimplantation development. *Genes Dev*. 12:2108-13.

Sadri, R., and P.J. Hornsby. 1996. Rapid analysis of DNA methylation using new restriction enzyme sites created by bisulfite modification. *Nucleic Acids Res*. 24:5058-9.

Santi, D.V., C.E. Garrett, and P.J. Barr. 1983. On the mechanism of inhibition of DNA-cytosine methyltransferases by cytosine analogs. *Cell*. 33:9-10.

Santoro, R., J. Li, and I. Grummt. 2002. The nucleolar remodeling complex NoRC mediates heterochromatin formation and silencing of ribosomal gene transcription. *Nat Genet*. 32:393-6.

Saxonov, S., P. Berg, and D.L. Brutlag. 2006. A genome-wide analysis of CpG dinucleotides in the human genome distinguishes two distinct classes of promoters. *Proc Natl Acad Sci U S A*. 103:1412-7.

Scheinbart, L.S., M.A. Johnson, L.A. Gross, S.R. Edelstein, and B.C. Richardson. 1991. Procainamide inhibits DNA methyltransferase in a human T cell line. *J Rheumatol*. 18:530-4.

Schermelleh, L., A. Haemmer, F. Spada, N. Rosing, D. Meilinger, U. Rothbauer, M. Cristina Cardoso, and H. Leonhardt. 2007. Dynamics of Dnmt1 interaction with the replication machinery and its role in postreplicative maintenance of DNA methylation. *Nucleic Acids Res*.

Schwille, P., F.J. Meyer-Almes, and R. Rigler. 1997. Dual-color fluorescence cross-correlation spectroscopy for multicomponent diffusional analysis in solution. *Biophys J*. 72:1878-86.

Sclafani, R.A., and T.M. Holzen. 2007. Cell Cycle Regulation of DNA Replication. *Annu Rev Genet*.

Sekar, R., A. Pernthaler, J. Pernthaler, F. Warnecke, T. Posch, and R. Amann. 2003. An improved protocol for quantification of freshwater Actinobacteria by fluorescence in situ hybridization. *Appl Environ Microbiol*. 69:2928-35.

Shapiro, R., B. Braverman, J.B. Louis, and R.E. Servis. 1973. Nucleic acid reactivity and conformation. II. Reaction of cytosine and uracil with sodium bisulfite. *J Biol Chem*. 248:4060-4.

Shapiro, R., V. DiFate, and M. Welcher. 1974. Deamination of cytosine derivatives by bisulfite. Mechanism of the reaction. *J Am Chem Soc*. 96:906-12.

Shen, L., Y. Kondo, Y. Guo, J. Zhang, L. Zhang, S. Ahmed, J. Shu, X. Chen, R.A. Waterland, and J.P. Issa. 2007. Genome-wide profiling of DNA methylation reveals a class of normally methylated CpG island promoters. *PLoS Genet*. 3:2023-36.

Smallwood, A., P.O. Esteve, S. Pradhan, and M. Carey. 2007. Functional cooperation between HP1 and DNMT1 mediates gene silencing. *Genes Dev*.

Spada, F., A. Haemmer, D. Kuch, U. Rothbauer, L. Schermelleh, E. Kremmer, T. Carell, G. Langst, and H. Leonhardt. 2007. DNMT1 but not its interaction with the replication machinery is required for maintenance of DNA methylation in human cells

10.1083/jcb.200610062. *J. Cell Biol.* 176:565-571.

Sporbert, A., P. Domaing, H. Leonhardt, and M.C. Cardoso. 2005. PCNA acts as a stationary loading platform for transiently interacting Okazaki fragment maturation proteins. *Nucleic Acids Res*. 33:3521-8.

Suetake, I., F. Shinozaki, J. Miyagawa, H. Takeshima, and S. Tajima. 2004. DNMT3L stimulates the DNA methylation activity of Dnmt3a and Dnmt3b through a direct interaction. *J Biol Chem*. 279:27816-23.

Sved, J., and A. Bird. 1990. The expected equilibrium of the CpG dinucleotide in vertebrate genomes under a mutation model. *Proc Natl Acad Sci U S A*. 87:4692-6.

Tate, P.H., and A.P. Bird. 1993. Effects of DNA methylation on DNA-binding proteins and gene expression. *Curr Opin Genet Dev*. 3:226-31.

Terpe, K. 2003. Overview of tag protein fusions: from molecular and biochemical fundamentals to commercial systems. *Appl Microbiol Biotechnol*. 60:523-33.

Tsukamoto, T., N. Hashiguchi, S.M. Janicki, T. Tumbar, A.S. Belmont, and D.L. Spector. 2000. Visualization of gene activity in living cells. *Nat Cell Biol*. 2:871-8.

Uetz, P., S.V. Rajagopala, Y.A. Dong, and J. Haas. 2004. From ORFeomes to protein interaction maps in viruses. *Genome Res*. 14:2029-33.

Valentin, G., C. Verheggen, T. Piolot, H. Neel, M. Coppey-Moisan, and E. Bertrand. 2005. Photoconversion of YFP into a CFP-like species during acceptor photobleaching FRET experiments. *Nat Methods*. 2:801.

van der Linden, R.H., L.G. Frenken, B. de Geus, M.M. Harmsen, R.C. Ruuls, W. Stok, L. de Ron, S. Wilson, P. Davis, and C.T. Verrips. 1999. Comparison of physical chemical properties of llama VHH antibody fragments and mouse monoclonal antibodies. *Biochim Biophys Acta*. 1431:37-46.

Vidal, M. 2005. Interactome modeling. *FEBS Lett*. 579:1834-8.

Vidal, M., R.K. Brachmann, A. Fattaey, E. Harlow, and J.D. Boeke. 1996a. Reverse two-hybrid and one-hybrid systems to detect dissociation of protein-protein and DNA-protein interactions. *Proc Natl Acad Sci U S A*. 93:10315-20.

Vidal, M., P. Braun, E. Chen, J.D. Boeke, and E. Harlow. 1996b. Genetic characterization of a mammalian protein-protein interaction domain by using a yeast reverse two-hybrid system. *Proc Natl Acad Sci U S A*. 93:10321-6.

Vidal, M., and P. Legrain. 1999. Yeast forward and reverse 'n'-hybrid systems. *Nucleic Acids Res*. 27:919-29.

Viegas-Pequignot, E., B. Dutrillaux, and G. Thomas. 1988. Inactive X chromosome has the highest concentration of unmethylated Hha I sites. *Proc Natl Acad Sci U S A*. 85:7657-60.

Vojtek, A.B., S.M. Hollenberg, and J.A. Cooper. 1993. Mammalian Ras interacts directly with the serine/threonine kinase Raf. *Cell*. 74:205-14.

Vu, K.B., M.A. Ghahroudi, L. Wyns, and S. Muyldermans. 1997. Comparison of llama VH sequences from conventional and heavy chain antibodies. *Mol Immunol*. 34:1121-31.

Walsh, C.P., J.R. Chaillet, and T.H. Bestor. 1998. Transcription of IAP endogenous retroviruses is constrained by cytosine methylation. *Nat Genet*. 20:116-7.

Weber, M., J.J. Davies, D. Wittig, E.J. Oakeley, M. Haase, W.L. Lam, and D. Schubeler. 2005a. Chromosome-wide and promoter-specific analyses identify sites of differential DNA methylation in normal and transformed human cells. 37:853-862.

Weber, M., J.J. Davies, D. Wittig, E.J. Oakeley, M. Haase, W.L. Lam, and D. Schubeler. 2005b. Chromosome-wide and promoter-specific analyses identify sites of differential DNA methylation in normal and transformed human cells. *Nat Genet*. 37:853-62.

Weber, M., I. Hellmann, M.B. Stadler, L. Ramos, S. Paabo, M. Rebhan, and D. Schubeler. 2007. Distribution, silencing potential and evolutionary impact of promoter DNA methylation in the human genome. *Nat Genet*. 39:457-66.

Wehr, M.C., R. Laage, U. Bolz, T.M. Fischer, S. Grunewald, S. Scheek, A. Bach, K.A. Nave, and M.J. Rossner. 2006. Monitoring regulated protein-protein interactions using split TEV. *Nat Methods*. 3:985-93.

Wolff, H., A. Hartl, H.M. Eilken, K. Hadian, M. Ziegler, and R. Brack-Werner. 2006. Live-cell assay for simultaneous monitoring of expression and interaction of proteins. *Biotechniques*. 41:688, 690, 692.

Xiong, Z., and P.W. Laird. 1997. COBRA: a sensitive and quantitative DNA methylation assay. *Nucleic Acids Res*. 25:2532-4.

Yoder, J.A., N.S. Soman, G.L. Verdine, and T.H. Bestor. 1997. DNA (cytosine-5)-methyltransferases in mouse cells and tissues. Studies with a mechanism-based probe. *J Mol Biol*. 270:385-95.

Zhang, X., J. Yazaki, A. Sundaresan, S. Cokus, S.W. Chan, H. Chen, I.R. Henderson, P. Shinn, M. Pellegrini, S.E. Jacobsen, and J.R. Ecker. 2006. Genome-wide high-resolution mapping and functional analysis of DNA methylation in arabidopsis. *Cell*. 126:1189-201.

Zhou, L., X. Cheng, B.A. Connolly, M.J. Dickman, P.J. Hurd, and D.P. Hornby. 2002. Zebularine: a novel DNA methylation inhibitor that forms a covalent complex with DNA methyltransferases. *J Mol Biol*. 321:591-9.

CHAPTER V. CURRICULUM VITÆ

Personal details:

Name:	**Kourosh Alexander Zolghadr**
Date of Birth:	11/ 11/ 1976
Place of Birth:	Teheran, Iran
Nationality:	German
Marital status:	unmarried

Current work address:

Ludwig-Maximilians-Universität (LMU) Munich
Biocenter, Department Biology II
Großhaderner Str. 2
82152 Planegg-Martinsried
Germany

Phone:	+49-(0)89-2180 74231
Fax:	+49-(0)89-2180 74236
E-mail:	k.zolghadr@lmu.de

Education:

2004 – present	PhD student in biology Ludwigs-Maximilians-Universität Munich Department of Biology, group of Prof. Dr. Heinrich Leonhardt
1997 – 2003	Diploma in biology Ludwigs-Maximilians-Universität Munich Department of Biology, lab of Prof. Dr. Thomas Cremer
1996	Allgemeine Hochschulreife Erasmus-Grasser Gymnasium, Munich

Societies:

Center for NanoScience – CeNS
Nanosystems Initiative Munich – NIM

V.1. PUBLICATIONS

Zolghadr, K., Mortusewicz, O., Rothbauer, U., Kleinhans, R., Goehler, H., Wanker, E., Cardoso, M.C., and Leonhardt, H. (2007). A fluorescent two-hybrid (F2H) assay for direct visualization of protein interactions in living cells. under revision at *Molecular & Cellular Proteomics (MCP)*

Rothbauer, U., **Zolghadr, K.**, Muyldermans, S., Schepers, A., Cardoso, M.C., and Leonhardt, H. (2007). A versatile nanotrap for biochemical and functional studies with fluorescent fusion proteins. accepted at *Molecular & Cellular Proteomics (MCP)*

Rothbauer, U.*, **Zolghadr, K.***, Tillib, S., Nowak, D., Schermelleh, L., Gahl, A., Backmann, N., Conrath, K., Muyldermans, S., Cardoso, M.C., and Leonhardt, H. (2006). Targeting and tracing antigens in live cells with fluorescent nanobodies. *Nat Methods* 3(11): 887-889.

* Joint first authors

Spada, F., Rothbauer, U., **Zolghadr, K.**, Schermelleh, L., and Leonhardt, H. (2006). Regulation of DNA methyltransferase 1. *Adv Enzyme Regul*. 46(1): 224-234

Schermelleh, L., Spada, F., Easwaran, H.P., **Zolghadr, K.**, Margot, J.B., Cardoso, M.C., and Leonhardt, H. (2005). Trapped in action: direct visualization of DNA methyltransferase activity in living cells. *Nat Methods* 2(10): 751-756.

Dietzel, S., **Zolghadr, K.**, Hepperger, C., and Belmont, A.S. (2004). Differential large-scale chromatin compaction and intranuclear positioning of transcribed versus non-transcribed transgene arrays containing β-globin regulatory sequences. *J Cell Sci* 117(Pt 19): 4603-4614.

V.2. AWARDS AND CONFERENCE CONTRIBUTIONS

Publication Award 2007 granted by the Center for NanoScience (CeNS) for
“Targeting and Tracing Antigens in Live Cells with Fluorescent Nanobodies”
Munich, November 23rd, 2007

2nd Transregio5 Symposium: Chromatin – Assembly and Inheritance of Functional States
Poster: “A versatile nanotrap for biochemical and functional studies with fluorescent fusion proteins.”
Munich, September 13 – 15, 2007

International Symposium on High Throughput Microscopy for Systems Biology
Poster: “Targeting and Tracing Antigens in Live Cells with Fluorescent Nanobodies”
EMBL Heidelberg, April 28 – 29, 2007

International Symposium on Optical Analysis of Biomolecular Machines
Poster: “Dynamics of DNA methyltransferases in living cells”
Max Delbrück Center for Molecular Medicine, Berlin, July 13 – 16, 2006

Workshop on Cell Biology and Microscopy
Talk and Poster: “Trapped in action - direct visualization of DNA methyltransferase activity in living cells”
Burg Altleiningen, December 7 – 11, 2005

Workshop on Molecular Labeling and FRET
Poster: “Dynamics of chromatin accessibility and proteome distribution in living cells”
Leibniz Institute for Neurobiology, Magdeburg, May 17 – 18, 2004